EDITORIAL BOARD

Please consider, when preparing the manuscript, the *Instructions for the Authors* at the end of each issue. Orders, exchange for other journals, manuscripts and all correspondences concerning off prints should be sent to the Executive Editors or to the editorial secretaries at the address:

Politehnica University Timisoara
Department of Mathematics
Victoriei Square, No. 2
300006–Timisoara, Romania
Tel.: +40-256-403099
Fax: +40-(0)256-403109
Politehnica University Timisoara
Department of Physical Fundamentals
of Engineering
B-dul. Vasile Parvan, No. 2
300223–Timisoara, Romania
Tel.: +40-256-403391
Fax: +40-(0)256-403392

Contents

BULETINUL ŞTIINŢIFIC
Al
UNIVERSITĂŢII "POLITEHNICA" DIN TIMIŞOARA

Tom 65 (79), 1	MATEMATICĂ – FIZICĂ	2020

ON CONTRIBUTION OF DYNAMICAL SYSTEMS TO EPIDEMIOLOGY

Gheorghe MOZA, Joan TORREGROSA

Abstract

The involvement of mathematical modeling in understanding the spreading of infectious diseases is briefly presented in this short review. The article addresses to different readers, from specialists familiar to the field of mathematical modeling to the larger public interested in these topics.

1 Introduction

The way an infectious disease (like Covid-19) spreads is a challenge both for science but also the large population. It is known from history that infectious diseases have caused much suffering to the humanity. From time to time and from place to place such pandemic plagues have appeared during the previous ages of the society. We can cite, at least, two very bad previous pandemic periods, with a very high number of death, the Black Plague and the Spanish flu. The first was one of the worst pandemic recorded in history, which stormed the humanity from 1346 to 1353 and has caused the death of 75–200 million people [1]. This number represented about one-third of the total world population at that time [2]. According to the World Health Organization, the Plague was created by the bacterium Yersinia pestis, which was spreading by fleas [3]. The second, and more recent, was the 1918 influenza pandemic, commonly known by the Spanish flu or as the Great Influenza epidemic. The estimated number of deaths was 17–50 million people [4] but due to the censors during World War I, this number could

arrive to 100 million. We will never know the actual number of total death. It was an exceptionally deadly global influenza pandemic caused by the H1N1 influenza A virus.

Various methods to constraint the disease and save people have been proposed over the years and more medical solutions have been tested and developed in this regard. Perhaps, the best medical solution against the plague caused by this bacteria was the invention of antibiotics, which saved the lives of millions of people over the years.

2 Models of population dynamics in epidemiology

Along with the research aimed at finding medical solutions, a new theoretical framework of mathematical modeling of various characteristics related to a pandemic has started to develop. Perhaps, the works of Lotka [5] and Volterra [6] around the year 1925 were the pioneering works in this new domain. They have studied different types of interactions between groups of preys and predators in real-life phenomena related to ecology. Their models of population dynamics are known in the literature as *predator-prey* models or *Lotka-Volterra* models. The field evolved rapidly, both in terms of new models being proposed but also in terms of new domains where the models may have applications.

One of the new domains is epidemiology and, particularly, the transmission of infectious diseases, since the ways an infectious disease spreads in a population have many links with predator-prey models. A mathematical model which studies the interactions of three groups of individuals in a population affected by an infectious disease is the so-called SIR model [7], [8]. The three interacting groups are S-susceptible, I-infected and R-recovered. In other words, the SIR model considers the whole population to be studied as being formed by three different groups of individuals: the group S which contains individuals which may become infected, the group I of infected individuals and, finally, the group R of recovered individuals. Notice that, all individuals from one of the three groups have the same characteristics related to the disease. At any time t, these three groups interact one to another and some individuals may pass from one group to another group. These interactions depending on time t are modeled by mathematical equations (particularly, differential or difference equations) of Lotka-Volterra type. Then, such equations are studied using different mathematical tools, such as the theory of dynamical systems, to discover different properties of the equations, which, in turn, explain different ways of possible interactions of the three groups in the studied population. There are many published scientific articles on SIR models and their variants, such as the models

SIS (Susceptible-Infected-Susceptible), SIRD (Susceptible-Infectious-Recovered-Deceased) [9], SIRV (Susceptible-Infectious-Recovered-Vaccinated) [10] and SEIR (Susceptible-Exposed-Infectious-Recovered) [11]. Such models received a special attention in the current pandemic caused by Covid-19. For example, a top Journal *Nonlinear Analysis: Real-World Applications* presents a list of most downloaded articles and, during May 2022, an article [12] on a variant of SIR models (the SAIRS epidemic model) was the first article in the list.

Another direction of research where mathematical models contribute in understanding the spreading of the culprits (microbes such as viruses, bacteria, parasites and fungi) in an infectious disease, is by modeling the interactions between microbes and different types of cells from immune system, such as neutrophils and lymphocytes. For example, in [13] are presented more such models to study interactions between host immunity and parasite spreading. A four-dimensional model based on differential equations studying interactions between an invading pathogen and the innate immune system is presented in [14], while a model for interactions between influenza A virus and local tissues such as respiratory tract, is reported in [15].

In conclusion, mathematical modeling and, in particular, tools and models from dynamical systems theory, represent a relevant domain which contributes to understanding the spreading of infectious diseases and other aspects in epidemiology.

3 Acknowledgments

This article was supported by Horizon2020-2017-RISE-777911 project.

References

[1] https://en.wikipedia.org/wiki/Black_Death

[2] Historical Estimates of World Population, https://www.census.gov/data

[3] World Health Organization, October 2017, `https://www.who.int/en/news-room/fact-sheets/detail/plague`

[4] https://en.wikipedia.org/wiki/Spanish_flu

[5] Lotka AJ, Elements of Physical Biology, Williams and Wilkins, Baltimore, MD, 1925.

[6] Volterra V, Variazioni e fluttuaziono del numero di individui in specie animali conviventi, Mem. Accad. Lincei 1926, 2: 31–113.

[7] Kendall DG (1956): Deterministic and stochastic epidemics in closed populations, Proceedings of the Third Berkeley Symposium on Mathematical Statistics and Probability: Contributions to Biology and Problems of Health 1956, 4:149–165.

[8] Kermack WO, McKendrick AG: A Contribution to the Mathematical Theory of Epidemics, Proceedings of the Royal Society of London 1927, Series A, 115 (772): 700–721.

[9] Bailey Norman TJ: The mathematical theory of infectious diseases and its applications (2nd ed.) 1975, London, Griffin. ISBN 0-85264-231-8.

[10] Schlickeiser R, Kröger M: Analytical Modeling of the Temporal Evolution of Epidemics Outbreaks Accounting for Vaccinations, Physics 2021, 3(2): 386-426.

[11] Carcione JM, Santos JE, Bagaini C and Ba J: A simulation of a COVID-19 epidemic based on a deterministic SEIR Model, Front. Public Health 2020, 8:230.

[12] Ottaviano S, Sensi M and Sottile S: Global stability of SAIRS epidemic models, Nonlinear Analysis: Real World Applications 2022, 65: 103501.

[13] Fenton A and Perkins SE: Applying predator-prey theory to modelling immune-mediated, within-host interspecific parasite interactions, Parasitology 2010, 137: 1027–1038.

[14] Stengel RF, Ghigliazza RM and Kulkarni NV: Optimal enhancement of immune response, Bioinformatics 2002, 18(9): 1227–1235.

[15] Quirouette C, Younis NP, Reddy MB, Beauchemin CAA: A mathematical model describing the localization and spread of influenza A virus infection within the human respiratory tract, PLOS Computational Biology 2020, 16(4): e1007705.

Prof. dr. Gheorghe MOZA
Department of Mathematics
Politehnica University of Timişoara
Piaţa Victoriei, nr.2, 300006 Timişoara, România
gheorghe.moza@upt.ro

Assoc. prof. dr. Joan TORREGROSA
Department of Mathematics
Autonomous University of Barcelona, SPAIN
torre@mat.uab.cat

BULETINUL ŞTIINŢIFIC
Al
UNIVERSITĂŢII "POLITEHNICA" DIN TIMIŞOARA

Tom 65 (79), 1	MATEMATICĂ – FIZICĂ	2020

ON THE PERIODIC AND HOMOCLINIC ORBITS OF A HAMILTON-POISSON SYSTEM

Cristian LĂZUREANU, Jinyoung CHO

Abstract

In this paper, we study a Hamilton-Poisson system that has a single family of equilibrium points. We show that there are periodic orbits around all the nonlinearly stable equilibrium points, and homoclinic orbits that connect each unstable equilibrium point with itself. We point out these properties in connection with the energy-Casimir mapping associated to the considered system. [1]

1 Introduction

Let Ω be an open set in $\mathbb{R}^3$ and $H, C \in C^\infty(\Omega)$. It is well known that the functions H and C define the three-dimensional system of differential equations

$$\dot{\mathbf{x}} = \nabla H \times \nabla C, \tag{1}$$

for which they are constants of motion. Moreover, (1) is a Hamilton-Poisson system, where the Poisson bracket in the smooth category is given by (see, e.g., [14])

$$\{f, g\} = \nabla C \cdot (\nabla f \times \nabla g). \tag{2}$$

This Poisson bracket can be written in matrix notation

$$\Pi = \begin{bmatrix} 0 & C_z' & -C_y' \\ -C_z' & 0 & C_x' \\ C_y' & -C_x' & 0 \end{bmatrix}. \tag{3}$$

[1] MSC(2010): 70H12, 70H14, 70K20, 70K42, 70K44.
Keywords and phrases: *Hamilton-Poisson system, energy-Casimir mapping, stability, periodic orbits, homoclinic orbits.*

The study of the common level sets of the independent constants of motion H and C may gives informations about the dynamics of (1). For instance, Holm and Marsden described such results in the case of rigid body dynamics [6].

In [15], the energy-Casimir mapping associated to a three-dimensional Hamilton-Poisson system was considered. If H is the Hamiltonian of the system and C is a Casimir function of the Poisson structure, then the energy-Casimir mapping is defined by

$$\mathcal{EC} : \mathbb{R}^3 \to \mathbb{R}^2 \ , \quad \mathcal{EC}(x, y, z) = (H(x, y, z), C(x, y, z)). \tag{4}$$

In order to classify the types of the orbits of system (1), a partition of the image of the energy-Casimir mapping given by the images of the equilibrium points through the energy-Casimir mapping was constructed [15] (also see [4, 5, 7, 8, 9, 10, 11, 12, 13, 16, 17]). In these papers, the considered Hamilton-Poisson systems have at least two families of equilibrium points, which lead to a partition of the image of $\mathcal{EC}$. Moreover, a topological classification of the fibers and the corresponding dynamical description is obtained. The aim of our work is to verify whether the connections between the above-mentioned partition and the dynamics of the system, reported in the above papers, hold for a system with a single family of equilibrium points. More precisely, we obtain that the boundary of the set $\mathrm{Im}(\mathcal{EC}) \subsetneq \mathbb{R}^2$ is the union of the images of some stable equilibrium points through $\mathcal{EC}$, and the image of the energy-Casimir mapping is convexly generated by these images. Furthermore, the fibers $\mathcal{F}_{(h,c)} = \mathcal{EC}^{-1}(h, c)$ corresponding to the pairs (h, c) that belong to the boundary of $\mathrm{Im}(\mathcal{EC})$ contain only nonlinearly stable equilibrium points. The images of the others critical points are in the interior of $\mathrm{Im}(\mathcal{EC})$ and the corresponding fibers are periodic orbits and homoclinic orbits for stable and unstable equilibria respectively. In addition, if Σ denotes an open subset of the semialgebraic partition of $\mathrm{Im}(\mathcal{EC})$ that has dimension 2 and $(h, c) \in \Sigma$, then the fiber $\mathcal{F}_{(h,c)}$ contains periodic orbits.

In this paper we study the system defined by the functions

$$H(x, y, z) = \frac{1}{4}x^2 + \frac{1}{4}y^2 - z \ , \quad C(x, y, z) = \frac{1}{2}x + \frac{1}{2}y + \frac{1}{2}z^2, \tag{5}$$

that is

$$\begin{cases} \dot{x} = \dfrac{1}{2}(1 + yz) \\ \dot{y} = -\dfrac{1}{2}(1 + xz) \\ \dot{z} = \dfrac{1}{4}(x - y) \end{cases} \tag{6}$$

The paper is set up as follows. In Section 2, we analyze the nonlinear stability of the equilibrium points of the considered system. In Section 3, we prove the existence of periodic orbits around all the nonlinearly stable equilibrium points.

In Section 4, we give two Hamilton-Poisson realizations of the considered system, which lead to an infinite family of Hamilton-Poisson realizations. In Section 5, we study some properties of the energy-Casimir mapping in connection with the dynamics of system (6). Particularly, we deduce parametric equations for some periodic and homoclinic orbits.

2 Stability

In this section we study the stability of the equilibrium points of system (6).

The equilibrium points of the system (6) satisfy the conditions

$$\begin{cases} \frac{1}{2}(1+yz)=0 \\ -\frac{1}{2}(1+xz)=0 \\ \frac{1}{4}(x-y)=0 \end{cases}.$$

Solving this system, we get the following family of equilibrium points of system (6)

$$\mathcal{E}=\left\{\left(M,M,-\frac{1}{M}\right)|M\in\mathbb{R}^*\right\}. \tag{7}$$

We obtain the following result regarding the stability of these equilibrium points.

Proposition 2.1. *Let $E_M=\left(M,M,-\frac{1}{M}\right)\in\mathcal{E}$ an arbitrary equilibrium point. Then E_M is unstable for every $M\in[1,+\infty)$ and nonlinearly stable for every $M\in(-\infty,0)\cup(0,1)$.*

Proof. Let $M\in\mathbb{R}^*$, the equilibrium point $E_M=\left(M,M,-\frac{1}{M}\right)$ and $J(x,y,z)$ be the matrix of linear part of system (6), that is

$$J(x,y,z)=\begin{bmatrix} 0 & \frac{1}{2}z & \frac{1}{2}y \\ -\frac{1}{2}z & 0 & -\frac{1}{2}x \\ \frac{1}{4} & -\frac{1}{4} & 0 \end{bmatrix} \tag{8}$$

The characteristic polynomial of $J(E_M)$ is given by

$$P_{J(E_M)}(\lambda) = -\lambda\left(\lambda^2 - \frac{M^3-1}{4M^2}\right) \tag{9}$$

and the roots of $P_{J(E_M)}$ are

$$\lambda_1 = 0, \quad \lambda_{2,3} = \pm\frac{\sqrt{M^3-1}}{2M} \tag{10}$$

For $M \in (1, +\infty)$ there is a positive eigenvalue and the equilibrium point E_M is unstable.

In the case $M = 1$, the equilibrium point E_M becomes $E_1(1, 1, -1)$ and the roots of the characteristic polynomial are all zero. We will show that there is a homoclinic orbit that connects E_1 with itself.

We remind that the functions H and C (5) are constants of motion, so we can define implicit equation of an orbit of system (6) by considering the level sets $H(x, y, z) = constant$ and $C(x, y, z) = constant$. Particularly, for the equilibrium point $E_1(1, 1, -1)$ we have

$$\begin{cases} H(x,y,z) = H(1,1,-1) \\ C(x,y,z) = C(1,1,-1) \end{cases},$$

which is equivalent to

$$\begin{cases} x^2 + y^2 - 4z = 6 \\ x + y + z^2 = 3 \end{cases}.$$

We get

$$x - y = \pm\sqrt{3 + 8z + 6z^2 - z^4}.$$

To obtain solution of system (6), we can reduce it from three degrees of freedom to one degree of freedom by rewriting the equation $\dot{z} = \frac{1}{4}(x - y)$ as

$$\dot{z} = \pm\frac{1}{4}\sqrt{3 + 8z + 6z^2 - z^4}. \tag{11}$$

Therefore

$$\int \frac{dz}{\sqrt{3 + 8z + 6z^2 - z^4}} = \pm\frac{1}{4}t.$$

Denoting $q = z + 1$, the above integral writes

$$\int \frac{dz}{\sqrt{3 + 8z + 6z^2 - z^4}} = \int \frac{dq}{q^2\sqrt{\frac{4}{q} - 1}}$$

Hence by integrating the equation (11), we get

$$-\frac{1}{2}\sqrt{\frac{4}{1+z}-1}=\pm\frac{1}{4}t$$

so we obtain

$$z(t)=\frac{12-t^2}{4+t^2} \tag{12}$$

Therefore we deduce

$$x(t)=\frac{t^4+24t^2-64t-48}{(4+t^2)^2}\ ,\ y(t)=\frac{t^4+24t^2+64t-48}{(4+t^2)^2}. \tag{13}$$

As a result, we get a solution of system (6).

Since $\lim\limits_{t\to\pm\infty}(x(t),y(t),z(t))=(1,1,-1)$, we get the homoclinic orbit

$$\mathcal{H}=(x,y,z):\mathbb{R}\to\mathbb{R}^3,\mathcal{H}(t)=(x(t),y(t),z(t)), \tag{14}$$

where the functions x,y,z are given by (12), (13).

For this reason, the equilibrium point $(1,1,-1)$ is unstable.

For $M\in(0,1)$, we will study stability of the equilibrium point E_M using the Arnold test [1] (also see [2]). We consider the function

$$F_\lambda(x,y,z)=C(x,y,z)-\lambda H(x,y,z),$$

where λ is a real parameter. Then we have successively the following:

1. $dF_\lambda\left(M,M,-\frac{1}{M}\right)=0$ if and only if $\lambda=\frac{1}{M}$.
2. $W=ker\ dC\left(M,M,-\frac{1}{M}\right)=span_{\mathbb{R}}\left\{\left(1,0,\frac{M}{2}\right),\left(0,1,\frac{M}{2}\right)\right\}$.
3. $d^2F_\lambda\big|_{W\times W}=\left(\frac{M^3-2}{4M}\right)dx^2+\frac{M^2}{2}dxdy+\left(\frac{M^3-2}{4M}\right)dy^2$ is negative definite for $M\in(0,1)$.

Hence, from the Arnold stability test we conclude that E_M is nonlinearly stable for $M\in(0,1)$.

To study the stability of the equilibrium point E_M in the case $M \in (-\infty, 0)$, we will consider the Lyapunov function $L \in C^\infty(\mathbb{R}^3, \mathbb{R})$,

$$L(x,y,z) = -\frac{1}{4M}(x-M)^2 - \frac{1}{4M}(y-M)^2 + \frac{1}{2}\left(z+\frac{1}{M}\right)^2.$$

Obviously, $L(x,y,z) > 0$, $\forall (x,y,z) \neq E_M$ and $L(E_M) = 0$, so L is positive definite. Moreover, $\dot{L} = \nabla L \cdot \dot{\mathbf{x}} = 0$, where $\dot{\mathbf{x}} = (\dot{x}, \dot{y}, \dot{z})$ is given by (6). Therefore the equilibrium point E_M is nonlinearly stable, which ends the proof. □

3 Periodic orbits

In this section we establish the existence of periodic orbits around the nonlinearly stable equilibrium points of system (6). We shall use the following version of the Moser-Weinstein theorem in the case of zero eigenvalue [3]:

Theorem 3.1. *([3]) Let $\dot{x} = X(x)$ be a dynamical system on a differentiable manifold U, x_0 an equilibrium point, i.e., $X(x_0) = 0$ and $C := (C_1, ..., C_j): U \to \mathbb{R}^j$ a vector valued constant of motion for the above dynamical system with $C(x_0)$ a regular value for C. If*
(i) the eigenspace corresponding to the eigenvalue zero of the linearized system around x_0 has dimension j,
(ii) $DX(x_0)$ has a pair of pure complex eigenvalues $\pm i\omega$ with $\omega \neq 0$,
(iii) there exist a constant of motion $I: U \to \mathbb{R}$ for the vector field X with $dI(x_0) = 0$ and such that $d^2I(x_0)|_{W\times W} > 0$, where $W = \bigcap_{l=1}^{j} \ker dC_l(x_0)$,
then for each sufficiently small $\varepsilon > 0$ any integral surface $I(x) = I(x_0) + \varepsilon^2$ contains at least one periodic solution of X whose period is close to the period of the corresponding linear system around x_0.

Using this theorem, we obtain the next result.

Proposition 3.2. *Let $E_M = \left(M, M, -\frac{1}{M}\right) \in \mathcal{E}$ be a nonlinearly stable equilibrium point of system (6) such that $M \in (-\infty, 0)$. Then for each sufficiently small $\varepsilon \in \mathbb{R}_+^*$, any integral surface*

$$\Sigma_\varepsilon^{E_M}: \; -\frac{1}{4M}(x-M)^2 - \frac{1}{4M}(y-M)^2 + \frac{1}{2}\left(z+\frac{1}{M}\right)^2 = \epsilon^2$$

contains at least one periodic orbit $\gamma_\varepsilon^{E_M}$ of system (6) whose period is close to $\frac{2\pi}{\omega}$, where $\omega = \frac{\sqrt{1-M^3}}{2|M|}$.

Proof. The characteristic polynomial associated with the linearization of system (6) at E_M has the eigenvalues $\lambda_1 = 0$ and $\lambda_{2,3} = \pm i\frac{\sqrt{1-M^3}}{2M}$. The eigenspace corresponding to the eigenvalue zero is $\operatorname{span}_{\mathbb{R}}\left\{(1, 1, \frac{1}{M^2})\right\}$, thus it has dimension 1.

Consider the constant of motion of system (6) given by

$$I(x, y, z) = \frac{1}{2}\left(x + y + z^2\right) - \frac{1}{M}\left(\frac{1}{4}x^2 + \frac{1}{4}y^2 - z\right).$$

We have

1. $dI(M, M, -\frac{1}{M}) = 0$.
2. $d^2I\left(M, M, -\frac{1}{M}\right)\big|_{W\times W} = \left(\frac{M^3-2}{4M}\right)dx^2 + \frac{M^2}{2}dxdy + \left(\frac{M^3-2}{4M}\right)dy^2 > 0$, where $W = \ker dC\left(M, M, -\frac{1}{M}\right) = \operatorname{span}_{\mathbb{R}}\left\{\left(1, 0, \frac{M}{2}\right), \left(0, 1, \frac{M}{2}\right)\right\}$.

Using Theorem 3.1, the conclusion follows. □

Similarly, we get the existence of periodic orbits around the other nonlinearly stable equilibrium points.

Proposition 3.3. *Let $E_M = \left(M, M, -\frac{1}{M}\right) \in \mathcal{E}$ be a nonlinear stable equilibrium point of system (6) such that $M \in (0, 1)$. Then for each sufficiently small $\varepsilon \in \mathbb{R}_+^*$, any integral surface*

$$\Sigma_\varepsilon^{E_M} \ : \ \frac{1}{4M}(x - M)^2 + \frac{1}{4M}(y - M)^2 - \frac{1}{2}\left(z + \frac{1}{M}\right)^2 = \epsilon^2$$

contains at least one periodic orbit $\gamma_\varepsilon^{E_M}$ of system (6) whose period is close to $\frac{2\pi}{\omega}$, where $\omega = \frac{\sqrt{1-M^3}}{2M}$.

4 Hamilton-Poisson realizations

In this section we prove that the considered system has infinitely many Hamilton-Poisson realizations.

Proposition 4.1. *The system* (6) *has the Hamilton-Poisson realization* $(\mathbb{R}^3, \Pi_1, H)$, *where*

$$\Pi_1 = \begin{bmatrix} 0 & z & -\frac{1}{2} \\ -z & 0 & \frac{1}{2} \\ \frac{1}{2} & -\frac{1}{2} & 0 \end{bmatrix} \tag{15}$$

is the matrix representation of the Poisson structure and H *is the Hamilton function defined in* (5).

Proof. Considering the Casimir function C given by (5), the matrix Π (3) becomes Π_1 and $\Pi_1 \cdot \nabla C = \mathbf{0}$. It is easy to see that system (6) writes $\Pi_1 \cdot \nabla H = \dot{\mathbf{x}}^t$, where $\mathbf{x} = (x, y, z)$, as required. □

Proposition 4.2. *The system* (6) *has another Hamilton-Poisson realization* $(\mathbb{R}^3, \Pi_2, C)$, *where the Poisson structure is given by*

$$\Pi_2 = \begin{bmatrix} 0 & 1 & \frac{1}{2}y \\ -1 & 0 & -\frac{1}{2}x \\ -\frac{1}{2}y & \frac{1}{2}x & 0 \end{bmatrix} \tag{16}$$

and C *is defined in* (5). *Moreover, system* (6) *is a bi-Hamiltonian system.*

Proof. Hence Π_2 verify $\Pi_2 \cdot \nabla C = \dot{\mathbf{x}}^t$ and $\Pi_2 \cdot \nabla H = \mathbf{0}$. We can observe that $\Pi_1 \cdot \nabla H = \Pi_2 \cdot \nabla C = \dot{\mathbf{x}}^t$. In addition, Π_1 and Π_2 are compatible Poisson structures, i.e. their sum is also a Poisson structure, thus (6) is a bi-Hamiltonian system. □

Proposition 4.3. *The system* (6) *has a family of Hamilton-Poisson realizations, namely* $(\mathbb{R}^3, \Pi_{a,b}, H_{c,d})$, *where the Hamiltonian function is given by*

$$H_{c,d} = \frac{d}{4}(x^2 + y^2) + \frac{c}{2}(x + y) + \frac{c}{2}z^2 - dz,$$

and the Poisson structure by

$$\Pi_{a,b} = \begin{bmatrix} 0 & az-b & -\frac{1}{2}a-\frac{1}{2}by \\ -az+b & 0 & \frac{1}{2}a+\frac{1}{2}bx \\ \frac{1}{2}a+\frac{1}{2}by & -\frac{1}{2}a-\frac{1}{2}bx & 0 \end{bmatrix},$$

for every $a,b,c,d \in \mathbb{R}$ that fulfill the condition $ad-bc=1$. A Casimir of the Poisson structure is

$$C_{a,b} = \frac{b}{4}(x^2+y^2) + \frac{a}{2}(x+y) + \frac{a}{2}z^2 - bz.$$

Proof. Let $a,b,c,d \in \mathbb{R}$ such that $ad-bc=1$. Let us denote $\Pi_{a,b} = a\Pi_1 - b\Pi_2$, $H_{c,d} = cC+dH$, and $C_{a,b} = aC+bH$, where Π_1 and Π_2 are given by (15) and (16) respectively. We observe that $\Pi_{a,b}$ verifies $\Pi_{a,b}\cdot\nabla H_{c,d} = \dot{\mathbf{x}}^t$ and $\Pi_{a,b}\cdot\nabla C_{a,b} = \mathbf{0}$ and the conclusion follows. □

5 Energy-Casimir mapping

In this section, we point out some connections between some properties of the energy-Casimir mapping (4) and the dynamics of the considered system (6).

In our case, the Hamiltonian H and a Casimir function C are given by (5). Then the energy-Casimir mapping is given by

$$\mathcal{EC}:\mathbb{R}^3\to\mathbb{R}^2\ ,\quad \mathcal{EC}(x,y,z) = \left(\frac{1}{4}x^2+\frac{1}{4}y^2-z,\ \frac{1}{2}x+\frac{1}{2}y+\frac{1}{2}z^2\right). \tag{17}$$

Recall that a point $(x_0,y_0,z_0)\in\mathbb{R}^3$ is a critical point of the energy-Casimir mapping if the rank of the Jacobian matrix of $\mathcal{EC}$ at this point is less than 2.

Remark 5.1. *Since system* (6) *has the form* (1)*, it results that the critical points of $\mathcal{EC}$ are the equilibrium points* (7) *of the considered system.*

The image of the equilibrium point $E_M\left(M,M,-\frac{1}{M}\right)\in\mathcal{E}$ trough the energy-Casimir mapping, given by

$$\mathcal{EC}(E_M) = \left(\frac{1}{2}M^2+\frac{1}{M}\ ,\ M+\frac{1}{2M^2}\right), \tag{18}$$

for every $M \in \mathbb{R}^*$, is a critical value of $\mathcal{EC}$. For $M < 0$, we consider the following curve of critical values

$$\Gamma : \begin{cases} h = \dfrac{1}{2}M^2 + \dfrac{1}{M} \\ c = M + \dfrac{1}{2M^2} \end{cases}, M < 0. \tag{19}$$

It immediately follows that Γ is a simple regular curve that defines a convex bijective function $c : \mathbb{R} \to \mathbb{R}, c = c(h)$ (Figure 1). For each $M < 0$, we denote a point of Γ by (h_e, c_e), where $h_e = \dfrac{1}{2}M^2 + \dfrac{1}{M}$, $c_e = M + \dfrac{1}{2M^2}$.

The image of the energy-Casimir mapping is the set

$$\mathrm{Im}(\mathcal{EC}) = \left\{(h, c) \in \mathbb{R}^2 | (\exists)(x, y, z) \in \mathbb{R}^3 : \mathcal{EC}(x, y, z) = (h, c)\right\}.$$

Now we can prove the next result.

Proposition 5.2. *Let $M < 0$ and $\mathcal{EC}$ (17) be the energy-Casimir mapping of system (6). Then the boundary of Im$(\mathcal{EC})$ is Γ and Im$(\mathcal{EC}) = \overline{co}\{\Gamma\}$, where $\overline{co}$ denoted the convex hull (Figure 1).*

Proof. A pair (h, c) belongs to the image of the energy-Casimir mapping if and only if the system

$$\begin{cases} h = \dfrac{1}{4}x^2 + \dfrac{1}{4}y^2 - z \\ c = \dfrac{1}{2}x + \dfrac{1}{2}y + \dfrac{1}{2}z^2 \end{cases} \tag{20}$$

or equivalent

$$\begin{cases} x^2 + y^2 - 4z = 4h \\ x + y + z^2 = 2c \end{cases} \tag{21}$$

has at least a solution.

First, it is obvious that the above system has solution for $h = h_e$ and $c = c_e$.

Now we show that there are no pairs $(h, c) \in \mathrm{Im}(\mathcal{EC})$ for $h = h_e$ and $c < c_e$, that is system (20) has no solution in this case.

Suppose that system (20) has solution for $h = h_e$ and $c < c_e$. Using (21) we get

$$(x - M)^2 + (y - M)^2 - 2M\left(z + \frac{1}{M}\right)^2 = 4M^2 + \frac{2}{M} - 4Mc,$$

or equivalent

$$(x-M)^2+(y-M)^2-2M\left(z+\frac{1}{M}\right)^2=4M(c_e-c). \tag{22}$$

But $M<0$ and $c<c_e$, which leads to a contradiction with (22). So for $h=h_e$ and $c<c_e$ system (20) has no solution.

Finally, let $h=h_e$ and $c\geq c_e$. Using (22), system (21) is equivalent with

$$\begin{cases} x^2+y^2-4z=2M^2+\dfrac{4}{M} \\ (x-M)^2+(y-M)^2-2M\left(z+\dfrac{1}{M}\right)^2=4M(c_e-c) \end{cases},$$

which has solution because it that represents the intersection between an ellipsoid with the center $E_M\left(M,M,-\frac{1}{M}\right)$ and a circular paraboloid that contains the point E_M. Therefore system (20) has solution for $h=h_e$ and $c\geq c_e$, that is the points situated above the curve Γ belong to $\mathrm{Im}(\mathcal{EC})$, which finishes the proof. □

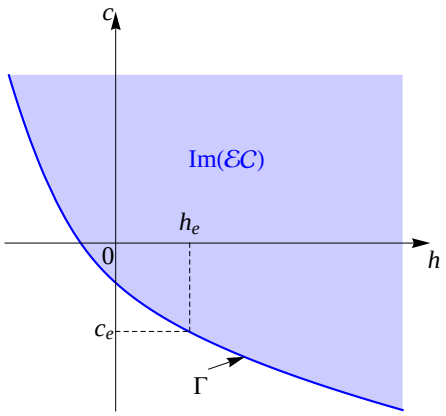

Figure 1: The image of the energy-Casimir mapping.

The images (18) of the equilibrium points through the energy-Casimir mapping allows us to define other two curves of critical values

$$\Gamma^s:\begin{cases} h=\dfrac{1}{2}M^2+\dfrac{1}{M} \\ c=M+\dfrac{1}{2M^2} \end{cases},M\in(0,1)\,,\quad \Gamma^u:\begin{cases} h=\dfrac{1}{2}M^2+\dfrac{1}{M} \\ c=M+\dfrac{1}{2M^2} \end{cases},M\in[1,\infty), \tag{23}$$

where "s" and "u" stand for stable and unstable respectively. These curves lead to the following semialgebraic partition of the set $\mathrm{Im}(\mathcal{EC})$ depicted in Figure 2

$$\mathrm{Im}(\mathcal{EC}) = \Gamma \cup \Sigma_1 \cup \Gamma^s \cup \Sigma_2 \cup \Gamma^u.$$

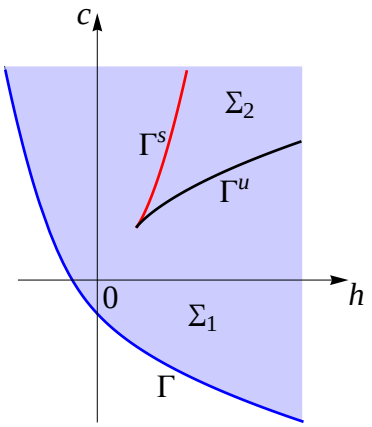

Figure 2: The semialgebraic partition of the image of the energy-Casimir mapping.

In the following, we point out connections between different types of the orbits of system (6) and pairs (h, c) from the subsets of the above partition of $\mathrm{Im}(\mathcal{EC})$.

The fiber of the energy-Casimir mapping $\mathcal{EC}$ corresponding to an element $(h_0, c_0) \in \mathrm{Im}(\mathcal{EC})$ is the set

$$\mathcal{F}_{(h_0,c_0)} = \left\{(x, y, z) \in \mathbb{R}^3 \mid \mathcal{EC}(x, y, z) = (h_0, c_0)\right\} \tag{24}$$

and an implicit equation of it is given by

$$\mathcal{F}_{(h_0,c_0)} : \begin{cases} H(x, y, z) = h_0 \\ C(x, y, z) = c_0 \ . \end{cases} \tag{25}$$

Since the dynamics of our system takes place at the intersection of the level sets $H(x, y, z) = constant$ and $C(x, y, z) = constant$, an orbit is given implicitly by (25). In Figure 3 we show such intersections.

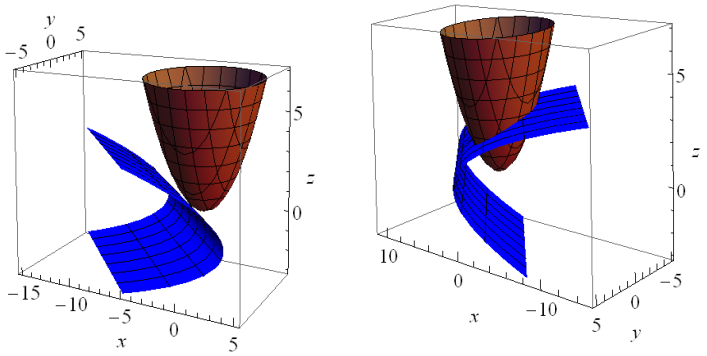

(a) $(h, c) \in \Gamma$ (b) $(h, c) \in \Sigma_1$

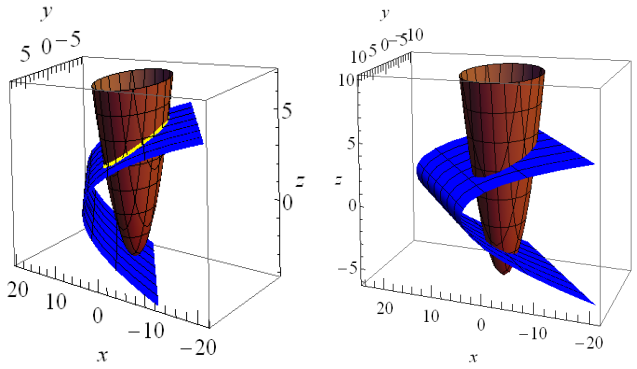

(c) $(h, c) \in \Gamma^s$ (d) $(h, c) \in \Sigma_2$

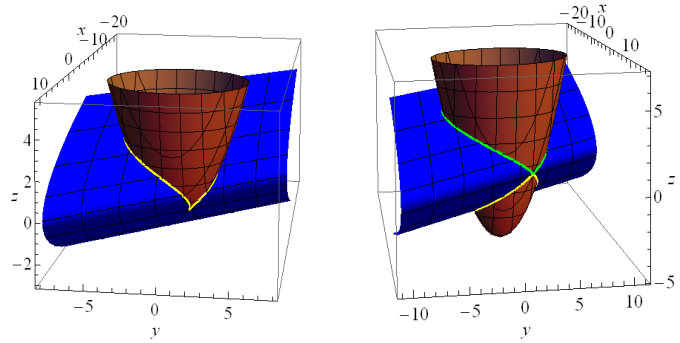

(e) $(h, c) \in \Gamma^u, M = 1$ (f) $(h, c) \in \Gamma^u, M > 1$

Figure 3: Intersections of the level sets $H(x, y, z) = h$ and $C(x, y, z) = c$:
(a) a stable equilibrium point; (b) a periodic orbit; (c) a stable equilibrium point and a periodic orbit; (d) two periodic orbits; (e) a homoclinic orbit; (f) a pair of homoclinic orbits.

We begin our study with the pairs (h,c) that belong to the boundary of $\mathrm{Im}(\mathcal{EC})$.

Proposition 5.3. *Let $(h,c)\in\Gamma$. Then the corresponding fiber contains only nonlinear stable equilibrium point,*

$$\mathcal{F}_{(h,c)}=\left\{\left(M,M,-\frac{1}{M}\right)\Big|M\in(-\infty,0)\right\}.$$

Proof. In this case, (5) and (25) lead to

$$-\frac{1}{4M}(x-M)^2-\frac{1}{4M}(y-M)^2+\frac{1}{2}\left(z+\frac{1}{M}\right)^2=c-\frac{1}{M}h-\frac{M}{2}+\frac{1}{2M^2}$$

Since $h=\frac{1}{2}M^2+\frac{1}{M}$, $c=M+\frac{1}{2M^2}$ (19), we get $c-\frac{1}{M}h-\frac{M}{2}+\frac{1}{2M^2}=0$ and

$$-\frac{1}{4M}(x-M)^2-\frac{1}{4M}(y-M)^2+\frac{1}{2}\left(z+\frac{1}{M}\right)^2=0$$

Therefore $x=y=M$ and $z=-\frac{1}{M}$, as required. □

In the proof of Proposition 2.1 we have determined the parametric equations of a homoclinic orbit (see Figure 3(e)) in connection with the equilibrium point $E_1(1,1,-1)$ and the critical value $(h,c)=\mathcal{EC}(E_1)\in\Gamma^u$. More precisely, we have obtained the following result.

Proposition 5.4. *Let $(h,c)=\mathcal{EC}(E_1)\in\Gamma^u$. Then the corresponding fiber contains the unstable equilibrium point $E_1(1,1,-1)$ and the homoclinic orbit $\mathcal{H}$ (14).*

Figure 3(f) indicates a pair of homoclinic orbits corresponding to the unstable equilibrium point E_M, $M>1$. Their parametrizations are given in the next result.

Proposition 5.5. *Let $(h,c)=\mathcal{EC}(E_M)\in\Gamma^u, M>1$. Then the corresponding fiber contains the unstable equilibrium point E_M and a pair of homoclinic orbits $\mathcal{H}_1$ and $\mathcal{H}_2$ given by*

$$\mathcal{H}_1(t)=(x_1(t),y_1(t),z_1(t))\ ,\ \mathcal{H}_2(t)=(x_2(t),y_2(t),z_2(t))\ ,\ t\in\mathbb{R},$$

where

$$x_1(t)=\frac{M^3+4p-4\left(-1+M^3\right)^{3/2}p+12M^3p^2-6M^6p^2+4M^3p^3+4M^3\left(-1+M^3\right)^{3/2}p^3+M^9p^4}{\left(M+2Mp+M^4p^2\right)^2}$$

$$y_1(t)=\frac{M^3+4p+4\left(-1+M^3\right)^{3/2}p+12M^3p^2-6M^6p^2+4M^3p^3-4M^3\left(-1+M^3\right)^{3/2}p^3+M^9p^4}{\left(M+2Mp+M^4p^2\right)^2}$$

$$z_1(t)=\frac{-1+2p-4M^3p-M^3p^2}{M(1+2p+M^3p^2)}$$

and

$$x_2(t)=\frac{M^3-4p+4\left(-1+M^3\right)^{3/2}p+12M^3p^2-6M^6p^2-4M^3p^3-4M^3\left(-1+M^3\right)^{3/2}p^3+M^9p^4}{\left(M-2Mp+M^4p^2\right)^2}$$

$$y_2(t)=\frac{M^3-4p-4\left(-1+M^3\right)^{3/2}p+12M^3p^2-6M^6p^2-4M^3p^3+4M^3\left(-1+M^3\right)^{3/2}p^3+M^9p^4}{\left(M-2Mp+M^4p^2\right)^2}$$

$$z_2(t)=\frac{-1-2p+4M^3p-M^3p^2}{M(1-2p+M^3p^2)},$$

with $p=p(t)=e^{\frac{\sqrt{-1+M^3}}{2M}(t-t_0)}$.

Proof. The implicit equation of the fiber (25) leads to

$$x-y=\pm\sqrt{8h+8z-4c^2+4cz^2-z^4}.$$

Let $M>1$ and $(h,c)\in\Gamma^u$ (23). Then

$$x-y=\pm\frac{1}{M^2}(1+Mz)\sqrt{4M^3-(Mz-1)^2},$$

and the last equation of system (6) becomes

$$\dot{z}=\pm\frac{1}{4M^2}(1+Mz)\sqrt{4M^3-(Mz-1)^2}.$$

Then

$$\int\frac{4M^2\,dz}{(1+Mz)\sqrt{4M^3-(Mz-1)^2}}=\pm(t-t_0).$$

By changing of variable $z=\dfrac{1}{v}-\dfrac{1}{M}$ we have

$$\int\frac{4dv}{\sqrt{4Mv^2-(1-\frac{2v}{M})^2}}=\mp(t-t_0). \tag{26}$$

Taking into account that $M > 1$, by integration we get the solutions $z_1(t)$ and $z_2(t)$. Using again (25) in this case, we obtain $x_1(t), y_1(t), x_2(t), y_2(t)$. It is easy to see that $\lim\limits_{t\to\pm\infty}(x_1(t), y_1(t), z_1(t)) = \lim\limits_{t\to\pm\infty}(x_2(t), y_2(t), z_2(t)) = E_M$, which finishes the proof. □

The next result regards the periodic orbit depicted in Figure 3(c).

Proposition 5.6. *Let $(h, c) = \mathcal{EC}(E_M) \in \Gamma^s$. Then the corresponding fiber contains the nonlinearly stable equilibrium point E_M and a periodic orbit $\mathcal{O}$ given by*

$$\mathcal{O}(t) = (x(t), y(t), z(t)) \ , \ t \in \mathbb{R},$$

where

$$x(t) = \frac{M^{3/2}\left(3-2M^3\right)-2\left(1-M^3\right)^{3/2}\cos q+\sin q\left(2+M^{9/2}\sin q\right)}{\sqrt{M}\left(1+M^{3/2}\sin q\right)^2}$$

$$y(t) = \frac{M^{3/2}\left(3-2M^3\right)+2\left(1-M^3\right)^{3/2}\cos q+\sin q\left(2+M^{9/2}\sin q\right)}{\sqrt{M}\left(1+M^{3/2}\sin q\right)^2}$$

$$z(t) = -\frac{1}{M} + \frac{2\left(1-M^3\right)}{M\left(1+M^{3/2}\sin q\right)},$$

with $q = q(t) = \frac{\sqrt{1-M^3}}{2M}(t - t_0)$.

Proof. As in the proof of Proposition 5.5, we obtain equation (26). Taking into account that $0 < M < 1$, we integrate this equation and get the solution $z(t)$, and then $x(t), y(t)$. The presence of the functions $\sin q(t)$ and $\cos q(t)$ shows the periodicity of the orbit. □

References

[1] V. Arnold, Conditions for nonlinear stability of stationary plane curvilinear flows on an ideal fluid, *Doklady Akademii Nauk SSSR*, **162**(5), (1965), 773–777.

[2] P. Birtea, M. Puta, Equivalence of energy methods in stability theory, *J. Math. Phys.*, **48**, (2007), 042704.

[3] P. Birtea, M. Puta, R. M. Tudoran, Periodic orbits in the case of zero eigenvalue, *C.R. Acad. Sci. Paris*, Ser. I, **344**, (2007), 779–784.

[4] T. Bînzar, C. Lăzureanu, On some dynamical and geometrical properties of the Maxwell-Bloch equations with a quadratic control, *Journal of Geometry and Physics*, **70**, (2013), 1–8.

[5] T. Bînzar, C. Lăzureanu, A Rikitake type system with one control, *Discrete and Continuous Dynamical Systems-B*, **18**(7), (2013), 1755–1776.

[6] D. D. Holm, J. E. Marsden, The rotor and the pendulum, in *Symplectic Geometry and Mathematical Physics*, Prog. Math. 99, P. Donato, C. Duval, J. Elhadad, and G. M. Tuynman, eds., Birkhäuser, Boston, Cambridge, MA, (1991), 189–203.

[7] C. Lăzureanu, On a Hamilton–Poisson approach of the Maxwell–Bloch equations with a control, *Mathematical Physics, Analysis and Geometry*, (2017), 20: 20.

[8] C. Lăzureanu, The real-valued Maxwell–Bloch equations with controls: From a Hamilton–Poisson system to a chaotic one, *International Journal of Bifurcation and Chaos*, **27**, (2017), 1750143-1–17.

[9] C. Lăzureanu, T. Bînzar, A Rikitake type system with quadratic control, *International Journal of Bifurcation and Chaos*, **22**(11), (2012), 1250274, 14 pages.

[10] C. Lăzureanu, T. Bînzar, Some geometrical properties of the Maxwell-Bloch equations with a linear control, *Proc. of the XIII-th Int. Conf. Math. App.*, Timişoara, 2012, 151–158.

[11] C. Lăzureanu, T. Bînzar, On a Hamiltonian version of controls dynamic for a drift-free left invariant control system on G_4, International Journal of Geometric Methods in Modern Physics, **9**(8), (2012) 1250065.

[12] C. Lăzureanu, T. Bînzar, Symmetries and properties of the energy-Casimir mapping in the ball-plate problem, Advances in Mathematical Physics, bf2017, (2017), 5164602.

[13] C. Lăzureanu, C. Petrişor, On the dynamics of a Hamilton-Poisson system, *Sci Bull Politehnica University of Timisoara, Transaction on Mathematics & Physics*, **63**(2), (2018), 14–28.

[14] R.M. Tudoran, A normal form of completely integrable systems, *Journal of Geometry and Physics*, **62**(5), (2012), 1167–1174.

[15] R.M. Tudoran, A. Aron, Ş. Nicoară, On a Hamiltonian Version of the Rikitake System, *SIAM Journal on Applied Dynamical Systems*, **8**(1), (2009), 454–479.

[16] R. M. Tudoran, A. Gîrban, On the Hamiltonian dynamics and geometry of the Rabinovich system, *Discrete and Continuous Dynamical Systems - B*, **15**(3), (2011), 789–823.

[17] R. M. Tudoran, A. Gîrban, On a Hamiltonian version of a three-dimensional Lotka-Volterra system, *Nonlinear Analysis: Real World Applications*, **13**, (2012), 2304–2312.

Cristian LĂZUREANU – Department of Mathematics
Politehnica University of Timişoara
Piaţa Victoriei 2, 300 006, Timişoara, România
E-mail: cristian.lazureanu@upt.ro

Jinyoung CHO – MSc student, Department of Mathematics,
Politehnica University of Timişoara
P-ta Victoriei 2, 300 006, Timişoara, România
E-mail: jinyoung.cho@student.upt.ro

BULETINUL ŞTIINŢIFIC
Al
UNIVERSITĂŢII "POLITEHNICA" DIN TIMIŞOARA
Tom 65 (79), 1 MATEMATICĂ – FIZICĂ 2020

A STATISCAL ANALYSIS OF DENTAL BRACKETS TYPES

Hazem ABBAS, Romeo NEGREA

Abstract

In paper we present a statistical analysis of a problem from real word, choose the adequate type of dental brackets for children in a dental clinic. A generalized regression model by Poisson type was used to analyzed two data group of children who use or used a dental brackets by different types. [1]

1 Introduction

Dental epidemiology involves studying and investigating the distribution and determinants of dental-related diseases in a specified population group to inform decisions in the management of health problems. In dental epidemiology studies, the hypothesis is typically followed by a cogent study design and data collection. Appropriate statistical analysis is essential to demonstrate the scientific association between the independent factors and the target variable. Analysis also helps to develop and build a statistical model. Poisson regression and its extensions have gained more attention in caries epidemiology than other working models such as logistic regression (see for example [1] , [2] ,[3])

[1]Mathematical Subject Classification (2010):*62P10, 62J12*
Keywords and phrases: *Poisson regression, generalized regression models, statistical tests*

2 Dental brackets

Dental braces (also known as brackets, orthodontic cases, or cases) are devices used in orthodontics that align and straighten teeth and help position them with regard to a person's bite, while also aiming to improve dental health. They are often used to correct underbites, as well as malocclusions, overbites, open bites, gaps, deep bites, cross bites, crooked teeth, and various other flaws of the teeth and jaw. Braces can be either cosmetic or structural. Dental braces are often used in conjunction with other orthodontic appliances to help widen the palate or jaws and to otherwise assist in shaping the teeth and jaws (see for example [4]).

Usually, the following types of dental appliances used in orthodontics are:

- Removable appliances – which can be taken out of the mouth by the patient;
- Functional appliances – which can be either removable or fixed;
- Fixed appliances – which are attached directly to the teeth.

Generally, removable appliances are used for simple tooth movement, such as individual tipping or limited expansion. They can also be used as an adjunct to fixed appliances, particularly during bite opening and molar distalization, or prior to functional appliance therapy to facilitate mandibular postural advancement. Functional appliances are used in the growing patient, often in conjunction with extra-oral force, to help correct both sagittal and vertical skeletal discrepancies, usually prior to the use of fixed appliances. Fixed appliances are the most popular form of appliance currently in use today because they can effect complex three-dimensional tooth movements in the management of many different types of malocclusion. Fixed devices can be made by different materials and it can be: aesthetic brackets or metal brackets.

2.1 Contemporary Metal Brackets

Metal brackets made from stainless steel are the most commonly used in orthodontic practice, but the color of the metal and its visibility may be objectionable to some adult patients. Manufacturers have tried to reduce the size of the bracket and hence its visibility by continuously redesigning the appliance. Another relatively recent introduction is a bracket made of titanium. A titanium bracket has the potential of working well in the small number of patients who experience nickel hypersensitivity from traditional metal brackets. Another variant of the

metal bracket is a stainless steel bracket coated with a micro-thin layer of zirconianitride to impart a gold color. Along with this bracket, gold arch wires are available to complement the color (see [4], [5]). Brackets are either routinely cast or injection-molded from stainless steel, although to reduce the chance of allergic reaction, nickel-free brackets made from titanium or cobalt chromium are now available. Bonding techniques rely on a physical interaction being established between the bracket base and an etched enamel tooth surface. Bracket bases are therefore roughened or sandblasted to improve this bond and often curved in both the horizontal and vertical planes, which aids in bracket location and seating on the tooth crown. A significant disadvantage of metallic orthodontic brackets is their poor aesthetics. bracket systems that are transparent, or more closely resemble natural tooth colour, have therefore been developed.

2.2 Plastic Brackets

The early aesthetic brackets were made of acrylic and polycarbonate, which discoloured quite rapidly and were prone to both permanent deformation and failure. To overcome these problems, plastic brackets were made in polyurethane or polycarbonate reinforced with ceramic or fibreglass fillers. Plastic brackets to be bonded directly to enamel were initially made of polycarbonate and plastic molding powder (Plexiglas). Plexiglas brackets did not last long because of their discoloration, fragility, and breakage under stress. Also, much of the energy in the wire was expended in distorting the brackets because of the poor integrity of the arch wire slot, and therefore forces were not transmitted to the tooth. In recent years there have been several improvements to reinforce plastic brackets, such as precision-made stainless steel slot inserts and ceramic material fillers (15% to 30%). Metal slot reinforcement of plastic brackets appears to strengthen the matrix adequately so that torque can be applied at the same level as with metal brackets. Ceramic-reinforced composite brackets without a metal slot insert have been shown to have fairly low frictional characteristics compared with ceramic and metal brackets .18 Hence the newly introduced ceramic-reinforced plastic brackets are suitable for clinical use because they are color stable, have lower friction,"' and have the structural integrity to transmit orthodontic forces without distorting.

2.3 Ceramic Brackets

Ceramic brackets were introduced in the 1980s and provide higher strength, more resistance to wear and deformation, better colour stability and superior aesthetics. They are manufactured from aluminium oxide and are described as either

monocrystalline or polycrystalline, depending upon whether they are made from one or many crystals. During the last decade, ceramic brackets have become the esthetic alternative to plastic brackets. The monocrystalline and polycrystalline ceramic materials used in manufacturing these brackets provide excellent color fidelity and stain resistance. However, clinicians may be inhibited from using ceramic brackets because of their reported fracture tendencies and, more importantly, their reported tendency to damage enamel during the debonding procedure. The manufacturers of these brackets have tried to improve bracket characteristics to facilitate easier debonding. These changes have included a shift from the purely chemical retention mechanism of resin bonding to the bracket base to a totally mechanical mode of bonding for the polycrystalline bracket. Investigations have found that debonding with sharp-edged pliers applies a bilateral force at the bracket base-adhesive interface and is the most effective method for debonding both polycrystalline and monocrystalline orthodontic brackets. Therefore forces applied at the interface rather than the bracket itself may prevent breakage on debonding. Brackets bonded by indirect techniques, which create a resin interlayer, facilitate debonding at the interface formed between this interlayer and the filled resin. Ceramic brackets may fracture during torsional and tipping movements, cause abrasion of opposing teeth, and have increased frictional resistance in sliding mechanics compared with plastic and metal brackets. Ceramic brackets have limitations and caution must be exercised in their use. Ceramic brackets should not be bonded to teeth that have cracks or signs of physical defects. A new design of the ceramic bracket is borrowed from the design of the metal reinforced plastic bracket. This bracket system incorporates a metal slot in the ceramic bracket, reducing the friction to levels experienced by stainless steel brackets. Another feature of this appliance is the ease of debonding via a vertical scribe line placed in the base of the bracket Despite these problems, adult patients often request ceramic brackets because of the improved aesthetics.

3 Preliminaries

3.1 Generalized linear regression models

Let $y_1, \ldots, y_n$ be a series of n observations on a characteristic Y from a statistical population. Of course, the (numerical) value y_i is only one of the possible realizations of the random variable Y_i. As we saw in the previous section, for linear models, we accept that all random variables Y_i are independent of each other and have a normal distribution of parameters the mean μ_i and the dispersion σ^2 i.e

$$Y_i \sim \mathcal{N}(\mu_i, \sigma^2)$$

and we will assume that the mean (expected) value μ_i is a linear function of k predictors that take the (numerical) values $\overline{x}_i = (x_{i1}, \ldots, x_{ik})^t$ or

$$\mu_i = \overline{x}_i \cdot \beta$$

where β is the vector of parameters (unknown).

It is known that the above model can be generalized in two stages, the first refers to the stochastic component and the second to the systematic component of the model (linear). We will describe the generalized linear model as formulated by Nelder and Wedderburn in 1972 (see [6]).

Let's assume that all the observations come from a distribution from a family of exponential distributions with the probability density function

$$f(y_i) = \exp\{\frac{y_i \cdot \theta_i - b(\theta_i)}{a_i(\phi)} + c(y_i, \phi)\} \tag{1}$$

where θ_i and ϕ are the parameters and $a_i(\phi)$, $b(\theta_i)$ and $c(y_i, \phi)$ are known functions.

The parameters θ_i and ϕ are, in essence, the location and scale parameters.

The family of exponential distributions as defined includes, as special cases, the normal distribution, the binomial distribution, the Poisson distribution, the exponential distribution, the gamma distribution and the inverse Gaussian distributions.

The second possible generalization of the linear model is based on the fact that instead of modeling the average, as before, we will introduce a transformation, i.e. a continuous, differentiable and bijective function $g(y_i)$ thus 'incåt

$$\eta_i = g(\mu_i). \tag{2}$$

The function $g(\mu_i)$ is called *link function*. Examples of related functions can be: the identical function, the inverse (hyperbolic) function, the logarithmic function, etc.

We will assume that the transformed model follows a linear model, i.e

$$\eta_i = \overline{x_i}\beta. \tag{3}$$

The quantity η_i is called *linear predictor*. Since the link function is bijective, we can invert and we get

$$\mu_i = g^{-1}(\overline{x_i}\beta). \tag{4}$$

We denote by $\hat{\mu_i}$ the values estimated (predicted) by the ω model and let $\hat{\theta}_i$ be the estimates corresponding to the canonical parameters. "similarly, we denote by $\tilde{\mu_i} = y_i$ 'and analogously $\tilde{\theta}_i$ for the canonical parameters under Ω.

The ratio criterion for comparing the two models in the family of exponential distributions is

$$-2\log\lambda = 2\sum_{i=1}^{n}\frac{y_i(\tilde{\theta}_i - \hat{\theta}_i - b(\tilde{\theta}_i) + b(\hat{\theta}_i)}{a_i(\phi)}.$$

The expression does not depend on the unknown parameters and it's called *deviation*

$$D(y,\hat{\mu}) = 2\sum_{i=1}^{n} p_i[y_i(\tilde{\theta}_i - \hat{\theta}_i) - b(\tilde{\theta}_i) + b(\hat{\theta}_i)] \tag{5}$$

The criterion of the likelihood ratio $-2\log L$ which represents the deviation divided by the scale parameter ϕ is called *scaled deviation*.

Let us return now to the comparison of two models ω_1, with p_1 parameters, and ω_2 with p_2 parameters, such that $\omega_1 \subset \omega_2$ 'and $p_2 > p_1$.

The logarithm of the ratio between the maximized likelihood functions for the two models can it is written as a difference of deviations, that is

$$-2\log\lambda = \frac{D(\omega_1) - D(\omega_2)}{\phi}. \tag{6}$$

The scale parameter is either known or estimated using a larger model ω_2.

The theory of large samples (law of large numbers) tells us that the asymptotic distribution of this criterion, under the usual regularity conditions is χ^2_ν with $\nu = p_2 - p_1$ degrees of freedom.

The problem of estimating the orders of linear models for data series was, for many mathematicians, an important object of study during the 1960s and 1970s. H. Akaike noticed that there is a similarity between choosing the number of factors in factorial analysis and determining the order of a linear model (that is, the number of predictor variables) (see [8]). . For example, in the case of a linear model, the idea of prediction is clear, but there is a problem that arises when parameters are estimated from the recorded data. In factorial analysis, the log-likelihoods are maximized and these maximizations are expected to be good models for the prediction distributions, but in this case the prediction no longer is a numerical value but a function that is estimated by the prediction distribution. The expected log-likelihood can be given by the Kullback-Leibler information.

Selecting the minimum of Kullback-Leibler information, comes back to maximizing $M_f \log g(y)$.

We considered n observations of some i.i.d. random variables. $y_1, \ldots, y_n$ having an unknown probability density $f(y)$. We assume that we have a lot of alternative or candidate models of the type $g_m(.|\theta_m),\ m = 1, 2, \ldots, M$, where θ_m is the vector of density parameters g_m. We will want to estimate $I(f, g_m(.|\theta_m))$. We assume that the parameter vector θ_m is known. Then, from the law of large numbers, we have

$$M_f \log g_m(y|\theta_m) = \int_{-\infty}^{\infty} f(y) \log g_m(y|\theta_m) dy = \frac{1}{N} \sum_{n=1}^{N} \log g_m(y_n|\theta_m). \qquad (7)$$

The vector of parameters θ_m for the densities $g_m(.|\theta_m)$ is unknown 'in practice'. Parameters must be estimated from the data and under the assumption that the model $g_m(|\theta_m)$ has been chosen. It is natural to use the maximum likelihood estimator $\hat{\theta}_m$ which maximizes the right member of (2.15). In this case, the law of large numbers no longer occurs when the vector of parameters is replaced with its estimates in the sense of maximum likelihood. so,

$$M\ M_f \log g_m(y|\hat{\theta}_m) \neq \frac{1}{N} M \sum_{n=1}^{N} \log g_m(y_n \hat{\theta}_m). \qquad (8)$$

This happens because the same set of data was used twice, for parameter estimation and for log-likelihood estimation

The log-likelihood estimator in the case above is a shifted estimator. This displacement (bias) is approximately equal to the number of parameters estimated in the model. An approximate correction for this bias is given in the definition of Akaike's estimator denoted by AIC (*Akaike's Informational Criterion*):

$$\text{AIC}(g) = -2(\text{log-maximum likelihood of the model}) +$$

$$+2(\text{the number of estimated parameters of the model}) =$$

$$= -2 \sum_{n=1}^{N} \log g_m(y_n|\hat{\theta}_m) + 2|\hat{\theta}_m|$$

where $|.|$ represents the cardinality of the estimated parameters in the model.

3.2 Poisson regression model

A random variable Y is said to have a Poisson distribution with parameter μ if a takes integer values $y = 0, 1, 2 \ldots$ with the probability

$$Pr[Y = y] = \frac{e^{-\mu}\mu^y}{y!} \tag{9}$$

for $\mu > 0$. The mean and variance are

$$M(Y) = Var(Y) = \mu$$

Since the mean is equal to the variance, any factor that affects one will affect the other. In other words, the usual assumption of homoscedasticity (equal variance) is not "fulfilled". for data with Poisson error (see [7]).

Suppose we have a sample with n observations $y_1, y_2, \ldots y_n$ which can be treated as realizations of independent Poisson random variables, with $Y_i \sim P(\mu_i)$, and suppose that we want the mean (and, therefore, the variance!) to depend on a vector of explanatory variables $\overline{x}_i$.

We could consider a simple linear shape model

$$\mu_i = \overline{x}_i \, \beta$$

but this model has the disadvantage that the linear predictor on the right can take any real value, while the Poisson mean on the left representing has a number of expectations, it must be non-negative.

A simple solution to this problem is to model the logarithm of the mean using a linear model. Thus, we calculated $\eta_i = \log(\mu_i)$ 'and we assume that the mean value of the transformation follows a linear model $\eta_i = \beta \ \overline{x}_i$. Thus, we will consider a generalized linear model with a (natural) logarithmic link function. Combine these two steps and we can write the log-linear model as

$$\log(\mu_i) = \overline{x}_i \, \beta. \tag{10}$$

We apply the exponential function to equation (4.2) and obtain a multiplicative model for the average:

$$\mu_i = \exp[\beta \ \overline{x}_i]$$

A measure of the discrepancy between the observed and estimated values is the statistical deviation. It is shown that for the Poisson responses the deviation is ia form

$$D = 2 \sum \{ y_i \log(\frac{y_i}{\hat{\mu}_i} - (y_i - \hat{\mu}_i) \}$$

The first term is identical to the binomial deviation. The second term, a sum of the differences between the observed and estimated values, is usually zero,

because the maximum likelihood estimates in Poisson models have the property of reproducing the marginal distributions.

For large samples, the distribution of the deviation is approximately χ^2 with $n - p$ degrees of freedom, where n is the number of observations and p is the number of parameters.

4 Methods and results

4.1 Methods

In this descriptive study, the dental data of two groups of children with dental apparatus, the first group with "in use" brackets and the second groups "out use", i.e. children who have used a dental brackets. In both groups, the children were randomly selected from a list of of patients from a dental clinic. Overall, 665 samples were selected and their data for dental brackets was evaluated, 330 in the first group and 335 for the second group.

The response variable (denoted with Y_a and respectively Y_b) represent the type of dental brackets and the predictor variables were the age and the sex of patients (denoted with $X1\_a$ and $X2\_a$ and respectively $X1\_b$ and $X2\_b$).

In the first step, it was analyzed, using appropriate statistical tests, if there are significant statistical differences between the two groups. More precisely, the F-test (to check the equality in the variance) and the t-test (for the equality in the mean) were applied.

The next step, the generalized Poisson regression model was applied for the two predictors in both groups.

The last step consisted in optimizing the number of predictors using the "backward" selection procedure. Data analysis was performed using the R software (4.2.0).

4.2 Results

A primary descriptive statistics was made for the both groups. For the first group they are 8 types of dental brackets : "metalic clasic", "damon metalic", "safir", "damon clear", "aparat mobil" (i.e. mobile brackets) ,"genius", "metalic+safir" The simple histogram is represented in Graph 1.

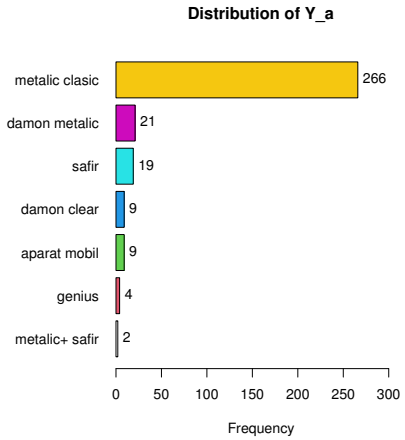

Figure 1: Distribution of brackets types for the first group

In analogous way, for the second group, where we have just 6 types, "metalic clasic", "safir", "damon metalic", "damon clear", "metalic+safir", "genius", the histogram is presented in Graph 2.

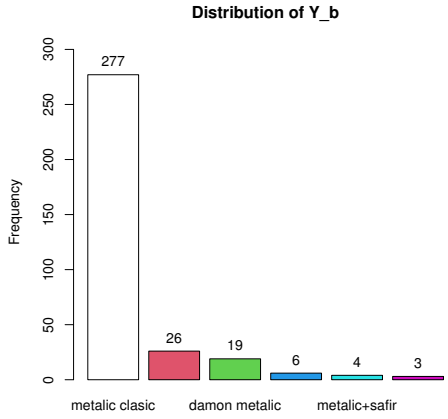

Figure 2: Distribution of brackets types for the second group

Using, successively, the F-test and the t-test, it was obtained that there are statistically significant differences between the two groups. Furthermore, the analysis using the regression method was performed separately, on each group of data (see Table 1 and Table 2, respectively).

Table 1: Results form F-test for comparison of the groups.

F test to compare two variances	
data:	Y_a and Y_b
F = 1.6683, num df = 329, denom df = 334,	p-value = 3.594e-06
alternative hypothesis:	true ratio of variances is not equal to 1
95 percent confidence interval:	(1.344735, 2.069989)
sample estimates:	ratio of variances 1.668261

Table 2: Results form t-test for comparison of the groups.

Welch Two Sample t-test	
data:	Y_a and Y_b
t = 1.6449, df = 619.49,	p-value = 0.1005
alternative hypothesis:	true difference in means is not equal to 0
95 percent confidence interval:	(-0.02507669, 0.28378315)
mean of x 1.466667	mean of y 1.337313

Because, the both statistical test suggest a statistical difference between these two groups, we will make the regression analyze for the each data groups.

Table 3: Statistical details on the Poisson regression with both predictors.

glm(formula = Y_a ∼ X1_a + X2_a, family = poisson)				
Deviance Residuals:				
Min	1Q	Median	3Q	Max
-1.2272	-0.3640	-0.3040	-0.2205	2.9523
Coefficients:				
	Estimate	Std. Error	z value	Pr(> |z|)
(Intercept)	0.026840	0.189632	0.142	0.887
X1_a	0.026091	0.005944	4.389	1.14e-05 ***
X2_a	-0.076660	0.092703	-0.827	0.408
Signif. codes: 0 ‘***’ 0.001 ‘**’ 0.01 ‘*’ 0.05 ‘.’ 0.1 ‘ ’ 1				
(Dispersion parameter for poisson family taken to be 1)				
Null deviance: 197.88 on 329 degrees of freedom				
Residual deviance: 180.04 on 327 degrees of freedom				
AIC: 912.73 Number of Fisher Scoring iterations: 5				

First, we consider the Poisson regression model with both predictor variables, i.e. X1=Age (as a normal random variable) and X2=Sex (as binary random variable with two states "M" and "F" transformed in "1" and "2") for each data group (we denote as X1_a and X2_a for group 1, respectively, X1_b and X2_b for the group 2). The response variable is considered as categorial variable following a Poisson distribution

(because de statistical mean value and variance value are almost the same , 1.466667 and 1.28308 for the first group and 1.337313 and 0.9691125 for the second group).

The results for the first group are presented in the Table 3.

Some detail about statistics indicators from above table.

- Coefficients and P-Values
  The coefficient estimate in the output indicate the average change in the log odds of the response variable associated with a one unit increase in each predictor variable.
  The standard error gives us an idea of the variability associated with the coefficient estimate. We then divide the coefficient estimate by the standard error to obtain a z value.
  The p-value $\Pr(> |z|)$ tells us the probability associated with a particular z value. This essentially tells us how well each predictor variable is able to predict the value of the response variable in the model.
- Null and Residual Deviance
  The null deviance in the output tells us how well the response variable can be predicted by a model with only an intercept term.
  The residual deviance tells us how well the response variable can be predicted by the specific model that we fit with p predictor variables. The lower the value, the better the model is able to predict the value of the response variable.
  To determine if a model is "useful" we can compute the Chi-Square statistic as: X^2 = Null deviance – Residual deviance with k degrees of freedom.
  We can then find the p-value associated with this Chi-Square statistic. The lower the p-value, the better the model is able to fit the dataset compared to a model with just an intercept term.
- AIC
  The Akaike information criterion (AIC) is a metric that is used to compare the fit of different regression models. The lower the value, the better the regression model is able to fit the data.

We observe that the predictor X2_a doesn't pass the z-test (the P-value is grater than alphs=0.05, i.e. there is a great probability such that the coefficient to be null from the statistical point of view), therefore, following the backward selection procedure, we can consider the regression model just with a single predictor, X1_a. The results are presented in the Table 4.

Table 4: Statistical details on the Poisson regression with a single predictor (Age).

glm(formula = Y_a ∼ X1_a, family = poisson)				
Deviance Residuals:				
Min	1Q	Median	3Q	Max
-1.1568	-0.3689	-0.3109	-0.2539	3.0215
Coefficients:				
	Estimate	Std. Error	z value	Pr(> |z|)
(Intercept)	-0.09393	0.12229	-0.768	0.442
X1_a	0.02597	0.00596	4.357	1.32e-05 ***
Signif. codes: 0 '***' 0.001 '**' 0.01 '*' 0.05 '.' 0.1 ' ' 1				
(Dispersion parameter for poisson family taken to be 1)				
Null deviance: 197.88 on 329 degrees of freedom Residual deviance: 180.72 on 328 degrees of freedom AIC: 911.41 Number of Fisher Scoring iterations: 5				

We can see that the intercept coefficient doesn't pass the z-test. Therefore we, consider the model with without intercept (this it is possible because we cannot put a dental bracket for a child of zero age). In the Table 5, is presented the statistical results for this model.

Table 5: Statistical details on the Poisson regression without intercept.

glm(formula = Y_a ∼ -1 + X1_a, family = poisson)				
Deviance Residuals:				
Min	1Q	Median	3Q	Max
-1.0428	-0.3927	-0.3439	-0.2958	2.9614
Coefficients:				
	Estimate	Std. Error	z value	Pr(> |z|)
X1_a	0.021682	0.002233	9.709	<2e-16 ***
Signif. codes: 0 '***' 0.001 '**' 0.01 '*' 0.05 '.' 0.1 ' ' 1				
(Dispersion parameter for poisson family taken to be 1) Null deviance: 260.62 on 330 degrees of freedom Residual deviance: 181.31 on 329 degrees of freedom AIC: 910 Number of Fisher Scoring iterations: 5				

We can observe that this model is very good and the predictor "age" it is essential for the choosing of dental bracket of a child. In fact the model give as the parameter for Poisson distribution, i.e. mean value

$$\mu = e^{0.021682 * \text{age}}$$

and with this value we can compute the probability to choose the k type from the

set of 8 types, using the formula

$$P(Y = y) = \frac{e^{-\mu}\mu^{y}}{y!}, \;\; y = 0, 1, \ldots, 7$$

In an analogous way, we analyse the data from the second group. The statistical results are given in Table 6 (the Poisson regression model with both predictors), Table 7 (regression with a single predictor after the optimization using the backward selection procedure). We observe that for this group, the intercept coefficient pass the t-test.

Table 6: Statistical details on the Poisson regression with both predictors, for the second group.

glm(formula = Y_b ∼ X1_b + X2_b, family = poisson)				
Deviance Residuals:				
Min	1Q	Median	3Q	Max
-1.4534	-0.2302	-0.1423	-0.0816	3.1830
Coefficients:				
	Estimate	Std. Error	z value	Pr(> |z|)
(Intercept)	-0.541685	0.203198	-2.666	0.00768 **
X1_b	0.041367	0.006065	6.821	9.04e-12 ***
X2_b	0.030077	0.102890	0.292	0.77004
Signif. codes: 0 ‘***’ 0.001 ‘**’ 0.01 ‘*’ 0.05 ‘.’ 0.1 ‘ ’ 1				
(Dispersion parameter for poisson family taken to be 1)				
Null deviance: 132.32 on 334 degrees of freedom Residual deviance: 93.14 on 332 degrees of freedom AIC: 822.43 Number of Fisher Scoring iterations: 4				

Table 7: Statistical details on the Poisson regression with a single predictors (Age), for the second group.

glm(formula = Y_b ∼ X2_b, family = poisson)				
Deviance Residuals:				
Min	1Q	Median	3Q	Max
-1.4518	-0.2192	-0.1311	-0.0879	3.1993
Coefficients:				
	Estimate	Std. Error	z value	Pr(> |z|)
(Intercept)	-0.495886	0.128849	-3.849	0.000119 ***
X2_b	0.041611	0.006008	6.925	4.35e-12 ***
Signif. codes: 0 ‘***’ 0.001 ‘**’ 0.01 ‘*’ 0.05 ‘.’ 0.1 ‘ ’ 1				
(Dispersion parameter for poisson family taken to be 1)				
Null deviance: 132.318 on 334 degrees of freedom Residual deviance: 93.226 on 333 degrees of freedom AIC: 820.52 Number of Fisher Scoring iterations: 4				

We can observe that this model is very good and the predictor "age" was essential for the choosing of dental bracket of a child. In this case the formula for

Poisson parameter it is

$$\mu = e^{-0.495886+0.041611*\text{age}}$$

and with this value we can compute the probability to choose the k type from the set of 6 types, using the formula

$$P(Y = y) = \frac{e^{-\mu}\mu^y}{y!}, \;\; y = 0, 1, \ldots, 5$$

5 Conclusions

We study the relation for the types of dental brackets and some records from patients files. A generalized regression model by Poisson type was proposed, based data from two different groups. In both cases, the mean value of the Poisson distribution depend by a single predictor – Age. These results are supported by dentists who note that the age of children is important for their teeth to support a certain type of bracket material. Our results give a simple computation for the probability of choosing a certain type of bracket based on the age of the children. Of course, there exists a little difference between the new group ("in use") and, somehow, the old group ("out of use") because there is a continuous development of new materials and new types for the dental brackets.

References

[1] Alex Man Him Chau Edward Chin Man Lo May Chun Mei Wong Chun Hung Chu, Interpreting Poisson Regression Models in Dental Caries Studies, *Caries Research*, Vol.52, 339—345 (2018).

[2] Maryam Taher, Mehdi Rahgozar , Enayatollah Bakhshi, Zahra Ghanbri, Reza Seraj, Application of the Poisson Regression Model with Zero Accumulation in the Analysis of Dental Data in 12- and 13-year-old adolescents, *Journal of Health Promotion Management*, Vol. 7 (1) (2018)

[3] Solinas G, Campus G, Maida C, Sotgiu G, Cagetti MG, Lesaffre E, Castiglia P. What statistical method should be used to evaluate risk factors associated with dmfs index? Evidence from the National Pathfinder Survey of 4-year-old Italian children, *Community Dent Oral Epidemiol*, Vol. 37, 539—546 (2009).

[4] Cobourne, M și DiBase, A. Handbook of Orthodontics, Elsevier (2016).

[5] Bishara, S. Textbook of Orthodontics, Saunders Company, (2001).

[6] J. A. Nelder, R. W. M. Wedderburn, Generalized Linear Models, *Journal of the Royal Statistical Society: Series A (General)*, Vol. 135 (3), 1972.

[7] McCullagh, P. and Nelder, J.A., Generalized Linear Models. 2nd Edition, Chapman and Hall, London (1989) http://dx.doi.org/10.1007/978-1-4899-3242-6

[8] Akaike, H. (1974), A new look at the statistical model identification, *IEEE Transactions on Automatic Control*, Vol. 19 (6), 716–723, (1974).

Hasem ABBAS, Master student
Casa Denti–Dental Clinic
Str. Aurelianus 5A, 300551, Timişoara, România
E-mail: hazem6070@gmail.com

Romeo NEGREA
Department of Mathematics
Politehnica University of Timişoara
P-ta Victoriei 2, 300006, Timişoara, România
E-mail: romeo.negrea@upt.ro

BULETINUL ŞTIINŢIFIC
Al
UNIVERSITĂŢII "POLITEHNICA" DIN TIMIŞOARA

Tom 65 (79), 1	MATEMATICĂ – FIZICĂ	2020

A SPRAY THEORY FOR THE GEOMETRIC METHOD IN HYDRODYNAMICS

Emanuel-Ciprian CISMAŞ

Abstract

We present a brief spray theory necessary for the geometric method in hydrodynamics and shape analysis. We make use of the convenient calculus to complete a unitary approach started by P. Michor and A. Kriegl.[1]

1 Introduction

The main goal of this article is to fix the lack o rigorousness in a few papers involving infinite dimensional Lie groups. For infinite dimensional Lie groups we have to do the things the right way: the "convenient way".

We will study infinite dimensional manifolds modelled on locally convex spaces. As is well-known, beyond Banach spaces a lot of pathologies occur: ordinary differential equations may not have solutions or the solutions may not be unique, there is no genuine inverse function theorem, there is no natural topology for the dual space and none of the candidates is metrizable. All these problems oblige us to handle carefully the geometric objects related to an infinite dimensional Fréchet manifold. There was a common belief between mathematicians that for infinite dimensional calculus each serious application needs its own foundation until 1982 when A. Frölicher and A. Kriegl presented independently the solution to the question regarding the right differential calculus in infinite dimension: *the convenient calculus*. P. Michor and A. Kriegl laid afterwards the foundations of

[1]2020 Mathematics Subject Classification. Primary: 22E65; Secondary: 58D05, 58B25, 35Q35.
Key words and phrases. Euler-Poincaré equations, diffeomoprhism group of the circle.
The first author is supported by NSF grant xx-xxxx.

the infinite dimensional differential geometry and brought everything together in their seminal book [30].

Twenty years before, in his influential article [1], V. Arnold had the idea to analyze the motion of hydrodynamical systems using geodesic flows. Actually he showed that the Euler equations of hydrodynamics can be recast as geodesic equations of a right-invariant Riemannian metric on the group of volume-preserving diffeomorphisms. Nowadays, similar methods are used in shape analysis [40]. This approach became the so called *geometric method in hydrodynamics* (see [15] for more details) and involves the use of geometric arguments to study issues like well-posedness or stability.

For example, the Camassa-Holm equation

$$u_t - u_{txx} = 2u_x u_{xx} + uu_{xxx} - 3uu_x$$

describes the geodesic flow on the group $\mathrm{Diff}^\infty_+(\mathbb{S}^1)$ of orientation-preserving diffeomorphisms of the circle. The right-invariant metric considered is obtained by right-translations from the inner product

$$\langle u, v\rangle = \int_{\mathbb{S}^1} uv + u_x v_x \, dx, \quad u, v \in T_{id}\mathrm{Diff}^\infty_+(\mathbb{S}^1),$$

One can observe that the differential operator $A = I - D^2$, called *inertia operator* in this context, generates the inner product by

$$\langle u, v\rangle = \int_{\mathbb{S}^1} u \cdot Av \, dx.$$

There is a high flexibility of this method given by the choice of an inertia operator or by the choice of an algebraic structure, usually involving diffeomorphism groups. In the last decade different inertia operators were studied starting with differential operators with constant coefficients [10], Hilbert transforms [14, 41] or Fourier multipliers [4, 13] and even pseudo-differential operators [7]. Among the algebraic structures studied one should mention homogeneous spaces [27], the Bott-Virasoro group [31], semi-direct products between a group and a vector space [23, 42] or semidirect products between two groups [6, 7].

The idea behind this geometric approach, initially developed by D.Ebin and J. Marsden in [12], is to use the right-invariance of the geodesic spray to obtain, via a "no gain, no loss" result (see [15] for details) a Cauchy-Lipschitz type theorem on a Fréchet space. Using this method we avoid the Nash-Moser schemes in order to obtain well-posedness in the smooth category. To formulate an inverse function theorem for Fréchet spaces we have to restrict to the category of tame Fréchet spaces, in the sense of R.S. Hamilton [20]. For example, the results obtained for $H^\infty(\mathbb{R}^d, \mathbb{R}^d)$ in [4], with geometric arguments, can not be obtained with a classical Nash-Moser approach, since $H^\infty(\mathbb{R}^d, \mathbb{R}^d)$ is no longer a tame space.

The article of V. Arnold is not rigorous enough for the infinite dimensional case. Most of the research work influenced by [1] uses the concept of Gâteaux smoothness. This concept of smoothness can be satisfactory for some problems but it is not the appropriate one to use in manipulating vector bundles or differential forms. The convenient smoothness defined below fixes this problem. In [31] and [30] the authors started to present a solid foundation of the aforementioned geometric method in hydrodynamics. There is still a missing piece: an introduction via convenient calculus of the geodesic spray theory. Thus, in Section 6, we will add the last piece of the puzzle.

2 Notations

In this article we will use the following notations:

- the letters $\mathbb{E}$, $\mathbb{F}$, $\mathbb{G}$ will be used to denote vector spaces.
- (spaces of linear mappings) $\mathrm{L}(\mathbb{E},\mathbb{F})$ denotes the space of linear and bounded mappings that in general do not coincide with the space $\mathcal{L}(\mathbb{E},\mathbb{F})$ of linear and continuous mappings, since $\mathbb{E}$ and $\mathbb{F}$ might not be bornological spaces.
- (dual spaces) because sometimes we work with locally convex spaces which may not be bornological we have two notions for the dual of a locally convex space $\mathbb{E}$: the bornological dual, denoted $\mathbb{E}'$, i.e. the set of all bounded linear functionals $f:\mathbb{E}\to\mathbb{R}$, and the topological dual, denoted $\mathbb{E}^*$, which is the set of all continuous linear functionals.
- (multiple derivatives) since we discuss different differentiability concepts we denote with Df the Fréchet derivative, with ∂f the Gâteaux derivative, and with df the derivative in the convenient setting.
- G is a Lie group, $\mathfrak{g}$ its Lie algebra and κ^r is the right Maurer-Cartan form.
- (different objects) for elements in $\mathfrak{g}$, or in some modelling space $\mathbb{E}$, we use small letters like u,v or x,y, for vector fields greek letters ξ,η, and for second order vector fields capital letters like X,Y.
- (too many r's) $\mathcal{R}$ is the bornological isomorphism between the convenient vector spaces $C^\infty(G,\mathfrak{g})$ and $\Gamma(TG)$ and R_g are the right translations on TG, the tangent mappings of $r_g(h):=hg$, for $g,h\in G$.
- if A,B,C are sets for two mappings $f:A\to C^B$ and $g:A\times B\to C$ one can define the cannonically attached mappings, sometimes called adjoint mappings:

$$f^\wedge:A\times B\to C,\quad f^\wedge(a,b):=f(a)(b),\ \ a\in A,b\in B,$$

$$g^\vee:A\to C^B,\quad g^\vee(a):=g(a,\cdot),\ \ a\in A.$$

3 Smooth differentiable mappings

To discuss about a smooth structure of an infinite dimensional topological manifold we need a notion of differentiability between Fréchet spaces. In Banach spaces we have a notion of differentiability, called *Fréchet differentiability*, which permits us to extend the differential calculus from finite dimension to infinite dimensional Banach spaces.

Definition 3.1. *Let $\mathbb{E}, \mathbb{F}$ be Banach spaces, and U an open subset of $\mathbb{E}$. A mapping f is said to be differentiable at a point $x \in U$, if there is an element $A_x \in \mathcal{L}(\mathbb{E}, \mathbb{F})$ such that*

$$\lim_{h \to 0} \frac{\|f(x+h) - f(x) - A_x(h)\|}{\|h\|} = 0.$$

In this way f can be approximated locally by an affine mapping generated by the linear mapping A_x, usually denoted by $D_x f$. If f is differentiable at every point $x \in U$, then Df can be regarded as a mapping of U into $\mathcal{L}(\mathbb{E}, \mathbb{F})$, and f is a C^1 differentiable mapping if and only if Df is continuous. Since $\mathcal{L}(\mathbb{E}, \mathbb{F})$ is a Banach space, a C^k differentiable mapping can be defined inductively.

When $\mathbb{E}, \mathbb{F}$ are non-normable Fréchet spaces we have to cope with the following phenomenon, namely the composition

$$\circ : \mathcal{L}(\mathbb{F}, \mathbb{G}) \times \mathcal{L}(\mathbb{E}, \mathbb{F}) \to \mathcal{L}(\mathbb{E}, \mathbb{G})$$

is not continuous for any locally convex topology which can endow the space of linear mappings, excepting the case when all the spaces are Banach. If we define a concept of smoothness that uses the continuity of the mapping

$$Df : U \to \mathcal{L}(\mathbb{E}, \mathbb{F})$$

the concept will not be conserved by compositions, i.e. there will be no chain rule. For a discussion on this topic one can consult [3] or [30].

The most used concept of smoothness for infinite dimensional manifolds, modelled on locally convex topological vector spaces, see [20, 32, 35, 37], avoids the topology of $\mathcal{L}(\mathbb{E}, \mathbb{F})$, using the product topology of $\mathbb{E} \times \mathbb{F}$ instead.

Definition 3.2. *Let $f : U \subseteq \mathbb{E} \to \mathbb{F}$ be a mapping between Fréchet spaces, where U is an open subset in $\mathbb{E}$. We say that f is Gâteaux differentiable at $x \in U$ in the direction $h \in \mathbb{E}$ if the following limit exists*

$$\partial_x f(h) := \lim_{t \to 0} \frac{f(x+th) - f(x)}{t}.$$

We say that f is C^1-Gâteaux differentiable on U if f is continuous, the limit exists for all $x \in U$ and $h \in \mathbb{E}$, and $\partial f : U \times \mathbb{E} \to \mathbb{F}$ is continuous relative to the product

topology. Inductively we define the C^k-Gâteaux differentiable mappings for $k \geq 2$, and the Gâteaux smooth mappings.

This notion of differentiability is weaker even in the context of Banach spaces, where C^{k+1}-Gâteaux differentiability implies C^k-Fréchet differentiability, but the classes of smooth mappings coincide. There is no need for the spaces to be Fréchet, one can use locally convex topological vector spaces in the above definition, but we are focused on our goal: the smooth Fréchet manifolds. This concept of C^k-Gâteaux differentiable mappings coincides with those of C^1_{MB}-mappings in the sense of Michal-Bastiani [3, 29] or C^k_c-mappings in the sense of Keller [21]. Using this differentiability concept one can introduce a smooth Fréchet manifold, as in [20].

Definition 3.3. *A smooth Fréchet manifold is a Hausdorff topological space with an atlas of coordinate charts taking their value in Fréchet spaces, such that the coordinate transition functions are all Gâteaux smooth mappings between Fréchet spaces.*

Although this definition is the most popular one, it raises serious barriers when one tries to define some elementary geometric objects, e.g. differential forms. Of course, there are attempts in this field to use a stronger notion of differentiability, see [34] for example, but most of them seem to fail in having serious applications in infinite dimensional differential geometry. To be able to do some decent analysis one has to consider smooth Fréchet manifolds as particular cases of a more general notion: the *smooth convenient manifolds.*

J. Boman had in [5] the idea to test the smoothness along smooth curves: a mapping f from $\mathbb{R}^d$ to $\mathbb{R}$ is smooth if and only if it sends smooth curves $u \in C^\infty(\mathbb{R}, \mathbb{R}^d)$ into smooth curves $f \circ u \in C^\infty(\mathbb{R}, \mathbb{R})$. This concept was extended to mappings between locally convex spaces by A. Frölicher and A. Kriegl and it will agree in the case of Fréchet spaces with most of the smoothness notions already defined there. One can consult [2, 21] for a comparison between different differentiability concepts for locally convex spaces. Thus, in [17], the authors constructed the so called convenient calculus for locally convex topological vector spaces. In this context the k-fold differentiability is defined directly as well as infinite differentiability and one can avoid the topology of the space $\mathcal{L}(\mathbb{E}, \mathbb{F})$. The remaining of this section is devoted to introducing the notion of convenient smoothness. We will explain why this notion coincides with the Gâteaux smoothness in the case of Fréchet manifolds.

For locally convex topological vector space $\mathbb{E}$ we call the final topology with respect to all smooth curves $c \in C^\infty(\mathbb{R}, \mathbb{E})$, the *$c^\infty$-topology.*

Definition 3.4. *A subset $U \subseteq \mathbb{E}$ is called c^∞-open iff $c^{-1}(U)$ is open in $\mathbb{R}$ for all $c \in C^\infty(\mathbb{R}, \mathbb{E})$, and we denote by $c^\infty\mathbb{E}$ the space $\mathbb{E}$ equiped with this topology.*

In other words the c^∞-topology is the finest topology on $\mathbb{E}$ such that all the smooth curves $c : \mathbb{R} \to \mathbb{E}$ become continuous. If $\mathbb{E}$ is a Fréchet space then the c^∞-topology coincides with the given locally convex topology, according to [30], but in general the c^∞-topology is finer than any locally convex topology with the same bounded sets. The space $c^\infty\mathbb{E}$ is not a topological vector space in general.

In a locally convex space $\mathbb{E}$ a curve $c{:}\mathbb{R} \to \mathbb{E}$ is called smooth if all its derivatives exist and are continuous. The smoothness of the curves does not depend on the topology given on $\mathbb{E}$, in the sense that for all topologies leading to the same dual we have the same family of smooth curves. In fact it depends only on the family of bounded sets, the *bornology* of $\mathbb{E}$, see the Appendix.

Definition 3.5. *Let $\mathbb{E}, \mathbb{F}$ be locally convex spaces, a mapping $f : U \subseteq \mathbb{E} \to \mathbb{F}$ defined on a c^∞-open subset U it is called convenient smooth if it maps smooth curves in U into smooth curves in $\mathbb{F}$.*

With this concept of smoothness there exist convenient smooth mappings which are not continuous, but all the convenient smooth mappings are continuous relative to the c^∞-topology, according to [17, 30]. The Gâteaux smoothness will imply convenient smoothness but not conversely. Anyway, on Fréchet spaces the two notions coincide.

Proposition 3.6. *Let $\mathbb{E}, \mathbb{F}$ be Fréchet spaces and $U \subseteq \mathbb{E}$ a c^∞-open subset, then U is open and the mapping $f : U \subseteq \mathbb{E} \to \mathbb{F}$ is Gâteaux smooth if and only if it is convenient smooth.*

Proof. As we mentioned before in the case of a Fréchet space $c^\infty\mathbb{E} = \mathbb{E}$ and thus U is open for the given topology on $\mathbb{E}$. If f is Gâteaux smooth then one can easily see that $f \circ c$ will be Gâteaux smooth for all smooth curves $c \in C^\infty(\mathbb{R}, \mathbb{E})$, thus f is convenient smooth. We denote by $d_x f$ the derivative of a convenient smooth mapping as in the Appendix. If f is smooth in the convenient sense then, by Proposition A.8 in the Appendix, the mapping $df : U \to \mathrm{L}(\mathbb{E}, \mathbb{F})$ exists and is convenient smooth. Here $\mathrm{L}(\mathbb{E}, \mathbb{F})$ denotes the space of bounded (not necessarily continuous) linear mappings between convenient vector spaces. See the Apppendix for the definition of a convenient vector space. The cartesian closedness property, Proposition A.9, implies that $\partial f := df : U \times \mathbb{E} \to \mathbb{F}$ is convenient smooth, thus continuous relative to the c^∞- topologies, which coincide here with the given topologies on $\mathbb{E}, \mathbb{F}$. □

Remark 3.7. *This notion of convenient smoothness or Boman smoothness can substitute the most used notion of smoothness for Fréchet spaces and implicitly for smooth Fréchet manifolds.*

4 Convenient manifolds. Regular Lie groups

Let us introduce now the geometric objects we will need. In order to do that we follow closely [30]:

Definition 4.1. *(Convenient manifolds) A chart $(\mathcal{U}, \varphi)$ on a set M is a bijection $\varphi : \mathcal{U} \to U \subseteq \mathbb{E}_{\mathcal{U}}$ from a subset $\mathcal{U} \subseteq M$ onto a c^∞-open subset U of a convenient vector space $\mathbb{E}_{\mathcal{U}}$. For two charts $(\mathcal{U}_\alpha, \varphi_\alpha)$ and $(\mathcal{U}_\beta, \varphi_\beta)$ on M the mapping*

$$\varphi_{_{\alpha\beta}} := \varphi_\alpha \circ \varphi_\beta^{-1} : \varphi_\beta(\mathcal{U}_\alpha \cap \mathcal{U}_\beta) \to \varphi_\alpha(\mathcal{U}_\alpha \cap \mathcal{U}_\beta)$$

is called the transition mapping. A family $(\mathcal{U}_\alpha, \varphi_\alpha)_{\alpha \in A}$ of charts on M is called an atlas for M, if the sets α form a cover of M and all transition mappings are defined on c^∞-open subsets.

An atlas for M is called smooth if all transition mappings $\varphi_{\alpha\beta}$ are convenient smooth. Two smooth atlases are called smooth-equivalent if their union is again a smooth atlas. An equivalence class of smooth atlases is a smooth structure for M. A smooth convenient manifold M is a set together with a smooth structure on it.

The isomorphism type of the modelling spaces $\mathbb{E}_{\mathcal{U}}$ is constant on the connected components of the manifold M, since the derivative of the chart changings are linear isomorphisms. The manifold $\mathrm{Diff}^\infty_+(\mathbb{S}^1)$, considered as an example in this article, is a connected manifold. Since we are focused only in offering a theoretical background for the Euler-Poincaré-Arnold equations, we are entitled to consider $\mathbb{E}_{\mathcal{U}} = \mathbb{E}$ in some of our reasonings to avoid further technicalities. In the case of manifolds modelled on Fréchet spaces the above definition coincides with the one presented before.

Definition 4.2. *A mapping $f : M \to N$ between convenient smooth manifolds is called convenient smooth if for each $p \in M$ and each chart $(\mathcal{V}_\beta, \psi_\beta)$ on N, with $f(p) \in \mathcal{V}_\beta$ there is a chart $(\mathcal{U}_\alpha, \varphi_\alpha)$ on M with $p \in \mathcal{U}_\alpha$, $f(\mathcal{U}_\alpha) \subseteq \mathcal{V}_\beta$ and the local representative $\psi_\beta \circ f \circ \varphi_\alpha^{-1}$ is convenient smooth. This is the case if and only if $f \circ c$ is a smooth curve on M for each smooth curve $c : \mathbb{R} \to M$.*

Definition 4.3. *A convenient smooth Lie group G is a convenient smooth manifold and a group such that the multiplication $m_G : G \times G \to G$ and the inversion $i_G : G \to G$ are convenient smooth.*

The conjugation mapping $c_g(x) := gxg^{-1}$ generates the adjoint representation of the Lie group G

$$\mathrm{Ad} : G \to GL(\mathfrak{g}) \subset L(\mathfrak{g}, \mathfrak{g}),$$

considered as a convenient smooth mapping into $L(\mathfrak{g},\mathfrak{g})$. In this way it makes sense to define the ajoint representation of the Lie algebra $\mathfrak{g}$ as

$$\mathrm{ad} := T_e \,\mathrm{Ad} : \mathfrak{g} \to \mathfrak{gl}(\mathfrak{g}) = L(\mathfrak{g},\mathfrak{g}).$$

In the particular case $G = \mathrm{Diff}^\infty_+(\mathbb{S}^1)$, the group of orientation-preserving diffeomorphisms of the circle, its Lie algebra is $\mathfrak{g} = \mathrm{C}^\infty(\mathbb{S}^1)$ the vector space of smooth real functions on the circle. The adjoint representation of $\mathfrak{g} = \mathrm{C}^\infty(\mathbb{S}^1)$ is given by

$$\mathrm{ad}_u\, v = -[u,v] = u_x v - v_x u, \quad u, v \in \mathrm{C}^\infty(\mathbb{S}^1). \tag{4.1}$$

For an infinite dimensional Lie group the Lie exponential mapping may not exist or may not be smooth. An attempt to find a condition which ensures both these properties led to the notion of regular Lie groups, introduced by J. Milnor [32].

Definition 4.4. *A convenient smooth Lie group is called regular if for every curve $u \in \mathrm{C}^\infty(\mathbb{R},\mathfrak{g})$ there exists a curve $g \in \mathrm{C}^\infty(\mathbb{R},G)$ such that*

$$\begin{cases} g(0) = e_{_G}, \\ R_{g(t)^{-1}} \dot g(t) = u(t). \end{cases}$$

and the evolution mapping

$$\mathrm{evol}^r_{_G} : \mathrm{C}^\infty(\mathbb{R},\mathfrak{g}) \to G, \qquad \mathrm{evol}^r_{_G}(u) := g(1)$$

exists and is convenient smooth.

Examples of regular Lie groups are offered by the *strong ILH-Lie groups* in the sense of H. Omori [37].

Definition 4.5. *A topological group G is a strong ILH-Lie group modelled on the Fréchet space $\mathfrak{g} := \mathbb{E} = \lim\limits_{\leftarrow q} \mathbb{E}^q, q \geq d$, if and only if there exists a system $G^q, q \geq d$, of topological groups G^q satisfying the following conditions:*

(G_1) every group G^q is a Hilbert manifold modelled on the Hilbert space $\mathbb{E}^q$,

(G_2) G^{q+1} is a dense subgroup in G^q, and the embedding $G^{q+1} \subset G^q$ is a mapping of class C^∞,

(G_3) $G = \bigcap\limits_{q \geq d} G^q$ with inverse limit topology,

(G_4) the group multiplication mapping $m_G : G \times G \to G$ extends to a mapping $G^{q+l} \times G^q \to G^q$ of class C^l,

(G_5) the inversion mapping $i_G : G \to G$ extends to a mapping $G^{q+l} \to G^q$ of class C^l,

(G_6) for each $g \in G^q$ the right translation $r_g : G^q \to G^q$ is a mapping of class C^∞,

(G_7) let $\mathfrak{g}^q := \mathbb{E}^q$ be the tangent space of G^q at the identity $e \in G^q$, and let TG^q be the tangent bundle. The mapping $Tr : \mathfrak{g}^{q+l} \times G^q \to TG^q$ defined by $Tr(u, g) := R_g u$ is a mapping of class C^l,

(G_8) there exists an open neighborhood U of zero in $\mathfrak{g}^d$ and a diffeomorphism Φ of U onto an open neighborhood $\mathcal{U}$ of the unity $e \in G^d$, $\Phi(0) = e$, such that the restriction of Φ to $U \cap \mathfrak{g}^q$ is a diffeomorphism of the open subset $U \cap \mathfrak{g}^q$ from $\mathfrak{g}^q$ onto an open subset $\mathcal{U} \cap G^q$ from G^q for any $q \geq d$.

In the case $G = \mathrm{Diff}^\infty_+(\mathbb{S}^1)$ for $q > \frac{3}{2}$, the set $G^q := \mathcal{D}^q(\mathbb{S}^1)$ of C^1-orientation preserving diffeomorphisms of the circle, which are of class H^q, has the structure of a Hilbert manifold modelled on $\mathbb{E}^q := H^q(\mathbb{S}^1)$. It is also a topological group. $\mathrm{Diff}^\infty_+(\mathbb{S}^1) = \cap_{q>\frac{3}{2}} \mathcal{D}^q(\mathbb{S}^1)$ is a strong ILH-Lie group according to [37], thus a regular convenient smooth Lie group.

5 Euler-Arnold equations on regular Lie groups

In oder to define a Riemannian metric on a regular convenient Lie group G an inner product on the Lie algebra $\mathfrak{g}$ is extended to every tangent space by right translations

$$\langle u_g, v_g \rangle_g = \langle R_{g^{-1}} u_g, R_{g^{-1}} v_g \rangle_e, \qquad u_g, v_g \in T_g G, \;\; g \in G. \tag{5.1}$$

If this inner product is generated by an isomorphism $A : \mathfrak{g} \to \mathfrak{g}^*$, which is positive-definite and symmetric with respect to the natural pairing $(\cdot, \cdot)$ between elements of $\mathfrak{g}^*$ and $\mathfrak{g}$

$$\langle u, v \rangle_e^A := (u, Av) = (Au, v), \qquad u, v \in \mathfrak{g}, \tag{5.2}$$

then this operator is called the *inertia operator* on G. The natural pairing is actually the evaluation mapping. By Remark B.3 in the Appendix, it is convenient smooth if, for example, the topological dual g^* is endowed with the strong topology and g is a convenient vector space. It will never be Gâteaux smooth because Gâteaux smoothness implies continuity.

Remark 5.1. *When working with an infinite dimensional Lie group one can not consider bi-invariant metrics because in this case the Riemannian exponential mapping and the Lie exponential mapping will coincide and the latter one can*

behave bizarrely. Another problem occurs, exemplified here for the Fréchet-Lie group $G = \mathrm{Diff}^\infty_+(\mathbb{S}^1)$. *In order to maintain the isomorphism property of the inertia operator, described above, we have to restrict* $\mathfrak{g}^*$ *to its regular dual*

$$\mathfrak{g}^*_{reg} \cong \mathrm{C}^\infty(\mathbb{S}^1),$$

defined as the space of linear functionals of the form

$$u \to \int_{\mathbb{S}^1} m \cdot u \, dx,$$

for $m \in \mathrm{C}^\infty(\mathbb{S}^1)$, *due to [22, 24]. The pairing between the elements of* $\mathfrak{g}^*_{reg}$ *and* $\mathfrak{g}$ *will be given by the* $L^2(\mathbb{S}^1)$*-inner product*

$$(u, v) := \langle u, v \rangle_{L^2(\mathbb{S}^1)} = \int_{\mathbb{S}^1} u \cdot v \, dx. \tag{5.3}$$

The topology on $\mathfrak{g}^*_{reg}$ *is not the induced one and now the pairing becomes even Gâteaux smooth, which is impossible without the above convention. With this convention the inertia operator* $A : \mathfrak{g} \to \mathfrak{g}^*_{reg}$ *will be called regular inertia operator.*

If the adjoint of ad_v relative to the inner product (5.2) exists then the geodesics can be determined with the help of this operator. We remind here that a bilinear operator is bounded if and only if it is convenient smooth by Theorem A.8. On $\mathrm{C}^\infty(\mathbb{S}^1)$ boundedness will be equivalent with continuity, being a bornological space.

Theorem 5.2. *(V. Arnold, [1]) If the inner product* $\langle \cdot, \cdot \rangle_e : \mathfrak{g} \times \mathfrak{g} \to \mathbb{R}$ *defined in* (5.2) *is bounded and there exists a bounded bilinear operator*

$$B : \mathfrak{g} \times \mathfrak{g} \to \mathfrak{g},$$

with the property

$$\langle B(u, v), w \rangle_e = \langle u, \mathrm{ad}_v \, w \rangle_e, \qquad w \in \mathfrak{g},$$

where ad_v *is the adjoint representation of* $\mathfrak{g}$, *then a smooth curve* $g(t)$ *on the regular convenient Lie group* G *is a geodesic for the right-invariant metric defined by* (5.1) *if and only if its Eulerian velocity* $u(t) = R_{g(t)^{-1}} \dot{g}(t)$ *satisfies the first order equation*

$$u_t = -B(u, u).$$

Proof. We present the proof adapted to the convenient approach, whereas the original proof of V. Arnold is not rigorous enough in the infinite dimensional

setting. Parts of the proof are presented in Section 46.4 of [30].

For a smooth $g : [a, b] \to G$ the energy functional of the curve g is

$$E(g) := \frac{1}{2}\int_a^b \langle \dot{g}(t), \dot{g}(t)\rangle_{g(t)} dt = \frac{1}{2}\int_a^b \langle g^*\kappa^r(\partial_t), g^*\kappa^r(\partial_t)\,\rangle_e dt,$$

where we pullback the Maurer-Cartan form κ^r on $T\mathbb{R}$, by g.

The first part uses arguments borrowed from the finite dimensional case. One has to introduce $g(s, t)$ a smooth variation of the curve g, $s \in (-\varepsilon, \varepsilon), t \in [a, b]$, with fixed endpoints $g(s, a) = g(a)$, $g(s, a) = g(b)$ and let us denote the curves $u(s, t) := R_{g(s,t)^{-1}}\partial_t g(s, t)$ and $v(s, t) := R_{g(s,t)^{-1}}\partial_s g(s, t)$. In particular we have $u_0(t) := u(0, t) : [a, b] \to \mathfrak{g}$ and $v_0(t) := v(0, t) : [a, b] \to \mathfrak{g}$.

$$\begin{aligned}\partial_s E(g) &= \frac{1}{2}\int_a^b 2\langle \partial_s(g^*\kappa^r(\partial_t)), g^*\kappa^r(\partial_t)\,\rangle_e\, dt\\ &= \int_a^b \langle \partial_t(g^*\kappa^r(\partial_s)) - d(g^*\kappa^r)(\partial_t, \partial_s), g^*\kappa^r(\partial_t)\,\rangle_e\, dt\end{aligned}$$

because $[\partial_t, \partial_s] = 0$ by Schwarz's theorem. Further

$$\begin{aligned}&\int_a^b -\langle g^*\kappa^r(\partial_s), \partial_t(g^*\kappa^r(\partial_t))\rangle_e - \langle [g^*\kappa^r(\partial_t), g^*\kappa^r(\partial_s)], g^*\kappa^r(\partial_t)\,\rangle_e\, dt\\ &= -\int_a^b \langle g^*\kappa^r(\partial_s), \partial_t(g^*\kappa^r(\partial_t)) + B(g^*\kappa^r(\partial_t), g^*\kappa^r(\partial_t))\,\rangle_e\, dt,\end{aligned}$$

exploiting the fixed endpoints of the variation and applying the right Maurer-Cartan equation.

The curve g is a geodesic for the metric (5.1) iff the derivative vanishes at $s = 0$ for all variations $g(s, t)$ of g with fixed endpoints. By Corollary 38.13 in [30] the group $\mathrm{C}^\infty(\mathbb{R}, G)$ is a regular convenient Lie group, if G is a regular convenient Lie group. It has the Lie algebra $\mathrm{C}^\infty(\mathbb{R}, \mathfrak{g})$ with the bracket $[X, Y](t) := [X(t), Y(t)]_{\mathfrak{g}}$. Thus, following the definition of a regular convenient Lie group, for every curve

$$v(s, t) \in \mathrm{C}^\infty(\mathbb{R}, \mathrm{C}^\infty(\mathbb{R}, \mathfrak{g})) = \mathrm{C}^\infty(\mathbb{R} \times \mathbb{R}, \mathfrak{g})$$

there exists a curve

$$g(s, t) \in \mathrm{C}^\infty(\mathbb{R}, \mathrm{C}^\infty(\mathbb{R}, G)) \subseteq \mathrm{C}^\infty(\mathbb{R} \times \mathbb{R}, G),$$

such that

$$\begin{cases} g(0, t) = g(t) \in \mathrm{C}^\infty(\mathbb{R}, G),\\ v(s, t) := R_{g(s,t)^{-1}}\partial_s g(s, t).\end{cases}$$

In particular, every smooth curve $v_0:[a,b]\to\mathfrak{g}$ corresponds to a variation with fixed endpoints of g. Eventually, for all v_0

$$\int_a^b \langle v_0(t), \dot{u}_0(t) + B(u_0(t), u_0(t))\rangle_e \; dt = 0.$$

Applying this identity for the smooth curve $v_0(t) := \dot{u}_0(t) + B(u_0(t), u_0(t))$ we get the conclusion, since the inner product (5.2) is positive definite and smoothness implies continuity for curves. □

In the case $G = \mathrm{Diff}^\infty_+(\mathbb{S}^1)$, for the right-invariant metric induced as in (5.1) and (5.2) by the inner product $\langle u, v\rangle = \int_{S^1} Au\cdot v\; dx$, with $A:\mathrm{C}^\infty(\mathbb{S}^1)\to\mathrm{C}^\infty(\mathbb{S}^1)$ continuous linear, invertible, positive definite and L^2-symmetric, one gets

$$B(u,v) = A^{-1}\left\{u\cdot(Av)_x + 2Av\cdot u_x\right\},$$

since $\mathrm{ad}_u\, v$ has the expression given in (4.1). Hence a curve $\varphi(t)$ is a geodesic of the right-invariant metric induced by the inertia operator A if and only if its Eulerian velocity $u(t) := R_{\varphi(t)^{-1}}\dot{\varphi}(t) = \dot{\varphi}(t)\circ\varphi(t)^{-1}$ satisfies the equation

$$u_t = -A^{-1}\left\{u\cdot(Au)_x + 2Au\cdot u_x\right\}.$$

The equation from the above theorem is called the *Euler-Arnold equation* induced by an inertia operator A. In general a Levi-Civita connection related to the Riemannian metric (5.1) is not granted, because a metric like (5.1) generates a flat mapping $v_g\mapsto\langle v_g,\cdot\rangle_g$ that is only injective. If the adjoint ad^T_u exists such a connection also exists. To derive its formula we have to identify the space $\Gamma(TG)$ of smooth sections with the convenient vector space $C^\infty(G,\mathfrak{g})$ of $\mathfrak{g}$-valued fuctions on G. The isomorphism is induced by the right trivialization $\rho = (\pi_G, \kappa^r):TG\to\to G\times\mathfrak{g}$.

Proposition 5.3. *The mapping* $\mathcal{R}: C^\infty(G,\mathfrak{g})\to\Gamma(TG)$

$$\overline{X}\to\mathcal{R}_{\overline{X}}$$

where $\mathcal{R}_{\overline{X}}$ *is defined by* $\mathcal{R}_{\overline{X}}(g) := R_g(\overline{X}(g))$, *for* $\overline{X}\in\mathrm{C}^\infty(G,\mathfrak{g})$, $g\in G$, *is a bornological isomorphism.*

Proof. We have to argue that $\mathcal{R}$ and $\mathcal{R}^{-1}$ send bounded sets into bounded sets. Of course, we refer here to the von Neumann bornology corresponding to the natural topologies on $C^\infty(G,\mathfrak{g})$ and $\Gamma(TG)$, presented in the Appendix. For $\mathcal{R}^{-1}$ one gets the conclusion observing that $\mathcal{R}^{-1}(\xi) = \kappa^r(\xi)$, for $\xi\in\Gamma(TG)$, and the insertion mapping $i:\Gamma(TG)\times\Omega^1(G,\mathfrak{g})\to\Omega^0(G,\mathfrak{g}) := C^\infty(G,\mathfrak{g})$ is convenient smooth.

Since TG is trivializable, let us denote by f_α:$\Gamma(TG) \to C^\infty(\mathbb{R}, \mathfrak{g})$, the mappings with respect to which $\Gamma(TG)$ has the initial topology (see the Appendix B)

$$f_\alpha := c^* \circ (u_\alpha^{-1})^* \circ (pr_2 \circ \rho)_* \circ (i_{\mathcal{U}_\alpha})^*.$$

Let us also denote by $g_\alpha : C^\infty(G, \mathfrak{g}) \to C^\infty(\mathbb{R}, \mathfrak{g})$ the mappings that give the topology on $C^\infty(G, \mathfrak{g})$. Then $\mathcal{R}$ is bounded if and only if $f_\alpha \circ \mathcal{R}$ is bounded, since the von Neumann bornology coincides with the initial bornology induced by f_α on $\Gamma(TG)$ (cf. [19]). But $f_\alpha \circ \mathcal{R} = g_\alpha \circ Id_{C^\infty(G,\mathfrak{g})}$, thus $\mathcal{R}$ is bounded.

□

As a consequence $\mathcal{R}$ and $\mathcal{R}^{-1}$ are convenient smooth. In order to avoid some cumbersome expressions we will use, in the next proposition, the same notation for the vector field and the curve attached via the isomorphism $\mathcal{R}$. Relation (5.4) should be written as $\nabla_{\mathcal{R}_{\overline{X}}} \mathcal{R}_{\overline{Y}} := \mathcal{R}_{\overline{\nabla_X Y}}$, for some mappings $\overline{X}, \overline{Y}, \overline{\nabla_X Y} \in \in \mathrm{C}^\infty(G, \mathfrak{g})$. Because the flat mapping is only injective the idea is to build the below candidate and to prove that this is the unique Levi-Civita connection, related to the right-invariant metric (5.1).

Proposition 5.4. *Assume that for all $u \in \mathfrak{g}$ the adjoint ad_u^T with respect to the bounded inner product $\langle \cdot, \cdot \rangle_e$ exists and that $u \mapsto \mathrm{ad}_u^T$ is bounded. Then the Levi-Civita connection related to the metric* (5.1) *exists and is given by*

$$\nabla_{\mathcal{R}_X} \mathcal{R}_Y := \mathcal{R}_{\nabla_X Y}, \quad \nabla_X Y \in \mathrm{C}^\infty(G, \mathfrak{g}), \tag{5.4}$$

where

$$\nabla_X Y(g) := T_g Y(\mathcal{R}_X(g)) - \frac{1}{2} \mathrm{ad}_{X(g)} Y(g) + \frac{1}{2} \mathrm{ad}^T_{X(g)} Y(g) + \frac{1}{2} \mathrm{ad}^T_{Y(g)} X(g), \tag{5.5}$$

for $X, Y \in \mathrm{C}^\infty(G, \mathfrak{g})$, $g \in G$.

Proof. See Section 46.5 in [30]. □

Remark 5.5. *This formula coincides pointwise with the corrected version of the formula given in [9], for the particular case $G = \mathrm{Diff}_+^\infty(\mathbb{S}^1)$*

$$(\nabla_X Y)_\varphi = [X, Y - Y_\varphi^R]_\varphi + \frac{1}{2} \left([X_\varphi^R, Y_\varphi^R]_\varphi + B(X_\varphi^R, Y_\varphi^R)_\varphi + B(Y_\varphi^R, X_\varphi^R)_\varphi \right),$$

where, for $X \in \Gamma(\mathrm{TDiff}_+^\infty(\mathbb{S}^1))$, the term X_φ^R denotes the right-invariant vector field whose value at $\varphi \in \mathrm{Diff}_+^\infty(\mathbb{S}^1)$ is X_φ, thus $X_\varphi^R = \mathcal{R}_{X_\varphi \circ \varphi^{-1}}$ and the operator $B(u, v) := \mathrm{ad}_v^T u$ was extended to the family of right-invariant vector fields by $B(Z, W)_\varphi = B(Z_{id}, W_{id}) \circ \varphi$.

6 The geodesic spray

An interesting phenomenon concerning the Euler-Poincaré-Arnold equations occurs for some Fréchet-Lie groups: the propagator of the evolution equation which describes the geodesic flow (Lagrangian coordinates) has better properties than the one corresponding to the Euler-Arnold equation (Eulerian coordinates).

We will exemplify this remark by considering the case $G = \mathrm{Diff}^\infty_+(\mathbb{S}^1)$, with a right-invariant metric constructed as in (5.2) and A a pseudo-differential operator of Hörmander class $S^r_{1,0}$, $r \geq 1$, as in [7]. The spray equation will be

$$\begin{cases} \varphi_t = v \\ v_t = S_\varphi(v) \end{cases}, \tag{6.1}$$

where

$$S_\varphi(v) = R_\varphi \circ S \circ R_{\varphi^{-1}}(v),$$

and

$$S(u) = A^{-1}\{[A,u]D(u) + u[A,D](u) - 2A(u)D(u)\}.$$

with $D := \frac{d}{dx}$ on S^1, defined as in [18].

The mapping $\mathrm{F} : \mathrm{TDiff}^\infty_+(\mathbb{S}^1) \to \mathrm{TTDiff}^\infty_+(\mathbb{S}^1)$, locally defined by

$$F(\varphi, v) := (\varphi, v, v, S_\varphi(v)), \tag{6.2}$$

extends to a smooth mapping $F : T\mathcal{D}^q(\mathbb{S}^1) \to TT\mathcal{D}^q(\mathbb{S}^1)$, mostly because of the commutators that appear in the above expressions. Hence, it is possible to recast the spray equation as an ODE on suitable Hilbert spaces and to work on the Hilbert approximations of the ILH Lie group $\mathrm{Diff}^\infty_+(\mathbb{S}^1)$. This phenomenon is exploited in order to obtain the existence of an integral curve of the geodesic spray, see [4, 7, 9, 12, 13, 23].

On the other hand, denoting $\varphi_t = u \circ \varphi$, one discovers via Theorem 5.2 that φ satisfies the spray equation iff the Eulerian velocity u satisfies the the Euler-Arnold equation

$$u_t = -A^{-1}\{u \cdot (Au)_x + 2Au \cdot u_x\}.$$

Unfortunately, this equation has a derivative loss when considered on the Hilbert approximations, thus it needs some Nash-Moser schemes in order to be solved in the smooth category. Such an approach is used in [8], with a comparison between these two methods.

The above discussion contains the essence of the so called "geometric method in hydrodynamics"[15]. Most of the papers concerned with this geometric method do not define rigorously the spray in the case of a Fréchet manifold. This is what

we intend to do in the sequel. We are interested here only in sprays related to a right-invariant metric on a regular Lie group. There is not a direct way to define a spray on a Fréchet-Lie group using the concept of Gâteaux smoothness, without introducing some conventions or losing generality. The convenient calculus permits us to define a geodesic spray on Fréchet manifolds and afterwards one can use the ILH structure of the Lie group for proving the existence of an integral curve.

6.1 Sprays on Banach manifolds

In the case of a Banach manifold M modelled on a Banach space $\mathbb{E}$, in order to define the spray related to a metric, the classical approach is to use the flat mapping

$$\widehat{g} : T_pM \to T_p^*M, \qquad \xi \to g(p)(\xi, \cdot),$$

where g is a smooth Riemannian metric on M. On the cotangent bundle of M we can define the canonical Liouville 1-form by

$$\Theta_\omega(X) := \omega(T\pi^*(X)), \qquad \omega \in T_x^*M, X \in T_\omega(T^*M),$$

where $\pi^* : T^*M \to M$ is the canonical projection. There is also a canonical symplectic form on T^*M obtained as

$$\Omega = -d\Theta,$$

where d is the exterior derivative of a 1-form.

We can pullback the Liouville form by the flat mapping $\widehat{g}$ to obtain a 1-form Θ^g on TM

$$\Theta_\xi^g(X) := g(p)(\xi, T\pi_M(X)), \qquad \xi \in TM, X \in T_\xi(TM),$$

and further a symplectic form on TM

$$\Omega^g := -d\Theta^g.$$

If the metric is strong we can associate to every function H on TM a Hamiltonian vector field F_H on TM defined as

$$d_\xi H(X) := \Omega^g(F_H(\xi), X), \tag{6.3}$$

where $\xi \in TM$ and $X \in T_\xi(TM)$. If the metric is weak the flat mapping and the symplectic form Ω^g are only injective and thus given a function H on TM the Hamiltonian vector field corresponding to it may not exist, but if exists it is given by the above relation (6.3).

Definition 6.1. *(see [26]) The geodesic spray F associated to a strong metric g is defined as the Hamiltonian vector field of the energy function*

$$E(\xi) := \frac{1}{2} g(p)(\xi, \xi).$$

In a local chart $U_{\mathbb{E}} \times \mathbb{E}$ of TM the Hamiltonian vector field F is

$$F(x, v) := (x, v, v, S(x, v)),$$

where $S(x, v)$ is defined by

$$g(x)(S(x, v), u) = \frac{1}{2} D_x g(u)(v, v) - D_x g(v)(v, u),$$

for $x \in U_{\mathbb{E}} \subseteq \mathbb{E}$ and $u, v \in \mathbb{E}$, where $D_x g$ represents the Fréchet derivative of the local representative of the metric. Since the flat mapping $\widehat{g}$ is bijective one gets

$$S(x, v) = pr_2[\widehat{g}^{-1}(x, \frac{1}{2} D_x g(u)(v, v) - D_x g(v)(v, u))].$$

6.2 Sprays for the geometric method

By TM we will denote the kinematic tangent bundle of an infinite dimensional manifold, modeled on a convenient vector space $\mathbb{E}$.

Definition 6.2. *We define a spray F to be a convenient smooth section of both $\pi_T M : TTM \to TM$ and $T\pi_M : TTM \to TM$ (symmetric vector field) which satisfies the quadratic condition*

$$F \circ m_\lambda^{TM} = T m_\lambda^{TM} \circ m_\lambda^{TTM} \circ F,$$

where $m_\lambda^{TM}, m_\lambda^{TTM}$ denote the fiber scalar multiplications.

Let G be a regular convenient Lie group and g a convenient smooth right-invariant metric defined as in (5.1) by a bounded inner product $\langle \cdot, \cdot \rangle$. Generally, a Riemannian metric g on an convenient manifold G can be defined as a convenient smooth section of the vector bundle $L(TG \oplus TG, G \times \mathbb{R})$, that gives a positive definite and symmetric bilinear form $g(p)(\cdot, \cdot)$ on each tangent space $T_p G$, $p \in G$. Let us consider the following mapping on TTG

$$\Theta_\xi^g(X) := g(\xi, T_\xi \pi_G(X)) = \langle \kappa^r(\xi), (\pi_G^* \kappa^r)_\xi(X) \rangle, \;\; X \in T_\xi TG,$$

where $\langle \cdot, \cdot \rangle$ is the inner product (5.2), κ^r the right Maurer-Cartan form and the mapping $\pi_G : TG \to G$ is the canonical projection. Θ^g is a convenient smooth section of the convenient convenient smooth vector bundle $L(TTG, TG \times \mathbb{R})$, thus a kinematic 1-form on the kinematic tangent bundle TG, when G is a regular convenient Lie group. The smoothness of $\xi \to \kappa^r(\xi)$ from $\Gamma(TG)$ to $C^\infty(G, \mathfrak{g})$ was justified in the previous section. Now, one can define a kinematic 2-form on TG by

$$\omega^g(Y, X) := -d\Theta^g(Y, X).$$

To every right-invariant metric on a regular convenient Lie group G one can associate the energy function $E : TG \to \mathbb{R}$

$$E(\xi) := \frac{1}{2} g(\xi, \xi) = \langle \kappa^r(\xi), \kappa^r(\xi) \rangle, \qquad \xi \in TG.$$

Proposition 6.3. *If there exists a vector field F on the kinematic tangent bundle TG satisfying*

$$i_F \omega^g = dE, \tag{6.4}$$

then it is unique and it is a right-invariant spray.

Proof. If $F(x, v) = (x, v, S_1(x, v), S_2(x, v))$ is the local representative of the vector field F then, using Remark A.11 in the Appendix, the local expression of $i_F \omega^g = = dE$ is

$$d_x g(u)(v, S_1(x, v)) + g(x)(w, S_1(x, v)) - d_x g(S_1(x, v))(v, u) - g(x)(S_2(x, v), u)$$

$$= \frac{1}{2} d_x g(u)(v, v) + g(x)(v, w),$$

for $X = (x, v, u, w)$. Choosing $u = 0$ implies $S_1(x, v) = v$. Hence F is a symmetric vector field and $S_2(x, v)$ satisfies

$$g(x)(S_2(x, v), u) = \frac{1}{2} d_x g(u)(v, v) - d_x g(v)(v, u).$$

Finally $S_2(x, \lambda v) = \lambda^2 S_2(x, v)$ and S_2 is quadratic in v, thus F is a spray.

The vector field (if exists) defined by (6.4) has to be unique because g is non-degenerate and one can easily see that F is actually invariant under any isometry of the metric (5.1) because E and ω^g are. □

There are two possible trivializations of $TTG \cong T(G \circledS \mathfrak{g})$, the first one is

$$tr^1_{TTG}(\xi_g, \xi_u) = (g, u, \kappa^r(\xi_g), \xi_u + [u, \kappa^r(\xi_g)]), \qquad g \in G, \xi_g \in T_g G, u \in \mathfrak{g}, \xi_u \in T_u \mathfrak{g}.$$

and is obtained decomposing $T(G\circledS\mathfrak{g})$ as the semidirect product between $G\circledS\mathfrak{g}$ and $\mathfrak{g}\circledS\mathfrak{g}$, see [16]. The second one is obtained using $tr^2_{TTG} = \sigma\circ(\rho\times id)\circ T\rho$, where $\sigma(g,u,v,w) = (g,v,u,w)$ is the canonical involution. Thus

$$tr^2_{TTG}(\xi_g,\xi_u) = (g,u,\kappa^r(\xi_g),\xi_u), \qquad g\in G, u\in\mathfrak{g}.$$

Of course, the symmetric vector fields on TG are invariant under these two trivializations. We prove now that, when the Arnold operator exists, also a spray related to the right-invariant metric (5.1) exists. The formula is similar to the one obtained in [25] in a more restrictive setting. Propositions 6.4 and 6.5 together with Theorem 5.2 and Proposition 5.4 form a unitary convenient approach of the so called geometric method in hydrodynamics.

Proposition 6.4. *If the inner product* (5.2) *is bounded and the Arnold operator* $ad^T:\mathfrak{g}\times\mathfrak{g}\to\mathfrak{g}$ *exists and is convenient smooth then the mapping*

$$F: TG\to TTG,$$

defined, with respect to any of the two trivializations of TTG*, by*

$$F(\xi) := (g,\kappa^r(\xi),\kappa^r(\xi),-ad^T_{\kappa^r(\xi)}\kappa^r(\xi)), \quad \xi\in T_gG, \tag{6.5}$$

is convenient smooth and satisfies the identity

$$i_F\omega^g(X) = dE(X), \quad \forall\, X\in TTG.$$

Proof. Let $\mathbb{E}$ be a convenient vector space and $f: M\to\mathbb{E}$ a convenient smooth mapping. Since, by [30], a kinematic vector field is also an operational vector field, then for a convenient smooth kinematic vector field ξ one obtains a convenient smooth $\mathbb{E}$-valued mapping by $\xi(f) := pr_2\circ Tf\circ\xi$. Here the right term is the differential of f, but in order to avoid another d in our arguments we prefer this notation, compare to Section 28.15 in [30]. The following formula holds

$$\xi\left(\langle f,g\rangle\right)(p) = \langle\xi(f),g\rangle(p) + \langle f,\xi(g)\rangle(p), \;\; p\in M,$$

for a bounded inner product $\langle\cdot,\cdot\rangle$ on $\mathbb{E}$, and $f,g: M\to\mathbb{E}$ smooth.

We will do the computations using the second trivialization of TTG. The kinematic vector field F defined above is symmetric, hence we get $\pi_G^*\kappa^r(F(\xi)) = \kappa^r(\xi)$. The global formula holds for the exterior derivative of a kinematic differential form, according to Section 33.12 in [30], thus

$$\begin{aligned}
\omega^g_\xi(F(\xi),X(\xi)) &= -F(\Theta^g\circ X)(\xi) + X(\Theta^g\circ F)(\xi) + (\Theta^g\circ[F,X])(\xi)\\
&= -\langle F(\kappa^r)(\xi),\pi_G^*\kappa^r(X(\xi))\rangle - \langle\kappa^r(\xi),F(\pi_G^*\kappa^r(X))(\xi)\rangle\\
&\quad + \langle X(\kappa^r)(\xi),\kappa^r(\xi)\rangle + \langle\kappa^r(\xi),X(\pi_G^*\kappa^r(F))(\xi)\rangle\\
&\quad + \langle\kappa^r(\xi),\pi_G^*\kappa^r([F,X](\xi))\rangle\\
&= -\langle F(\kappa^r)(\xi),\pi_G^*\kappa^r(X(\xi))\rangle + \langle X(\kappa^r)(\xi),\kappa^r(\xi)\rangle\\
&\quad - \langle\kappa^r(\xi),d(\pi_G^*\kappa^r)(F(\xi),X(\xi))\rangle.
\end{aligned}$$

But

$$d(\pi_G^*\kappa^r)(F,X) = \pi_G^*\, d\kappa^r(F,X) = \pi_G^*\left(\frac{1}{2}[\kappa^r,\kappa^r]_\wedge(F,X)\right)$$
$$= [\kappa^r(T\pi_G(F)),\kappa^r(T\pi_G(X))] = \mathrm{ad}_{\kappa^r(T\pi_G(F))}\,\kappa^r(T\pi_G(X)),$$

by applying the Maurer-Cartan equation. In the same time $T\pi_G(F(\xi)) = \xi$ and $F(\kappa^r)(\xi) = pr_2\,(T_\xi\kappa^r(F(\xi))) = -\,\mathrm{ad}^T_{\kappa^r(\xi)}\,\kappa^r(\xi)$, since $\sigma\circ(\rho\times id)\circ(T\pi_G, T\kappa^r)$ gives the chosen trivialization of TTG. Eventually

$$\begin{aligned}\omega^g_\xi(F(\xi),X(\xi)) =& -\langle -\,\mathrm{ad}^T_{\kappa^r(\xi)}\,\kappa^r(\xi),\kappa^r(T\pi_G(X(\xi))\rangle + \langle X(\kappa^r)(\xi),\kappa^r(\xi)\rangle\\ &-\langle \mathrm{ad}^T_{\kappa^r(\xi)}\,\kappa^r(\xi),\kappa^r(T\pi_G(X(\xi))\rangle\\ =&\langle X(\kappa^r)(\xi),\kappa^r(\xi)\rangle = d_\xi E(X(\xi)).\end{aligned}$$

□

Written in the manner of Proposition 5.4 the above result becomes.

Proposition 6.5. *Assume that for all $u\in\mathfrak{g}$ the adjoint ad^T_u with respect to the bounded inner product $\langle\cdot,\cdot\rangle_e$ exists and that $u\mapsto \mathrm{ad}^T_u$ is bounded. Then the metric spray is given by*

$$F = \mathcal{R}_{\overline{S}},$$

where $\mathcal{R}: C^\infty(TG,T\mathfrak{g})\to\Gamma(TTG)$ is the canonical isomorphism and the mapping $\overline{S}: TG\to T\mathfrak{g}$ is defined as

$$\overline{S}(\xi) = \left(\kappa^r(\xi), -\,\mathrm{ad}^T_{\kappa^r(\xi)}\,\kappa^r(\xi)\right),\quad \xi\in TG.$$

Proof. One has only to argue that

$$(\sigma\circ(\rho\times id)\circ T\rho)\,(\mathcal{R}_{\overline{S}}(\xi)) = \left(g,\kappa^r(\xi),\kappa^r(\xi),-\,\mathrm{ad}^T_{\kappa^r(\xi)}\,\kappa^r(\xi)\right)$$

which is straightforward, since by its very definition

$$\mathcal{R}_{\overline{S}}(\xi) = R_\xi(\overline{S}(\xi)) = \left(\xi,\kappa^r(\xi),\mathrm{ad}^T_{\kappa^r(\xi)}\,\kappa^r(\xi)\right)$$

□

Proposition 6.6. *If the inner product* (5.2) *is bounded and the operator ad^T exists and is bounded, then a smooth curve $g:\mathbb{R}\to G$ is a geodesic of the right-invariant metric* (5.1) *if and only if $\dot{g}(t):\mathbb{R}\to TG$ is an integral curve of the right-invariant spray F defined by* (6.4)*, and we call it the geodesic spray corresponding to this metric.*

Proof. It is a straightforward consequence of Proposition 5.2 and of Proposition 6.4, since $\kappa^r(\dot{g}(t)) = R_{g(t)^{-1}}\dot{g}(t)$. □

Remark 6.7. *Since we work on manifolds modelled on non normable locally convex spaces the existence of an integral curve for a smooth vector field is not granted. Most of the times we speculate the right invariance of the geodesic spray. It is a challenge to find new ways for proving the existence of integral curves for a given spray, motivated in practice by metrics which are not right-invariant. These kind of metrics can appear in fields like image processing or shape analysis.*

In order to prove the existence of an integral curve of the geodesic spray one has to visualize it in an appropriate way. The Lie group $G = \mathrm{Diff}^\infty_+(\mathbb{S}^1)$ is a good ambient group for exemplifying the construction of Euler-Arnold's equation or the connection compatible with a given right-invariant weak Riemannian metric, but not for aspects regarding the geodesic spray. The occurrence of some particular phenomena (existence of an universal cover, for example) makes this group inappropriate if one wants to grasp the overall picture. That's why we have to switch to the more general case $G = \mathrm{Diff}^\infty(M)$, with M a compact manifold.

6.3 The EPDiff equation

Let us consider a compact manifold M and the Lie group $G = \mathrm{Diff}^\infty(M)$ of diffeomorphisms isotopic to the identity. We define an inner product on its Lie algebra $\Gamma(TM)$, the set of all smooth sections of TM, via

$$\langle u_1, u_2\rangle := \int_M g\,(Au_1, u_2)\,d\mu\,,$$

where $u_1, u_2 \in \Gamma(TM)$, g is the Riemannian metric on TM, $d\mu$, the Riemannian density and the inertia operator

$$A : \Gamma(TM) \to \Gamma(TM)$$

is a L^2-symmetric, positive definite, continuous linear operator. In order to get an inner product on each tangent space $T_\varphi\mathrm{Diff}^\infty(M)$, we translate the above inner product using the right translations R_φ

$$G_\varphi(v_\varphi, w_\varphi) = \int_M g\left(A(R_{\varphi^{-1}}v_\varphi), R_{\varphi^{-1}}w_\varphi\right)d\mu\ ,$$

where $v_\varphi, w_\varphi \in T_\varphi\mathrm{Diff}^\infty(M)$, and $A_\varphi := R_\varphi \circ A \circ R_{\varphi^{-1}}$.

Let $u(t) := R_{\varphi^{-1}(t)}\dot{\varphi}(t)$ be the *Eulerian velocity* of the geodesic curve $\varphi(t)$. Then $u(t)$ is a solution of the *Euler-Poincaré equation* (EPDiff) *on* $\mathrm{Diff}^\infty(M)$

$$m_t + \nabla_u m + (\nabla u)^t\, m + (\mathrm{div} u)m = 0, \quad m := Au\,, \tag{6.6}$$

where $(\nabla u)^t$ is the Riemannian adjoint (with respect to the metric g) of ∇u.

When A is invertible, the EPDiff equation (6.6) can be recast as

$$u_t = -A^{-1}\left\{\nabla_u Au + (\nabla u)^t Au + (\mathrm{div} u)Au\right\}, \tag{6.7}$$

which is the *Euler–Arnold* equation for $\mathrm{Diff}^\infty(M)$.

In the sequel we would like to introduce the spray related to the metric G_φ, but one has to find the best way to visualize it. We need some terminology from classical mechanics, in order to give an interpretation to some abstract computations. The *configuration space* of the fluid motion (the space of all physically valid states) is $\mathrm{Diff}^\infty(M)$ and every $\varphi \in \mathrm{Diff}^\infty(M)$ takes a particle $p \in M$ to a particle $\varphi(p)$. Thus every φ is a *symmetry* of the mechanical system. A *motion* of the fluid is a curve $\varphi(t) \in \mathrm{Diff}^\infty(M)$. Obviously during a motion every particle p describes a path $t \to \varphi(t,p)$ and we call $\varphi(t,p)$ the *Eulerian points* of this path. The *Lagrangian velocity field* $\dot\varphi(t,p)$ is the time derivative of this trajectory. The *Eulerian velocity* is defined as $u(t,q) = \dot\varphi(t, \varphi^{-1}(t)(q))$ and is the velocity at time t of the particle currently in position q.

The covariant derivative along the path $\varphi(t,p)$ is called the *material derivative* and connects the *Eulerian derivative* u_t with the Lagrangian and Eulerian velocity fields

$$\left(\nabla_{_t}\dot\varphi(t,p)\right)(t_0) = (u_t + \nabla_u u)(\varphi(t_0,p)) \ . \tag{6.8}$$

Locally on TTM the second order tangent vector $\ddot\varphi(t,p)$ is expressed as

$$\Big(\varphi(t,p), \dot\varphi(t,p), \dot\varphi(t,p), -\Gamma_{\varphi(t,p)}(\dot\varphi(t,p),\dot\varphi(t,p)) + \nabla_{_t}\dot\varphi(t,p)\Big) \tag{6.9}$$

because of $\nabla_{_t}\dot\varphi(t,p) = \ddot\varphi(t,p) + \Gamma_\varphi(\dot\varphi(t,p),\dot\varphi(t,p))$. Here Γ is the Christoffel symbol corresponding to the metric given on M.

We start now with the connection ∇ of M and we build a connection $\widetilde{\nabla}^q$ on $\mathcal{D}^q(M)$, in the way done in Section 9 of [12]. Usually the restriction $q > \frac{3}{2}$ is taken into consideration. The projections π_M, π_{TM} and connector K ascend to smooth mappings $\widetilde{\pi}^q_M, \widetilde{\pi}^q_{TM}$ and $\widetilde{K}^q$, respectively. Here by $\widetilde{K}^q$ we mean $\widetilde{K}^q(X) := K \circ X$, when $X \in TT\mathcal{D}^q(M)$, with similar meaning for $\widetilde{\pi}^q_M, \widetilde{\pi}^q_{TM}$.

By their very definition:

$$T\mathcal{D}^q(M) = \{\xi \in H^q(M,TM) : \ \widetilde{\pi}^q_M \circ \xi \in \mathcal{D}^q(M)\},$$

$$TT\mathcal{D}^q(M) = \{X \in H^q(M,TTM) : \ \widetilde{\pi}^q_{TM} \circ X \in T\mathcal{D}^q(M)\},$$

thus first and second order vector fields on $\mathcal{D}^q(M)$ can be seen as mappings on M. Since the connecting morphisms of the inverse systems $\{\mathcal{D}^q(M)\}_q$, $\{T\mathcal{D}^q(M)\}_q$

and $\{TT\mathcal{D}^q(M)\}_q$ are inclusion mappings it is straightforward to argue the existence of the inverse limits $\widetilde{K} = \lim_{\leftarrow q} \widetilde{K}^q$, $\widetilde{\pi}_M = \lim_{\leftarrow q} \widetilde{\pi}^q_M$, and $\widetilde{\pi}_{TM} = \lim_{\leftarrow q} \widetilde{\pi}^q_{TM}$.

We consider now $\varphi(t) \in \mathrm{Diff}^\infty(M)$ a motion of the fluid. The mapping $\widetilde{K}$ will induce an ILH connection $\widetilde{\nabla}$ on $\mathrm{Diff}^\infty(M)$, in the sense of [36, 37]. Using $\widetilde{\nabla}$ we get a covariant derivative along the motion $\varphi(t)$ that satisfies

$$\left(\widetilde{\nabla}_{\dot{\varphi}}\dot{\varphi}\right)(t_0)(p) = \left(\nabla_{\dot{\varphi}(t,p)}\dot{\varphi}(t,p)\right)(t_0).$$

Because of (6.8) one can recast the Euler-Arnold equation (6.7) in the form

$$\widetilde{\nabla}_{\dot{\varphi}}\dot{\varphi} = S_\varphi(\dot{\varphi}) = R_\varphi \circ S \circ R_{\varphi^{-1}}(\dot{\varphi}), \tag{6.10}$$

where

$$S(u) = A^{-1}\left\{[A, \nabla_u]u - (\nabla u)^t Au - (\mathrm{div} u)Au\right\}.$$

Further, we will relate the above Lagrangian description (6.10) of the EPDiff equation to the spray equation. First of all, we need an image of the spray equation. Since the local charts on $\mathrm{Diff}^\infty(M)$ use the Riemannian exponential of M, see [37], it will not be helpful to switch from the Eulerian description (6.7) of the spray equation to a local description on $T\mathrm{Diff}^\infty(M)$.

The double tangent bundle $TT\mathcal{D}^q(M)$ has also a fiber bundle structure over $\mathcal{D}^q(M)$ which is identified with $T\mathcal{D}^q(M) \oplus T\mathcal{D}^q(M) \oplus T\mathcal{D}^q(M)$, via Dombrowski's isomorphism [26]. In order to get an appropriate image of the spray equation, let us consider the fiber subbundle of 2-velocities, see also [33]

$$T^2\mathcal{D}^q(M) = \left\{\xi \in TT\mathcal{D}^q(M) :\ \widetilde{\pi}^q_{TM}(\xi) = T\widetilde{\pi}^q_M(\xi)\right\}.$$

The advantage of $T^2\mathcal{D}^q(M)$ consists in its vector bundle structure over $\mathcal{D}^q(M)$, apart from its canonical identification with $T\mathcal{D}^q(M) \oplus T\mathcal{D}^q(M)$. Moreover, for $\widetilde{\nabla}$ exists, one can construct the inverse limit of vector bundles

$$T^2\mathrm{Diff}^\infty(M) = \lim_{\leftarrow q} T^2\mathcal{D}^q(M)$$

as in [11], for example. The identification of $T^2\mathrm{Diff}^\infty(M)$ with the Whitney sum $T\mathrm{Diff}^\infty(M) \oplus T\mathrm{Diff}^\infty(M)$ is via

$$(\varphi, \dot{\varphi}, \ddot{\varphi}) \to (\dot{\varphi}, \widetilde{\nabla}_{\dot{\varphi}}\dot{\varphi}).$$

The equation (6.10) corresponds, under the above identification, to the spray equation. Thus, it makes sense to call the mapping

$$v_\varphi \mapsto (v_\varphi, S_\varphi(v_\varphi)),\quad T\mathrm{Diff}^\infty(M) \mapsto T\mathrm{Diff}^\infty(M) \oplus T\mathrm{Diff}^\infty(M)$$

the *geodesic spray* related to the right-invariant metric (6.3). The idea is to prove the existence of geodesics φ^q on Banach approximations $\mathcal{D}^q(M)$ and then to obtain geodesics on $\mathrm{Diff}^\infty(M)$ as an inverse limit $\varphi = \lim_{\leftarrow q} \varphi^q$. The big stake is the well-posedness, in the smooth category, of the EPDiff equation on a compact manifold, with an inertia operator A of a pseudo-differential type, an extension of the results presented in [7, 13].

In the end, in order to help the reader to follow some of the arguments presented in this paper, we will list in an Appendix some basic facts from convenient calculus.

Acknowledgments

I would like to express my very great appreciation to Cornelia Vizman and Boris Kolev for their valuable and constructive suggestions during the planning and development of this research work. The research was partially supported by CNCS UEFISCDI, project number PN-III-P4-ID-PCE-2016-0778 and partially by Horizon2020-2017-RISE-777911.

A A glimpse into the convenient calculus

We add some details about the convenient calculus of A. Frölicher and A. Kriegl. All the missing proofs of the statements presented below can be found in [30].

In locally convex spaces there is a weaker notion than that of Cauchy sequences, namely the *Mackey-Cauchy sequences*.

Definition A.1. *A sequence $(x_n)_n$ in $\mathbb{E}$ is called Mackey-Cauchy if there exists a bounded and absolutely convex set B and for every $\varepsilon > 0$ an integer $n_\varepsilon \in \mathbb{N}$ such that*

$$x_n - x_m \in \varepsilon B, \quad \forall n > m > n_\varepsilon.$$

This is equivalent with $t_{nm}(x_n - x_m) \to 0$ for some $t_{nm} \to \infty$ in $\mathbb{R}$.

Definition A.2. *A convenient vector space is a locally convex topological vector space which is Mackey complete (every Mackey-Cauchy sequence converges in $\mathbb{E}$).*

Any sequentially complete topological vector space is Mackey-complete.

Definition A.3. *(Bornology) Let X be a set, a bornology on X is a collection $\mathcal{B}$ of subsets such that:*

(i) $\mathcal{B}$ *covers* X, *i.e.* $X = \bigcup_{B\in\mathcal{B}} B$.

(ii) $\mathcal{B}$ *is stable under inclusions, if* $B \in \mathcal{B}$ *and* $B_0 \subseteq B$, *then* $B_0 \in \mathcal{B}$.

(ii) $\mathcal{B}$ *is stable under finite unions, if* $B1, \ldots, B_n \in \mathcal{B}$, *then* $\bigcup_{i=1}^{n} B_i \in \mathcal{B}$.

Given a locally convex space $(\mathbb{E}, \tau)$ we obtain a natural bornology on $\mathbb{E}$ (von Neumann bornology) consisting of all bounded sets. We call a set $U \subseteq \mathbb{E}$ *bornivorous* if it absorbs every bounded set from its von Neumann bornology.

Definition A.4. *A Hausdorff locally convex space* $\mathbb{E}$ *is called bornological if each convex, balanced and bornivorous set in* $\mathbb{E}$ *is a neighborhood of* 0.

Definition A.5. *Let* $(\mathbb{E}, \tau)$ *be a locally convex topological vector space, then the collection of all absolutely convex bornivorous subsets forms a locally convex topology* τ_{born} *called the bornologification of the initial topology. The space* $\mathbb{E}_{born} := := (\mathbb{E}, \tau_{born})$ *is called the attached bornological space and it is the finest locally convex structure having the same bounded sets as* $(\mathbb{E}, \tau)$.

Remark A.6. *A subset* U *in* $\mathbb{E}$ *is* c^∞*-open iff for every* $x \in U$ *there is a bornivorous set* B *such that* $x + B \subset U$. *Instead, a subset* U *is open relative to the bornologification of the initial topology iff for every* $x \in U$ *there exists a convex, balanced and bornivorous set* B *such that* $x + B \subset U$.

A convenient vector space $\mathbb{E}$ *interacts naturally with the* c^∞*-topology: a convenient smooth map between convenient vector spaces will be continuous relative to this topology and usually is not continuous relative to the initial topology on* $\mathbb{E}$. *But, in general, the* c^∞*-topology is not a liniar topology ! For linear mappings the above phenomenon is not a problem: a linear mapping between convenient vector spaces is bounded iff it is convenient smooth. Besides the cartesian closedness, another cornerstone of the convenient calculus is the fact that the two fundamental spaces* $\mathrm{C}^\infty(\mathbb{E}, \mathbb{F})$ *and* $\mathrm{L}(\mathbb{E}, \mathbb{F})$ *(linear and bounded) will remain in this category, when* $\mathbb{E}, \mathbb{F}$ *are convenient vectors spaces. The smoothness of a curve* $c : \mathbb{R} \to \mathbb{E}$ *does not depend on the initial topology on* $\mathbb{E}$, *it depends only on its bornology. Usually we substitute the initial locally convex topology with its bornologification and work with bornological locally convex spaces. In this way we can exploit the characteristic property: on bornological spaces a linear mapping is continuous if and only if it is bounded.*

We equip $\mathrm{C}^\infty(\mathbb{R}, \mathbb{F})$ with the bornologification of the topology of uniform convergence on compact sets, in all derivatives separately. The space $\mathrm{C}^\infty(\mathbb{E}, \mathbb{F})$ will be equiped with the bornologification of the initial topology relative to all pullback mappings $c^*{:}\mathrm{C}^\infty(\mathbb{E}, \mathbb{F}) \to \mathrm{C}^\infty(\mathbb{R}, \mathbb{F})$, $c^*(f) := f \circ c$, for all $c \in \mathrm{C}^\infty(\mathbb{R}, \mathbb{E})$. If a locally

convex space $\mathbb{E}$ is Mackey-complete (convenient) then its attached bornological space, $\mathbb{E}_{born}$, having the same bounded sets, will be Mackey-complete.

Proposition A.7. *For locally convex spaces $\mathbb{E}, \mathbb{F}$ we have:*

(i) If $\mathbb{F}$ is a convenient vector space then $\mathrm{C}^\infty(\mathbb{E}, \mathbb{F})$ is a convenient vector space, for any $\mathbb{E}$. The space $\mathrm{L}(\mathbb{E}, \mathbb{F})$ is a closed linear subspace and it is a convenient vector space endowed with the initial topology relative to the inclusion mapping.

(ii) If $\mathbb{E}$ is a convenient vector space then a curve $c : \mathbb{R} \to \mathrm{L}(\mathbb{E}, \mathbb{F})$ is smooth if and only if $t \mapsto c(t)(x)$ is a smooth curve in $\mathbb{F}$, for all $x \in \mathbb{E}$.

Proposition A.8. *Let $\mathbb{E}, \mathbb{F}, \mathbb{G}$ be convenient vector spaces, $U \subset \mathbb{E}$, $V \subset \mathbb{F}$ c^∞-open subsets:*

(i) If $f : U \to \mathbb{F}$ is convenient smooth, then the mapping $df : U \to \mathrm{L}(\mathbb{E}, \mathbb{F})$ is convenient smooth and linear bounded in the second component, where:

$$d_x f(h) := \left.\frac{d}{dt}\right|_{t=0} f(x + th).$$

(ii) The differentiation operator $d : \mathrm{C}^\infty(U, \mathbb{F}) \to \mathrm{C}^\infty(U, \mathrm{L}(\mathbb{E}, \mathbb{F}))$ exists, is linear and bounded (smooth) and the chain rule holds:

$$d_x(f \circ g)(v) = d_{g(x)} f(d_x g(v)).$$

(iii) Convenient smooth mappings are continuous with respect to the c^∞-topology.

(iv) Multilinear mappings are convenient smooth if and only if they are bounded and for the derivative we have the product rule:

$$d_{(x_1,\dots x_n)} f(v_1, \dots, v_n) = \sum_{i=1}^{n} f(x_1, \dots, x_{i-1}, v_i, x_{i+1}, \dots, x_n).$$

(v) (Smooth uniform boundedness) A linear mapping $f : \mathbb{E} \to \mathrm{C}^\infty(V, \mathbb{G})$ is convenient smooth (bounded) if and only if $ev_v \circ f : \mathbb{E} \to \mathbb{G}$ is convenient smooth, for each $v \in V \subset \mathbb{F}$, where $\mathrm{ev}_v : \mathrm{C}^\infty(V, \mathbb{G}) \to \mathbb{G}$ denotes the evaluation mapping.

(vi) (Smooth detection principle) A mapping $f : U \subset \mathbb{E} \to \mathrm{L}(\mathbb{F}, \mathbb{G})$ is convenient smooth if and only if $\mathrm{ev}_y \circ f : U \to \mathbb{G}$ is convenient smooth for all $y \in \mathbb{F}$.

(vii) A mapping $f : U \to \mathrm{L}(\mathbb{F}, \mathbb{G})$ is convenient smooth if and only if the mapping $f : U \to \mathrm{C}^\infty(\mathbb{F}, \mathbb{G})$ is convenient smooth, i.e. $\mathrm{L}(\mathbb{F}, \mathbb{G}) \hookrightarrow \mathrm{C}^\infty(\mathbb{F}, \mathbb{G})$ is initial.

Proposition A.9. *(Cartesian closedness) Let $U_i \subseteq \mathbb{E}_i$, $i = \overline{1,2}$, be two c^∞-open subsets in locally convex spaces which need not to be convenient. Then a mapping $f : U_1 \times U_2 \to \mathbb{F}$ is convenient smooth if and only if the cannonically associated mapping $f^\vee : U_1 \to \mathrm{C}^\infty(U_2, \mathbb{F})$ exists and is convenient smooth:*

$$\mathrm{C}^\infty(U_1 \times U_2, \mathbb{F}) = \mathrm{C}^\infty(U_1, \mathrm{C}^\infty(U_2, \mathbb{F})).$$

As a consequence of the cartesian closedness property let us note that the evaluation mapping

$$\mathrm{ev} : \mathrm{C}^\infty(U, \mathbb{F}) \times U \to \mathbb{F}, \;\; \mathrm{ev}(f, x) := f(x),$$

and the composition mapping

$$\circ : \mathrm{C}^\infty(\mathbb{F}, \mathbb{G}) \times \mathrm{C}^\infty(U, \mathbb{F}) \to \mathrm{C}^\infty(U, \mathbb{G})$$

are convenient smooth.

Proposition A.10. *Let $f : \mathbb{E} \to \mathbb{F}$ and $A : \mathbb{E} \to \mathrm{L}(\mathbb{F}, \mathbb{G})$ be convenient smooth mappings, then*

$$d_x(A(\cdot)f(\cdot))v = d_xA(v)(f(x)) + A(x)(d_xf(v)),$$

for all $x, v \in \mathbb{E}$.

Proof. The evaluation mapping $\mathrm{ev} : \mathrm{C}^\infty(\mathbb{F}, \mathbb{G}) \times \mathbb{F} \to \mathbb{G}$ is convenient smooth and the curve $c : \mathbb{R} \to \mathrm{L}(\mathbb{F}, \mathbb{G})$ is smooth iff $c : \mathbb{R} \to \mathrm{C}^\infty(\mathbb{F}, \mathbb{G})$ is smooth by Proposition A.8 (vii). Thus $\mathrm{ev} : \mathrm{L}(\mathbb{F}, \mathbb{G}) \times \mathbb{F} \to \mathbb{G}$ is convenient smooth and bilinear. Hence

$$d_x(A(\cdot)f(\cdot))v = d_x(\mathrm{ev}(A(\cdot), f(\cdot)))(v) = d_{(A(x),f(x))}\mathrm{ev}(d_xA(v), d_xf(v))$$

$$= \mathrm{ev}_{d_xf(v)}A(x) + \mathrm{ev}_{f(x)}d_xA(v) = d_xA(v)(f(x)) + A(x)(d_xf(v)),$$

using Proposition A.8 (iii). □

Remark A.11. *The identity is also true for $L^k(\mathbb{E}, \mathbb{F})$ instead of $L(\mathbb{E}, \mathbb{F})$.*

B Vector bundles over a convenient manifold

For $x \in \mathbb{E}$ the *kinematic tangent vector* with foot point x is the pair (x, X), $X \in \mathbb{E}$. The space $T_x\mathbb{E} = \mathbb{E}$ of kinematic tangent vectors with foot point x consists

of all derivatives $c^{'}(0)$ of the smooth curves $c{:}\mathbb{R} \to \mathbb{E}$ with $c(0) = x$. For a convenient smooth mapping $f : \mathbb{E} \to \mathbb{F}$ the *kinematic tangent mapping* at x is defined by

$$T_x f : T_x\mathbb{E} \to T_{f(x)}\mathbb{F}, \;\; T_x f(x, X) := (f(x), d_x f(X)).$$

If M is a convenient smooth manifold on the set

$$\bigcup_{\alpha\in A} \mathcal{U}_\alpha \times \mathbb{E}_\alpha \times \{\alpha\},$$

we consider the equivalence relation

$$(p, v, \alpha) \sim (q, w, \beta) \iff p = q, \;\text{ and }\; d_{\varphi_\beta(p)}(\varphi_{\alpha\beta})w = v$$

and denote the quotient set by TM, the *kinematic tangent bundle* of M. We define $\pi_M : TM \to M$ by $\pi_M([p, v, \alpha]) = p$ and $T\mathcal{U}_\alpha := \pi_M^{-1}(\mathcal{U}_\alpha) \subset TM$. The mapping $Tu_\alpha : T\mathcal{U}_\alpha \to u_\alpha(\mathcal{U}_\alpha) \times \mathbb{E}_\alpha$ defined by

$$Tu_\alpha([p, w, \beta]) = (u_\alpha(p), d_{u_\beta(p)}(u_{\alpha\beta})w)$$

is giving a chart for an atlas $(T\mathcal{U}_\alpha, Tu_\alpha)_{\alpha\in A}$ of TM.

The set $T_pM := \pi_M^{-1}(p)$ is called the *fiber* over p of the tangent bundle. It carries a canonical convenient vector space structure induced by

$$T_pu_\alpha := Tu_\alpha|_{T_pM} : T_pM \to \{p\} \times \mathbb{E}_\alpha \cong \mathbb{E}_\alpha,$$

for $p \in \mathcal{U}_\alpha$. For connected convenient manifolds, e.g. $\mathrm{Diff}^\infty_+(\mathbb{S}^1)$, the fiber of the tangent bundle coincides with the modelling space. The same observation holds, in particular, for the Lie algebra of a connected Lie group.

The kinematic tangent bundle can be also defined as the quotient of the space $C^\infty(\mathbb{R}, M)$ by the equivalence relation: $c_1 \sim c_2 \iff c_1(0) = c_2(0)$ and in each chart $(\mathcal{U}_\alpha, u_\alpha)$ with $c_1(0) = c_2(0) \in \mathcal{U}_\alpha$ we have $(u_\alpha \circ c_1)^{'}(0) = (u_\alpha \circ c_2)^{'}(0)$. In this way any curve $c \in \mathrm{C}^\infty(\mathbb{R}, M)$ corresponds to the kinematic tangent vector $[c(0), (u_\alpha \circ c)^{'}(0), \alpha]$. For a convenient smooth mapping $f : M \to N$ the tangent mapping Tf will send the equivalence class $[c]$ in the equivalence class $[f \circ c]$ and its local representative with respect to some charts is the kinematic tangent mapping of the local representative of f.

Remark B.1. *On convenient vector spaces another kind of tangent vectors are available: the operational tangent vectors, see Section 28.1 in [30]. The two notions will not coincide in general and will give two different tangent bundles of a convenient manifold. This difference causes some headaches and leads to the existence of* 12 *different notions of differential forms in the convenient setting. The "right" notion for a convenient manifold is the kinematic tangent bundle, the*

other one does not even preserve products or there exist no vertical lifts. Anyway, for manifolds modelled on nuclear Fréchet spaces the two notions coincide and one recovers the result from the finite dimensional case: any tangent vector is a derivation.

In the convenient setting it's worth reducing everything to curves, thus the convenient vector space $C^\infty(\mathbb{R}, \mathbb{E})$ will play a central role. First of all, the space of $\mathbb{E}$-valued functions on a manifold M will be endowed with the initial topology with respect to the mappings

$$C^\infty(M,\mathbb{E}) \xrightarrow{(i_{\mathcal{U}_\alpha})^*} C^\infty(\mathcal{U}_\alpha,\mathbb{E}) \xrightarrow{(u_\alpha^{-1})^*} C^\infty(U_\alpha,\mathbb{E}) \xrightarrow{c^*} C^\infty(\mathbb{R},\mathbb{E})$$

The space of smooth sections of TM is endowed with the topology given by the closed embedding

$$\Gamma(TM) \to \prod_\alpha C^\infty(\mathcal{U}_\alpha,\mathbb{E})$$

$$s \to (pr_2 \circ \psi_\alpha \circ s|_{\mathcal{U}_\alpha})_\alpha$$

which is actually the initial topology with respect to the family of mappings

$$\Gamma(TM) \xrightarrow{(i_{\mathcal{U}_\alpha})^*} \Gamma(TM|_{\mathcal{U}_\alpha}) \xrightarrow{(pr_2\circ\psi_\alpha)_*} C^\infty(\mathcal{U}_\alpha,\mathbb{E}) \xrightarrow{(u_\alpha^{-1})^*} C^\infty(U_\alpha,\mathbb{E}) \xrightarrow{c^*} C^\infty(\mathbb{R},\mathbb{E})$$

where $i_{\mathcal{U}_\alpha}$ is the restriction to $\mathcal{U}_\alpha$ and ψ_α is a local trivialization of TM.

Let now $\pi : E \to M$ be a convenient smooth mapping between convenient smooth manifolds. By a *vector bundle chart* on $(E, \pi, M, \mathbb{F})$ we mean a pair $(\mathcal{U}, \psi)$, where $\mathcal{U}$ is an open subset in M, and where ψ is a fiber respecting diffeomorphism $\psi : E_\mathcal{U} := \pi^{-1}(\mathcal{U}) \to \mathcal{U} \times \mathbb{E}$ such that

$$pr_1 \circ \psi = \pi,$$

where $\mathbb{E}$ is a fixed convenient vector space, called the *standard fiber*.

Two vector bundle charts $(\mathcal{U}_\alpha, \psi_\alpha), (\mathcal{U}_\beta, \psi_\beta)$ are called *compatible*, if the mapping $\psi_1 \circ \psi_2^{-1}$ is a fiber linear isomorphism

$$\psi_\alpha \circ \psi_\beta^{-1}(p, v) = (p, \psi_{\alpha\beta}(p)v), \qquad v \in \mathbb{E},$$

for some mapping $\psi_{\alpha\beta} : \mathcal{U}_{\alpha\beta} := \mathcal{U}_\alpha \cap \mathcal{U}_\beta \to GL(\mathbb{E})$. The mapping is then unique and convenient smooth into $L(\mathbb{E}, \mathbb{E})$, and is called the *transition function* between the two vector bundle charts.

Remark B.2. *Compare this definition with the definition of a Banach vector bundle, presented in [26]. An extension of a result known for Banach spaces ([26] Proposition III.1.1, [37] Theorem 5.3) holds if the mapping $f : U \times \mathbb{E} \to \mathbb{F}$ is a convenient smooth and linear in the second argument, then the mapping of U into $L(\mathbb{E}, \mathbb{F})$, $x \mapsto f(x, \cdot)$, is a convenient smooth mapping. The converse also holds, by Proposition A.9, since $L(\mathbb{E}, \mathbb{F}) \subset \mathrm{C}^\infty(\mathbb{E}, \mathbb{F})$ is initial. In [26] the author has omitted the veracity of the result for infinite dimensional Banach spaces and thus the conditions VB1 and VB2, in Chapter III, are enough to define a Banach vector bundle. With VB1 and VB2 in Definition III.1 of [26] we obtain the above formulation for Banach manifolds.*

If $(E, \pi, M, \mathbb{E})$ is a convenient smooth vector bundle with a vector bundle atlas $(\varphi_\alpha, \pi^{-1}(\mathcal{U}_\alpha))_{\alpha \in A}$, then we define the dual vector bundle

$$E^{'} := \bigcup_{p \in M} E_p^{'},$$

with the standard fiber the bornological dual $\mathbb{E}^{'}$ and the transition functions

$$\psi_{\alpha\beta}(p) := (\varphi_{\beta\alpha}(p))^t,$$

naturally obtained using the transpose mapping relative to the bornological duals. For two convenient smooth vector bundles $(E, \pi_1, M, \mathbb{E})$ and $(F, \pi_2, M, \mathbb{F})$ with $(\pi_1^{-1}(\mathcal{U}_\alpha), \varphi_\alpha)_{\alpha \in A_1}$, and $(\pi_2^{-1}(\mathcal{V}_\alpha), \phi_\alpha)_{\alpha \in A_2}$ the corresponding vector bundle atlases, one can construct another vector bundle over M, the Hom-bundle

$$L(E, F) := \bigcup_{p \in M} L(E_p, F_p),$$

having the standard fiber the convenient vector space $L(\mathbb{E}, \mathbb{F})$. The transition functions are

$$\psi_{\alpha\beta}(p)(T) := \phi_{\alpha\beta}(p) \circ T \circ \varphi_{\alpha\beta}^{-1}(p), \qquad T \in L(\mathbb{E}, \mathbb{F}).$$

With this terminology we have $E^{'} := L(E, M \times \mathbb{R})$. We are ready to define now the *kinematic cotangent bundle* $T^{'}M$, having the transition functions

$$\psi_{\alpha\beta}(p) := T_{\varphi_\alpha(p)}(\varphi_\beta \circ \varphi_\alpha^{-1})^t \in GL(\mathbb{E}^{'}) \subset L(\mathbb{E}^{'}, \mathbb{E}^{'}).$$

If we use the Gâteaux smoothness to define a manifold modelled by locally convex spaces then we can not define differential forms as Gâteaux smooth sections of a vector bundle, see [35] for a discussion. This is the case because for non normable locally convex spaces the evaluation mapping:

$$\mathrm{ev} : \mathbb{E} \times \mathbb{E}^{'} \to \mathbb{R},$$

is not continuous for any linear topology on $\mathbb{E}'$, by a theorem of B. Maissen [28].

In the convenient setting a kinematic differential k-form is defined as a convenient smooth section of the vector bundle $L^k_{alt}(TM, M \times \mathbb{R})$:

$$\Omega^k(M) := \Gamma(L^k_{alt}(TM, M \times \mathbb{R})),$$

with the modelling space $L^k_{alt}(\mathbb{E}, \mathbb{R})$, the space of bounded k-linear alternating mappings, where $\mathbb{E}$ is the modelling space of M. This construction is the only one which is invariant under Lie derivatives, pullbacks or exterior derivatives. There are a lot of other candidates but all have major drawbacks, see Section 33 of [30] for a discussion.

Remark B.3. *The reason why this construction is possible is the following: the evaluation mapping* $\mathrm{ev} : \mathbb{E} \times \mathbb{E}' \to \mathbb{R}$ *is always convenient smooth, thus continuous relative to the* c^∞*-topology on* $c^\infty(\mathbb{E} \times \mathbb{E}')$*. But* $c^\infty(\mathbb{E} \times \mathbb{E}')$ *is not a topological vector spaces in general (if* $\mathbb{E}$ *is not normable), and thus* ev *is not continuous relative to some linear topology on the space* $\mathbb{E}'$*, to avoid any contradiction with Maissen's theorem.*

The space $\Omega^k(M)$ carries the structure of a convenient vector space, induced by the closed embedding

$$\Omega^k(M) \to \prod_\alpha C^\infty(\mathcal{U}_\alpha, L^k_{alt}(\mathbb{E}, \mathbb{R})),$$

$$\omega \mapsto pr_2 \circ \psi_\alpha \circ (\omega | \mathcal{U}_\alpha),$$

having the initial topology induced by the mappings

$$\Gamma(L^k_{alt}(TM, M \times \mathbb{R})) \xrightarrow{(pr_2 \circ \psi_\alpha)_* \circ (i_{\mathcal{U}_\alpha})^*} C^\infty(\mathcal{U}_\alpha, L^k_{alt}(\mathbb{E}, \mathbb{R})) \xrightarrow{c^* \circ (u_\alpha^{-1})^*} C^\infty(\mathbb{R}, L^k_{alt}(\mathbb{E}, \mathbb{R}))$$

where $u_\alpha : \mathcal{U}_\alpha \to \mathbb{E}$ is a smooth atlas of M, ψ_α the induced vector bundle chart, a similar construction to the one for $\Gamma(TM)$. In the same manner the space $\Omega^k(M, V)$, of differential forms with values in a convenient vector space V, becomes a convenient vector space.

Remark B.4. *The following mappings are convenient smooth:*

$$d : \Omega^k(M) \to \Omega^{k+1}(M) \quad \textit{(exterior differentiation operator)}$$

$$i : \Gamma(TM) \times \Omega^k(M) \to \Omega^{k-1}(M) \qquad \textit{(insertion operator)}$$

$$f^* : \Omega^k(M) \to \Omega^k(N) \qquad \textit{(pullback operator)}$$

References

[1] V. I. Arnold, Sur la géométrie différentielle des groupes de Lie de dimension infinie et ses applications à l'hydrodynamique des fluides parfaits, *Ann. Inst. Fourier (Grenoble)*, **16** (1966), 319–361.

[2] V. I. Averbukh, O. G. Smolyanov. The various definitions of the derivative in linear topological spaces. *Russian Math. Surveys 23*, no 4, 67-113, 1968.

[3] A. Bastiani, Applications différentiable et variétés différentiables de dimension infinie, *J. Anal. Math* , **13** (1964), 1–114.

[4] M. Bauer, J. Escher and B. Kolev, Local and global well-posedness of the fractional order EPDiff equation on R^d, *Journal of Diff. Equations* , **258** (2015), 2010–2053.

[5] J. Boman. Differentiability of a function and of its compositions with functions of one variable, *Math. Scand.* , **20** (1967), 249–268.

[6] E.C. Cismas, Euler-Poincaré equations on semi-direct products, *Monatshefte für Math.*, **179** (2014), 491–507.

[7] E.C. Cismas, Euler-Poincaré-Arnold equations on semi-direct products II *Discrete and Continuous Dynamical Systems- Series A*, **36** (2016), 5993-6022

[8] E.C. Cismas and N. Lupa, A Nash-Moser approach for the Euler-Arnold equations, *Monatsh Math (2019)*, https://doi.org/10.1007/s00605-019-01344-z

[9] A. Constantin and B. Kolev, On the geometric approach to the motion of inertial mechanical systems, *J. Phys. A*, **35** (2002), 51–79.

[10] A. Constantin and B. Kolev, Geodesic flow on the diffeomorphism group of the circle, *Comment. Math. Helv.*, **78** (2003), 787–804.

[11] C.T.J. Dodson and G.N. Galanis, Second order tangent bundles of infinite dimensional manifolds. *Journal of Geometry and Physics*, **52** (2004), 127–136.

[12] D. G. Ebin and J. E. Marsden, Groups of diffeomorphisms and the motion of an incompressible fluid, *Ann. of Math.* , **2** (1970), 102–163.

[13] J. Escher and B. Kolev, Right-invariant Sobolev metrics of fractional order on the diffeomorphisms group of the circle, *Journal of Geometric Mechanics* **6** (2014), 335–372.

[14] J. Escher, B. Kolev, and M. Wunsch, The geometry of a vorticity model equation, *Commun. Pure Appl. Anal.*, **11** (2012), 1407–1419.

[15] J. Escher and B. Kolev, Geometrical methods for equations of hydrodynamical type, *J. Nonlinear Math.Phys.* **19**, (2012), 161–178.

[16] O. Esen and H.Gümral, Tulczyjew's triplet for Lie groups I: Trivializations and reductions *Journal of Lie Theory* **24**, (2014), 1115–1160.

[17] A. Frölicher, A. Kriegl. Linear Spaces and differentiation Theory. *J. Wiley, Chichester* , 1988.

[18] L. Guieu and C. Roger. L'algèbre et le groupe de Virasoro. *Les Publications CRM, Montreal, QC*, 2007. Aspects géométriques et algébriques, généralisations.

[19] F. Gach. Topological versus Bornological Concepts in Infinite Dimensions, *Master thesis, Univ. Vienna*, 2004.

[20] R. S. Hamilton, The inverse function theorem of Nash and Moser, *Bull. Amer. Math. Soc.*, **7** (1982) 65–222.

[21] H. H. Keller, *Differential Calculus in Locally Convex Spaces*, Lecture Notes in Math., Springer-Verlag, 1974.

[22] A. A. Kirillov, Infinite dimensional Lie groups: their orbits, invariants and representations. The geometry of moments, *Twistor Geometry and Non-Linear Systems*, **970** (1982), 101–123.

[23] J. Escher, M. Kohlmann and J. Lenells, The geometry of the two-component Camassa–Holm and Degasperis–Procesi equations. *Journal of Geometry and Physics*, **61** (2011), 436–452.

[24] B. Kolev, Lie groups and mechanics: An introduction, *J. Nonlinear Math. Phys.*, **11** (2004), 480–498.

[25] S. Kouranbaeva, The Camassa-Holm equation as a geodesic flow on the diffeomorphism group. *J. Math.Phys.* 40, 857-868, 1999.

[26] S. Lang, *Fundamentals of Differential Geometry*, Graduate Texts in Mathematics„ **191**, Springer-Verlag, New York, 1999.

[27] J. Lenells, The Hunter-Saxton equation: a geometric approach, *Math. Anal.*, **40**, (2008), 266-277.

[28] B. Maissen. Über Topologien im Endomorphismenraum eines topologischen Vektorraumes. *Math. Annalen*, 151, 283-285, 1963.

[29] A. D. Michal, Differentiable calculus in linear topological spaces, *Proc. Natl. Acad. Sci.* **24** (1938), 340–342.

[30] P. Michor and A. Kriegl, *The Convenient Setting of Global Analysis*, Math. Surveys and Monographs, **53**, AMS 1997.

[31] P. Michor and T. Ratiu, *On the geometry of the Virasoro-Bott group*, Journal of Lie Theory, **8**, 2 (1998), 293-309

[32] J. Milnor, Remarks on infinite-dimensional Lie groups, *Relativity, groups and topology, II (Les Houches,* , North-Holland, Amsterdam, (1984), 1007–1057.

[33] K. Modin, Generalized Hunter–Saxton equations, optimal information transport, and factorization of diffeomorphisms. *The Journal of Geometric Analysis*, (2014) **25** (2): 1306—1334.

[34] O. Muller, A metric approach to Fréchet geometry, *J. Geom. Phys.*, **58** (2008), 1477–1500.

[35] K. H. Neeb, Towards a Lie theory of locally convex groups. *Japan. J. Math.* , **1** (2006), 291–468.

[36] H. Omori, Groups of diffeomorphisms and their subgroups, *Translations of Amer. Math. Soc.*, **179**, 1973.

[37] H. Omori, Infinite-dimensional Lie Groups, *Translations of Math. Monographs*, **158**, 1997.

[38] G. Rezaie. R. Malekzadeh. Sprays on Fréchet modelled manifolds. *Int. Math. Forum* 5, No. 59, 2901-2909, 2010.

[39] N. K. Smolentsev. Diffeomorphism groups of compact manifolds. *Journal of Math. Sciences* Vol. 146. No. 6, 2007.

[40] L. Younes, F. Arrate and M. Miller Evolutions equations in computational anatomy *N*euroImage 45 (1), S40-S50, 2009.

[41] M. Wunsch. On the geodesic flow on the group of diffeomorphisms of the circle with a fractional Sobolev right-invariant metric. *J. Nonlinear Math. Phys.*, 17(1):7–11, 2010.

[42] C. Vizman. Geodesic equations and diffeomorphisms groups. *J.Symmetry, Integrability and Geometry: Methods and Applications*, SIGMA, 4, 030, 2008.

Emanuel-Ciprian CISMAŞ
Department of Mathematics
Politehnica University of Timişoara
Piaţa Victoriei, nr.2, 300006 Timişoara, România
emanuel.cismas@upt.ro

BULETINUL ŞTIINŢIFIC
Al
UNIVERSITĂŢII "POLITEHNICA" DIN TIMIŞOARA

Tom 65 (79), 1	MATEMATICĂ – FIZICĂ	2020

PIECEWISE POLYNOMIAL LEAST SQUARES METHOD FOR NONLINEAR HEAT TRANSFER PROBLEMS

Mădălina Sofia PAŞCA

Abstract

In this paper is used a recently introduced approximation method, namely the Piecewise Polynomial Least Squares Method (PWPLSM), in order to compute analytical approximate polynomial solutions for several nonlinear heat transfer problems.

Analyzing the errors obtained by applying the Piecewise Polynomial Least Squares Method with those found in the literature, the accuracy of the method is illustrated. [1]

1 Introduction

The heat transfer phenomena are mainly nonlinear and thus they are best modeled by using nonlinear equations. These equations most of the time can not be solved analytically using traditional methods and, when the numerical solutions are not sufficient, an approximate analytical solution must be computed. In recent years many methods have been developed to compute approximate solutions for nonlinear heat transfer problems. Is mentioned only some of the methods that led to obtaining approximate solutions for this type of equations:

- the Homotopy perturbation method (HPM)([2],[1],[3]),

[1]Mathematical Subject Classification(2010):*34K28, 45L05*
Keywords and phrases:*Nonlinear heat transfer problems, Piecewise Polynomial Least Squares Method (PWPLSM), analyrical approximate polynomial solutions*,

- the Optimal Homotopy Asymptotic Method (OHAM)([4]),
- the Homotopy analysis method (HAM)([5],[6]),
- the Squared remainder minimization method (SRMM)([7]),
- the Generalized approximation method (GAM)([8]),
- the Least Squares Differential Quadrature Method (LSDQM) ([9]).

In this paper is computed approximate analytical solutions for some well-known nonlinear heat transfer problems ([16],[17],[18]) modeled by using nonlinear ordinary differential equations.

In the second section is described the Piecewise Polynomial Least Squares Method (PWPLSM), which is used for determine analytical approximate polynomial solutions for the above-mentioned type of problems. In the last section with numerical application, is compared approximate solutions obtained by using PWPLSM with previous approximate solutions presented in ([4],[8],[7],[10],[9]). The computations show that by using Piecewise Polynomial Least Squares Method we obtain approximations with an error smaller than the errors obtained by using other methods thus the usefulness of the method being demonstrated.

2 Piecewise Polynomial Least Squares Method (PWPLSM)

We consider a problem consisting of a nonlinear differential equation of order n:

$$y^{(n)}(x) = F(y^{(n-1)}(x), y^{(n-2)}(x), \cdots, y^{(1)}(x), y(x), x) \tag{1}$$

where F is a continuous function, y is an absolutely continuous function, $x \in [a, b]$ and the boundary conditions:

$$\begin{aligned} d_{1i}y^{(n-1)}(a) + d_{2i}y^{(n-1)}(b) + d_{3i}y^{(n-2)}(a) + d_{4i}y^{(n-2)}(b) + \cdots + \\ + d_{(2n-3)i}y^{(1)}(a) + d_{(2n-2)i}y^{(1)}(b) + d_{(2n-1)i}y(a) + d_{2ni}y(b) = \mu_{1i}, \quad i = \overline{1,n} \end{aligned} \tag{2}$$

are satisfied.

We will consider a division Δ_M of the interval $I = [a, b]$ consisting of $M + 1$ equidistant points: $a = a_0 < a_1 < a_2 < \cdots < a_{M-1} < a_M = b$.

To the equation (1) we attach the following operator:

$$\mathcal{D}(y(x)) = y^{(n)}(x) - F(y^{(n-1)}(x), y^{(n-2)}(x), \cdots, y^{(1)}(x), y(x), x). \tag{3}$$

We denote by $\tilde{y}_i(x)$ an approximate solution of the equation (1) on each subinterval $I = [a_i, a_{i+1}]$.

By replacing in $\mathcal{D}$ the exact solution $y(x)$ with this approximate solution we obtain the *reminder* on each subinterval:

$$\mathcal{R}_i(x, \tilde{y}_i(x)) = \mathcal{D}(\tilde{y}_i(x)), \qquad x \in [a_i, a_{i+1}]. \tag{4}$$

Definition 1. *We call an* ***ϵ-approximate piecewise polynomial (pwpl) solution*** *of the problem (1 - 2) related to the division Δ_M an approximate polynomial solution $\tilde{y}(x) = \tilde{y}_i(x), x \in I_i$ which satisfies on each subinterval the following relations:*

$$\mathcal{R}_i(x, \tilde{y}_i(x)) < \varepsilon, \quad \varepsilon > 0, \quad i = \overline{0, M}, \tag{5}$$

$$\begin{aligned} d_{1i}\tilde{y}^{(n-1)}(a) + d_{2i}\tilde{y}^{(n-1)}(b) + d_{3i}\tilde{y}^{(n-2)}(a) + d_{4i}\tilde{y}^{(n-2)}(b) + \cdots + \\ d_{(2n-3)i}\tilde{y}^{(1)}(a) + d_{(2n-2)i}\tilde{y}^{(1)}(b) + d_{(2n-1)i}\tilde{y}(a) + d_{2ni}\tilde{y}(b) = \mu_{1i}, \quad i = \overline{1, n} \end{aligned} \tag{6}$$

Definition 2. *We call a* ***week ϵ-approximate piecewise polynomial (pwpl) solution*** *of the problem (1 - 2) an approximate polynomial solution $\tilde{y}(x) = \tilde{y}_i(x), x \in I_i$ which satisfies on each subinterval the relations:*

$$\int_{a_i}^{a_{i+1}} |\mathcal{R}_i(x, \tilde{y}_i(x)) < \varepsilon, \quad \varepsilon > 0, \quad i = \overline{0, M}, \tag{7}$$

$$\begin{aligned} d_{1i}\tilde{y}^{(n-1)}(a) + d_{2i}\tilde{y}^{(n-1)}(b) + d_{3i}\tilde{y}^{(n-2)}(a) + d_{4i}\tilde{y}^{(n-2)}(b) + \cdots + \\ d_{(2n-3)i}\tilde{y}^{(1)}(a) + d_{(2n-2)i}\tilde{y}^{(1)}(b) + d_{(2n-1)i}\tilde{y}(a) + d_{2ni}\tilde{y}(b) = \mu_{1i}, \quad i = \overline{1, n} \end{aligned} \tag{8}$$

Definition 3. *Let*

$$P_{im}(x) = c_{i0} + c_{i1}x + c_{i2}x^2 + \cdots + c_{im}x^m,$$

$c_{ij} \in \mathbb{R}, i = \overline{0, M}, \ j = \overline{0, m}.$

We call the sequence of polynomials $P_{im}(x)$ ***convergent*** *to the solution of the problem (1 - 2) if:*

$$\lim_{m \to \infty} \mathcal{R}_i(x, P_{im}(x)) = 0. \tag{9}$$

According to the Weierstrass Theorem on Polynomial Approximation, it follows that there exists a sequence of polynomials $P_{im}(x)$ which converges to the solution of the equation (1).

It is computed a weak ϵ - approximate pwpl solution, in the sense of the Definition 1, of the type:

$$\tilde{y}_i(x) = \sum_{k=0}^{m} c_{ik}x^k, m > 0 \tag{10}$$

where the coefficients $c_{i0}, c_{i1}, \cdots, c_{im}$ are calculated using the following algorithm:

1. By substituting the approximate solutions (10) in the equation (1) is obtained the expressions:

$$\mathcal{R}_i(x,\tilde{y}_i(x)) = y_i^{(n)}(x) - F(y_i^{(n-1)}(x), y_i^{(n-2)}(x), \cdots, y_i^{(1)}(x), y_i(x), x)$$
$$i = \overline{0, M-1}, \quad x \in [a_i, a_{i+1}] \tag{11}$$

2. On each interval I_i is attached to the equation (1) the following functional:

$$\mathcal{J}_i(c_{i0}, c_{i1}, c_{i2}, \cdots, c_{im}) = \int_{a_i}^{a_{i+1}} \mathcal{R}_i^2(x, \tilde{y}_i(x))dx \tag{12}$$

3. Is computed the real values $c_{i0}^0, c_{i1}^0, \cdots, c_{im}^0$ as the values which give the minimum of the functionals $\mathcal{J}_i$.

4. With coefficients $c_{i0}^0, \cdots, c_{im}^0$ previously determined is constructed the polynomials:

$$T_{im}(x) = \sum_{k=0}^{m} c_{ik}^0 x^k. \tag{13}$$

Theorem 2.1. *The sequence of polynomials $T_{im}(x)$ from (13) satisfies the property:*

$$\lim_{m\to\infty} \int_{a_i}^{a_i+1} \mathcal{R}_i^2(x, T_{im}(x))dx = 0. \tag{14}$$

Proof: Based on the way the polynomials $T_{im}(t)$ are computed and taking into account the relations (11)-(13), the following inequalities are satisfied:

$$0 \leq \int_{a_i}^{a_{i+1}} \mathcal{R}_i^2(x, T_{im}(x))dx \leq \int_{a_i}^{a_{i+1}} \mathcal{R}_i^2(x, P_{im}(x))dx, \ \forall m \in \mathbb{N}. \tag{15}$$

It follows that:

$$0 \leq \lim_{m\to\infty} \int_{a_i}^{a_{i+1}} \mathcal{R}_i^2(x, T_{im}(x))dx \leq \lim_{m\to\infty} \int_{a_i}^{a_{i+1}} \mathcal{R}_i^2(x, P_{im}(x))dx = 0. \tag{16}$$

and:

$$\lim_{m\to\infty} \int_{a_i}^{a_{i+1}} \mathcal{R}_i^2(x, T_{im}(x))dx = 0. \tag{17}$$

Moreover, $\forall \epsilon > 0,\ \exists m_o \in \mathbb{N},\ m > m_0$ it follows that $T_{im}(x)$ is a *weak ϵ-approximate polynomial solution* of the equation (1) to each interval I_i and the piecewise polynomial:

$$T_m(x) = \begin{cases} T_{1m}(x), x \in [a_0, a_1] \\ T_{2m}(x), x \in [a_1, a_2] \\ \cdots \\ T_{Mm}(x), x \in [a_{M-1}, b] \end{cases} \tag{18}$$

is a *weak ϵ-approximate piecewise polynomial solution* of the equation, on the interval $I = [a, b]$.

3 Application

We consider a lumped system of combined convective–radiative heat transfers. The specific heat coefficient is a linear function of temperature ([7],[10],[11]):

$$c = c_a(1 + \gamma(T - T_a))$$

where γ is a constant and c_a is the specific heat at T_a.

The cooling process of the system is:

$$\rho V c \frac{dT}{d\tau} + hA(T - T_a) + E\sigma A(T^4 - T_s^4) = 0, \qquad T(0) = T_i \tag{19}$$

Performing the changes of variables:
$y = \dfrac{T}{T_i},\ y_a = \dfrac{T_a}{T_i},\ x = \dfrac{\tau(hA)}{\rho V c_a},\ \varepsilon_1 = \gamma T_i, \varepsilon_2 = \dfrac{E\sigma T_i^3}{h},\ y_s = \dfrac{T_s}{T_i}$ and $y_a = y_s = 0$
we obtain the following problem:

$$\begin{gathered} y'(x)(1 + \varepsilon_1 y(x)) + y(x) + \varepsilon_2 y^4(x) = 0, \\ y(0) = 1 \end{gathered} \tag{20}$$

Case 1: $\epsilon_1 = 1, \epsilon_2 = 1$

To verify the effectiveness of the method described in the previous section, an approximate annalytical solution is determined as follows:

- it divides the interval $I = [0, 1]$ into four subintervals of equal length:
  $0 = a_0 < a_1 < \cdots a_4 = 1$ and is computed on each subinterval $I_i = [a_i, a_{i+1}]$ an approximate solution of the type:

$$\tilde{y}_i(x) = \sum_{k=0}^{m} c_{ik} x^k, \quad m > 0, \quad i = \overline{0,4}.$$

- from initial conditions is determined c_{i0}.
- the corresponding remainders are: $\mathcal{R}_i(x, \tilde{y}_i(x))$.
- the following functionals are computed:

$$\mathcal{J}_i(c_{i1}, c_{i2}, \cdots c_{ik}) = \int_{a_i}^{a_{i+1}} \mathcal{R}_i^2(x, \tilde{y}_i(x))dx$$

Using an mathematical soft for minimizing $\mathcal{J}_i$ it obtaining the PWPLSM solution of the problem (20).

To the interval $I_1 = [0, 0.25]$, we conssider a third degree polynomial:

$$\tilde{y}_1(x) = c_{10} + c_{11}x + c_{12}x^2 + c_{13}x^3$$

and from initial condition $\tilde{y}_1(0) = 0.25$ is determined c_{10}.

The corresponding remainder is:

$$\mathcal{R}_1(x, \tilde{y}_1(x)) = \left(c_{11}x + c_{12}x^2 + c_{13}x^3 + 0.25\right)^4 + \left(c_{11} + 2c_{12}x + 3c_{13}x^2\right)\left(c_{11}x + c_{12}x^2 + c_{13}x^3 + 1.25\right) + c_{11}x + c_{12}x^2 + c_{13}x^3 + 0.25$$

The following functionals is computed: $\mathcal{J}_1(c_{11}, c_{12}, c_{13}) = \int_0^{0.25} \mathcal{R}_1^2(x, \tilde{y}_1(x))dx$

Minimizing $\mathcal{J}_1(c_{11}, c_{12}, c_{13})$ with respect to the real coefficients c_{11}, c_{12}, c_{13}, the PWPLSM solution of the problem (20) on the interval I_1 is:

$$\tilde{y}_1(x) = -0.01156x^3 + 0.0696x^2 - 0.2031x + 0.25$$

Going through the algorithm for each of the four subintervals I_i, the PWPLSM solution is obtained:

$$\tilde{y}(x) = \begin{cases} -0.01156x^3 + 0.0696x^2 - 0.2031x + 0.25, & x \in [0, 0.25] \\ 0.02558x^4 - 0.08186x^3 + 0.1922x^2 - 0.4573x + 0.6035, & x \in [0.25, 0.5] \\ 0.1646x^4 - 0.6051x^3 + 1.02x^2 - 1.258x + 1.189, & x \in [0.5, 0.75] \\ 0.852x^4 - 3.698x^3 + 6.431x^2 - 5.843x + 3.055, & x \in [0.75, 1] \end{cases}$$

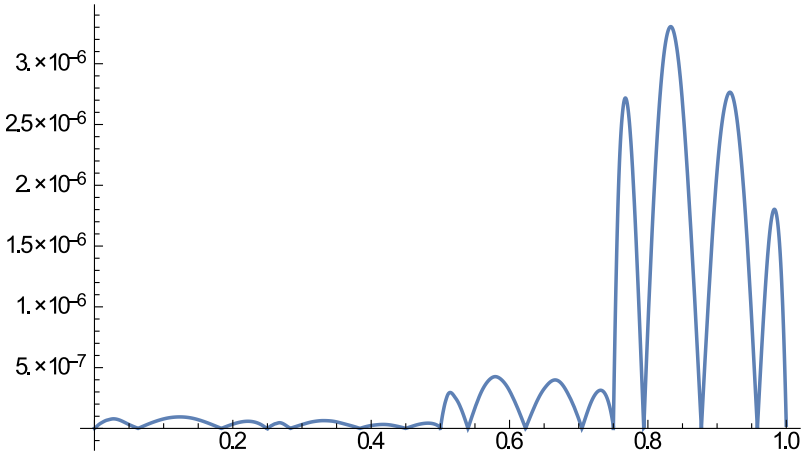

Figure 1: The absolute errors corresponding to $\tilde{y}(x)$ case $\epsilon_1 = 1, \epsilon_2 = 1$ App. 1

Table 1 presents the comparison between the erors obtained by different methods.

Table 1: Comparison of HPM, HAM, SRMM, LSDQ and PWPLSM for $\epsilon_1 = \epsilon_2 = 1$

x	HPM	HAM	$SRMM3^{rd}$ deg	$LSDQ3^{rd}$ deg	$PWPLSM$
0.1	1.209	1.86×10^{-2}	1.704×10^{-3}	5.38×10^{-4}	7.81×10^{-8}
0.2	7.24×10^{-1}	5.82×10^{-3}	4.66×10^{-4}	1.403×10^{-3}	3.49×10^{-8}
0.3	4.27×10^{-1}	6.18×10^{-3}	1.19×10^{-3}	3.37×10^{-3}	3.16×10^{-8}
0.4	2.47×10^{-1}	1.709×10^{-2}	2.12×10^{-3}	4.302×10^{-3}	2.36×10^{-8}
0.5	1.38×10^{-1}	2.68×10^{-2}	1.99×10^{-3}	3.89×10^{-3}	8.45×10^{-9}
0.6	7.49×10^{-2}	3.52×10^{-2}	9.44×10^{-4}	2.38×10^{-3}	3.09×10^{-7}
0.7	3.81×10^{-2}	4.25×10^{-2}	5.48×10^{-4}	3.06×10^{-4}	7.73×10^{-8}
0.8	1.78×10^{-2}	4.85×10^{-2}	1.78×10^{-3}	1.57×10^{-3}	8.41×10^{-7}
0.9	7.303×10^{-2}	5.34×10^{-2}	1.93×10^{-3}	2.35×10^{-3}	2.11×10^{-6}

We will compare the absolute errors for approximate PWPLSM solutions with previous solutions: HPM obtained by Ganji et all in ([10]), HAM obtained by

Damiary et all in ([12]) and $SRMM$ obtained by Caruntu and Bota in ([7]), obtained by Pasca et all in ([9]). Since the problem (20) does not have a known exact solution, we computed for each approximate solution the relative error as the difference (in absolute value) between the approximate solution and the numerical solution given by the Wolfram Mathematica software.

Better errors are observed in the case of the PWPLSM solution, even if the approximation was made with a polynomial of third degree.

Case 2: $\epsilon_1 = 1, \epsilon_2 = 0$

Using PWPLSM we computed the following piecewise polynomial approximate solution of equation (20):

$$\tilde{y}(x) = \begin{cases} 0.0613117x^2 - 0.199774x + 0.25, & x \in [0, 0.25] \\ 0.0738664x^2 - 0.370244x + 0.587944, & x \in [0.25, 0.5] \\ 0.0712664x^2 - 0.499941x + 0.982154, & x \in [0.5, 0.75] \\ 1.41134 - 0.596745x + 0.064394x^2, & x \in [0.75, 1] \end{cases}$$

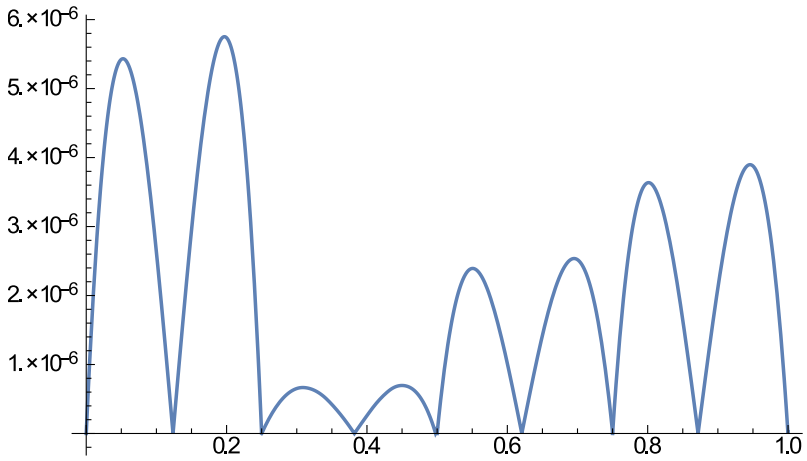

Figure 2: The absolute errors corresponding to $\tilde{y}(x)$ case $\epsilon_1 = 1, \epsilon_2 = 0$ App. 1

As in Case 1, we compare in Table 2 the erors from PWPLSM solutions with previous one: HPM obtained by Ganji in ([13]), HAM obtained by Abbasbandy in ([14]), $OHAM$ by Marinca and Herisanu in ([4]), $SRMM$ by Caruntu and Bota in ([7]) and Pasca et all in ([9]).

Table 2: Comparison erors of HPM, HAM, OHAM, SRMM, LSDQ and PWPLSM for $\epsilon_1 = 1, \epsilon_2 = 0$ in Application 1

x	HPM	HAM	$OHAM$	$SRMM2^{nd}$ deg	$LSDQ2^{nd}$ deg	$PWPLSM$
0.1	3.35×10^{-2}	3.67×10^{-5}	3.708×10^{-2}	1.56×10^{-3}	1.07×10^{-4}	2.63×10^{-4}
0.2	4.345×10^{-2}	1.954×10^{-3}	5.366×10^{-2}	8.024×10^{-5}	2.67×10^{-4}	5.73×10^{-6}
0.3	4.029×10^{-2}	4.091×10^{-3}	5.658×10^{-2}	1.138×10^{-3}	5.698×10^{-5}	6.51×10^{-7}
0.4	3.071×10^{-2}	5.415×10^{-3}	5.113×10^{-2}	1.669×10^{-3}	4.325×10^{-5}	2.58×10^{-7}
0.5	1.886×10^{-2}	5.541×10^{-3}	4.118×10^{-2}	1.730×10^{-3}	1.571×10^{-4}	7.42×10^{-8}
0.6	7.170×10^{-3}	4.432×10^{-3}	2.942×10^{-2}	1.379×10^{-3}	2.600×10^{-4}	1.01×10^{-6}
0.7	3.062×10^{-3}	2.243×10^{-3}	1.762×10^{-2}	6.736×10^{-4}	3.292×10^{-4}	2.51×10^{-6}
0.8	1.125×10^{-2}	7.827×10^{-4}	6.855×10^{-3}	3.304×10^{-4}	3.449×10^{-4}	3.63×10^{-6}
0.9	1.726×10^{-2}	4.372×10^{-3}	2.320×10^{-3}	1.575×10^{-3}	2.903×10^{-4}	2.11×10^{-6}

Case 3: $\epsilon_1 = 0, \epsilon_2 = 1$

In this case, the solution was calculated keeping, as in the other two cases, four equidistant subintervals of the interval $I = [a.b]$. On each subinterval $I_i = [a_i, a_{+i+1}]$ the approximate solution $\tilde{y}(x)$ is a third degree polynomial, the four coefficients were calculated to determine the approximate polynomial $\tilde{y}_i$.

For this case is computed the following piecewise polynomial least squares annalytical approximate solution:

$$\tilde{y}(x) = \begin{cases} 0.25 - 0.253847x + 0.133416x^2 - 0.0453598x^3, & x \in [0, 0.25] \\ 0.669223 - 0.806281x + 0.574651x^2 - 0.22838x^3, & x \in [0.25, 0.5] \\ 1.73516 - 3.16098x + 2.94193x^2 - 1.12119x^3, & x \in [0.5, 0.75] \\ 6.39624 - 14.8875x + 13.5242x^2 - 4.35673x^3, & x \in [0.75, 1] \end{cases}$$

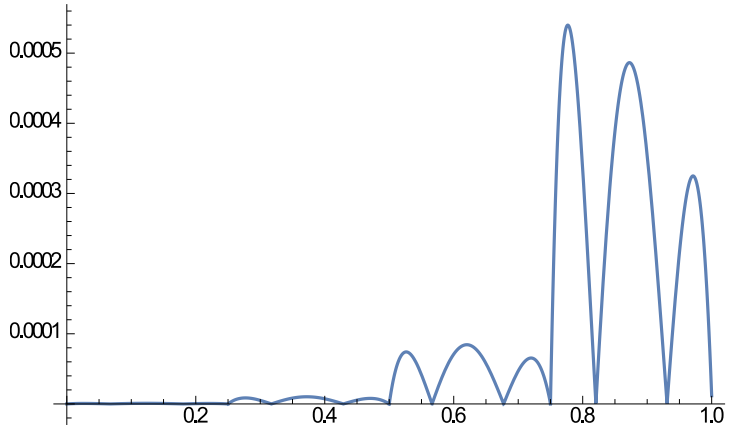

Figure 3: The absolute errors corresponding to $\tilde{y}(x)$ case $\epsilon_1 = 0, \epsilon_2 = 1$ App. 1

In Table 3 we present the comparison between the errors of solutions obtained

by PWPLSM and the erors of solution obtained by Rajabi et all in ([15]) using HPM, Domairry et all in ([12]) using HAM, Caruntu and Bota in ([7]) using $SRMM$ and Pasca et all usind LSDQM in ([9]).

Table 3: Comparison of HPM, HAM, SRMM, LSDQ and PWPLSM erors for $\epsilon_1 = 0, \epsilon_2 = 1$ in Application 1

t	HPM	HAM	$SRMM5^{th}$ deg	$LSDQ5^{nd}$ deg	$PWPSM$
0.1	2.24×10^{-3}	1.18×10^{-5}	6.08×10^{-5}	2.52×10^{-3}	7.18×10^{-7}
0.2	9.47×10^{-3}	8.72×10^{-4}	1.25×10^{-3}	3.51×10^{-3}	4.47×10^{-7}
0.3	1.79×10^{-2}	1.25×10^{-3}	3.12×10^{-3}	1.40×10^{-3}	5.05×10^{-6}
0.4	2.51×10^{-2}	1.54×10^{-2}	9.67×10^{-3}	7.42×10^{-3}	7.31×10^{-6}
0.5	3.004×10^{-2}	2.09×10^{-2}	1.12×10^{-3}	1.06×10^{-3}	1.25×10^{-9}
0.6	3.27×10^{-2}	3.04×10^{-2}	1.78×10^{-4}	2.87×10^{-3}	7.08×10^{-5}
0.7	3.37×10^{-2}	4.35×10^{-2}	8.14×10^{-4}	1.83×10^{-4}	4.69×10^{-5}
0.8	3.35×10^{-2}	5.95×10^{-2}	7.43×10^{-3}	1.94×10^{-3}	3.34×10^{-4}
0.9	3.23×10^{-2}	7.72×10^{-2}	3.59×10^{-3}	2.69×10^{-3}	3.54×10^{-4}

4 Conclusions

In the present paper we obtain analytical approximate solutions for nonlinear heat transfer problems using the recently introduced Piecewise Polynomial Least Squares Method. Using the Piecewise Polynomial Least Squares Method one obtains the analytical solution of the problem, not only numerical solutions, fact which demonstrates the usefulness of the method (PWPLSM).

The application presented clearly illustrate the accuracy of the method. The very good errors (smaller than those existing in the literature) that can be observed in each of the three tables, were calculated starting from approximate solutions, polynomial of not very high degree. If in ([7]) using SRMM and in ([9]) with LSDQ, the approximation polynomial had five degree, with this new method we only used third degree polynomial and the approximate analytical solution found being closer to the exact solution. The degree of the approximation polynomial being lower, fewer coefficients are calculated that minimize the functional $\mathcal{J}$, which means that the required resources are also fewer.

For all these reasons, it appears that the proposed method is useful and easy to use in practice.

References

[1] J.H. He, *Application of homotopy perturbation method to nonlinear wave equations*, Chaos, Solitons and Fractals 26 (3) (2005) 695–700.

[2] J.H. He, *Homotopy perturbation technique*, Journal of Computer Methods in Ap- plied Mechanics and Engineering 17 (8) (1999) 257–262.

[3] V. Marinca, *Application of modified homotopy perturbation method to nonlinear oscillations*, Archives of Mechanics 58 (3) (2006) 241–256.

[4] V. Marinca, N. Herisanu, *Application of Optimal Homotopy Asymptotic Method for solving nonlinear equations arising in heat transfer*, International Communi- cations in Heat and Mass Transfer 35 (2008) 710–715.

[5] S.J. Liao, *Beyond Perturbation: Introduction to the Homotopy Analysis Method*, Chapman and Hall/CRC Press, Boca Raton, (2003).

[6] S.J. Liao, *On the homotopy analysis method for nonlinear problems*, Applied Mathematics and Computation 147 (2004) 499–513.

[7] B.Caruntu, C.Bota, *Approximate polynomial solutions for nonlinear heat transfer problems using the squared remainder minimization method*, International Communications in Heat and Mass Transfer 39 (2012) 1336 - 1341.

[8] R.A. Khan, *The generalized approximation method and nonlinear heat transfer equations*, Electronic Journal of Qualitative Theory of Differential Equations 2 (2009) 1–15.

[9] M.S.Paşca, M. Lăpădat: *Approximate solutions by the least squares differential quadrature method for nonlinear heat transfer problems*, Scientific Buletin of The Politehnica University of Timisoara, Transactions on Mathematics and Physics, Volume 64(78), Issue 1, 2019, pag 4-13

[10] D.D. Ganji, A. Rajabi,*Assessment of homotopy-perturbation and perturbation methods in heat radiation equations*, International Communications in Heat and Mass Transfer 33 (2006) 391–400.

[11] S. Abbasbandy, *Homotopy analysis method for heat radiation equations*, Interna- tional Communications in Heat and Mass Transfer 34 (2007) 380–387.

[12] G. Domairry, N. Nadim, *Assessment of homotopy analysis method and homotopy perturbation method in non-linear heat transfer equation*, International Communications in Heat and Mass Transfer 35 (2008) 93–102.

[13] D.D. Ganji, *The application of He's homotopy perturbation method to nonlinear equations arising in heat transfer*, Physics Letters A 355 (2006) 337–341.

[14] S. Abbasbandy, *The application of homotopy analysis method to nonlinear equations arising in heat transfer*, Physics Letters A 360 (2006) 109–113.

[15] A. Rajabi, D.D. Ganji, H. Taherian, *Application of homotopy perturbation method in nonlinear heat conduction and convection equations*, Physics Letters A 360 (2007) 570–573.

[16] O. Abdulaziz, I. Hashim, *Fully developed free convection heat and mass transfer of a micropolar fluid between porous vertical plates*, Numerical Heat Transfer, Part A: Applications 55 (3) (2009) 270–288.

[17] C.M. Fan, H.F. Chan *Modified collocation Trefftz method for the geometry boundary identification problem of heat conduction*, Numerical Heat Transfer, Part B: Fundamentals 59 (1) (2011) 58–75.

[18] D. Slota, *Homotopy perturbation method for solving the two-phase inverse stefan problem*, Numerical Heat Transfer, Part A: Applications 59 (10) (2011) 755–768.

Mădălina Sofia PAŞCA
Department of Mathematics
Politehnica University of Timişoara
Piaţa Victoriei 2, 300006 Timişoara, România
E-mail: madalina.pasca@upt.ro
West University Timişoara
Bv. V.Pârvan 4, 300223 Timişoara, România
E-mail: madalina.pasca79@e-uvt.ro

INSTRUCTIONS FOR THE AUTHORS

The "Buletinul Ştiinţific al Universităţii Politehnica Timişoara" is a direct successor of the "Buletin scientifique de l'École Polytechnique de Timişoara" which was started in 1925. Between 1982 – 1989 it was published as the "Lucrările Seminarului de Matematică şi Fizică ale Institutului Politehnic "Traian Vuia" din Timişoara".

Publication program: one volume per year in two issues, each series.

The "Mathematics-Physics" series of the "Buletinul Ştiinţific al Universităţii Politehnica Timişoara" publishes original papers in all areas of the pure and applied mathematics and physics.

1. The manuscript should be sent to the Editor, written in English (or French, or German, or Russian). The manuscript should be prepared in LATEX.
2. Maximum length of the paper is 8 pages, preferably in an even number of pages, in Times New Roman (12 pt).
3. For the first page the authors must bear in view:
   - an Abstract single spaced (at most 150 words) will be placed before the beginning of the text as: ABSTRACT. The problem of ...
   - footnote with MSC (Mathematics Subjects Classification) or PACS (Physics Abstracts Classification System) Subject Classification Codes (10 pt)
4. Graphs. illustrations and tables should placed into the manuscript (send it as .eps or .pdf file), with the corresponding consecutively number and explanations under them.
5. The complete author's (authors') address(es) will be placed after References.
6. A Copyright Transfer Agreement is required together with the paper. By submitting a paper to this journal, authors certify that the manuscript has not been submitted to, nor is it under consideration for publication by another journal, conference proceedings, or similar publications.
7. There is no page charge and after registration a paper is sent to two independent referees. After acceptance and publication the author will receive 5 reprints free of charge. If a larger amount is required (fee of 2 USD per copy per article) this should be communicated to the Editor.
8. Manuscripts should be sent to:

For Mathematics

Dr. Liviu CĂDARIU
POLITEHNICA UNIVERSITY TIMISOARA
Department of Mathematics
Victoriei Square, No. 2
300006 – TIMIŞOARA, ROMANIA
liviu.cadariu-brailoiu@mat.upt.ro

For Physics

Dr. Dušan POPOV
POLITEHNICA UNIVERSITY TIMISOARA
Department of Physical Fundamentals of Engineering
B-dul. V. Parvan, No.2
300223 – TIMIŞOARA, ROMANIA
dusan.popov@et.upt.ro